Tropical Ecosystem Sustainability: A large mammal approach

By

Jennifer Leigh Bradham

Dissertation

Submitted to the Faculty of the

Graduate School of Vanderbilt University

in partial fulfilment of the requirements

for the degree of

DOCTOR OF PHILOSOPHY

in

Earth and Environmental Sciences

December 14, 2019

Nashville, Tennessee

Approved:

Maria Luisa S.P. Jorge, Ph.D.

Jessica Oster, Ph.D.

Jonathan Gilligan, Ph.D.

James Clarke, Ph.D.

Mauro Galetti, Ph.D.

Milton Ribeiro, Ph.D.

To the majestic white-lipped peccary

ACKNOWLEDGEMENTS

The acknowledgements section of this dissertation could easily be equally as long and verbose as the subsequent pages detailing the last six years of my academic accomplishments. I composed, rephrased, deleted, and re-wrote this section numerous times over the past month, never feeling like it quite captured what I wanted to say. In the end, words were committed to paper, but please know they fall short of truly expressing my ineffable gratitude to those who made this journey possible.

There is no other way to begin than by thanking my advisor, Malu. When I said it was a challenge to write the Acknowledgements for this dissertation, I particularly meant writing this section, as nothing that I compose seems to convey exactly how I feel. You will never know what an impact you have had on my life. Over the past six years you have not only been an advisor, but you have become one of my closest friends. You championed my successes and shared in my struggles. You gave me the freedom to explore, the freedom to fail, and perhaps most importantly words of reassurance when I was certain I was not capable. Working with you has not only made me a better scientist, it has made me a better person. No matter what obstacles appeared, we faced them as team, and I felt supported at every turn. As I look forward to advising my own students, I can only hope to be half as impactful of an advisor as you were to me.

I am incredibly grateful to the phenomenal group of scientists who served on my committee: Jessica Oster, Jonathan Gilligan, Jim Clarke, Miltinho Ribeiro and Mauro Galetti. Jessica – you are proof that it is possible to have it all, to be a successful scientist, a dedicated mother and wife, and a genuinely kind human being. Thank you for leading by example and for being such a great friend. Jonathan – I have learned more from you than you will ever know. Your confidence in my abilities, insightful advice, and positive outlook when challenges arose were foundational pillars that made this work possible. Jim – thank you for your constant positivity and uplifting feedback. Graduate school is an incredibly challenging time, but your support (and willingness to let an ecologist infiltrate your engineering classes!) were key to my success. Miltinho e Mauro - o conhecimento científco e a criatividade em resolver problemas que vocês têm são qualidades que eu espero poder ter um dia. Sou eternamente agradecida por vocês terem aceitado serem parte do meu comitê. Mauro, muito obrigada por me ensinar a sempre procurar exergar os problemas ecológicos de forma mais abrangente. Enquanto eu olhava os dados e via números, você sempre enxergava uma história. Você sempre celebrou cada um dos meus sucessos e sempre me fez me sentir capaz. Muito obrigada! Miltinho, sua alegria e sua visão sempre positiva da vida são contagiosas. Muito origada por ter me aceitado no seu grupo de pesquisa e ter dividido comigo sua animação sobre tudo relacionado com Ecologia da Paisagem. Mas talvez mais importante que tudo, muito obrigada a vocês dois por terem aguentado o meu Portunhol!

Thank you to the rest of the EES faculty; you each have played a role in my success whether you

knew it or not. Gente (Guil), simply put - thank you for caring, for treating me like part of your family, and for always helping put things into perspective. Steve, your support at critical junctions is the reason I am here today; thank you for believing I was capable of making this journey. I am also grateful to David Furbish for sharing in my excitement of "super diffusive jungle pigs", for mercilessly (read: painfully) throwing me off the ledge into the world of coding, and for serving as a sounding board when making difficult life choices.

This work would have been severely diminished without the collaborative knowledge and constant support from the amazing group of graduate students in the Earth and Environmental Sciences Department. You all were the reason I chose Vanderbilt and you are the reason I am where I am today. A few of you warrant special mention. Greg, your excitement for all things science is infectious and I could not have made it this far without such a dear friend to nerd out with (I feel like I sufficiently paid you back though, right?). Thank you to Chris "Linda" Tasich for teaching me how to code when I opened Matlab for the first time and cried because I didn't even know where to enter data. To Chelsea Peters, Rachel Bain, Megan Patrick Dejter, Elizabeth Stone Gerding, and Emily Burchfield, thank you for endless laughs, late night study sessions, long runs, hot yoga classes, feeding me when I was too stressed to eat, and helping care for my little human so I could maintain sanity. I don't know what I did to deserve such amazing friends, but I am so thankful to have you all in my life.

Minha querida amiga Julia, muito obrigada por ter me ajudado com as aranhas na mata, tirado os carrapatos das minhas costas, me ensinado português, ter me emprestado a sua bucha de banho, me recebido na sua casa e me ensinado a fazer sopa de mandioca. Você me é a minha Walking Dead deconhecida preferida e minha parceira de campo preferida também!

To the greatest friends and most fun OG lab group ever – Trina, Kristy, Dan, and Avarna – it was never a dull moment and I'm smiling as I write this sentence just thinking about how fun the past years have been. From crashing ecology pool parties to traipsing through the jungle sharing granola bars and picking up giant tarantulas, some of my best memories of graduate school come from moments spent with all of you. Sharing in your diverse research interests and enthusiasm for all things ecology expanded my horizons and made me a better scientist. I can't wait for the ESA where we finally all get matching peccary tattoos (you too, Malu).

Speaking of great ecologists, I am humbled to have worked with such phenomenal undergraduate students while completing this dissertation research, especially Ted Maertens, Clara Yip, Melissa Halstead, and Amy Nguyen. I can't wait to see what amazing things you accomplish, and I'm honored to have been a part of your journey.

To the amazing members of the NewG lab group, Michaela, Dara, Maya, Noam, and Taber – I am grateful to you for participating in half made teaching demonstrations, providing insightful

feedback on my research talk, and your general all around awesomeness.

This work would not have been possible without the expertise of some incredible collaborators, namely Alexine Keuroghlian, Felipe Pedrosa, Valesca Zipparo, William Bercê, and Vladimir Costa as well as the extensive knowledge of Brazilian ecosystems shared by Duca Andrade Santos, Paulino Angelo, and Vadico.

To Lilly, Molly and our Vanderbilt Women's group - I am grateful that you gave me a place to feel supported, where my struggles and successes fell upon understanding and welcoming ears.

Finally, I would like to thank my family. Gia, Leith, and Flora – if there were an award for most patient family members in the world, you all would get it. Leith, you have always been the voice of reason and I would have never even made it past the first year without your unwavering support and belief in my abilities. Thank you for riding this roller coaster with me mi amor. Flora, you remind me every day that life is worth living. Your awe at the natural world around you inspires me to be a better person, to slow down and just be present. I love you, tiny toot. A special thanks to my very best friend, Gia, for 12 years of snuggles, tating, and making me feel loved when the imposter syndrome was taking root. Mom, dad, Kell, Jules, and the one and only Granster – I love you all so much and I hope this work makes you proud. For my grandad, the original 'doc', I hope you're looking down and smiling now that there is competition for your nickname. Sheldon and Janice, the greatest in-laws of all time, I am grateful for your love and support over the years. A special thank you to Rebecca and Ryan for being pretty much the most awesome people in the world because wine, Newfoundland, scary flights in small planes, and a listening ear are key to surviving graduate school.

This work was generously funded by Vanderbilt University College of Arts and Science Vanderbilt Summer Research Grant, Vanderbilt University Earth and Environmental Science Department, the Earth Science Department Jewell Williams Grant, the Geological Society of America, the Vanderbilt Center for Latin American Studies Tinker Grant, and the Fundação de Amparo á Pesquisa do Estado de São Paulo.

TABLE OF CONTENTS

Page

LIST OF TABLES

LIST OF FIGURES

CHAPTER 1

INTRODUCTION

1.1 Overview

Tropical forests are rapidly being altered by habitat loss and fragmentation, with tropical deforestation rates in some areas, such as Brazil and Indonesia, exceeding 500,000 hectares per year between 1990 to 2015 (FAO 2015a). As tropical forests provide irreplaceable ecosystem services, or benefits to society, the consequences of forest loss and fragmentation can be detrimental to human well-being at both global and local scales. For example, tropical forests act as carbon sinks, removing carbon from the atmosphere through their growth (Soepadmo 1993; Pan et al. 2011). As a result, cutting down forests reduces carbon uptake, leaving more carbon to reside in the atmosphere (Baccini et al. 2017). On a more local scale, approximately 1.2 to 1.5 billion people directly depend on tropical forests for provisioning services such as medicine, food, clean water, and timber for home construction (Vira et al. 2015), provisions which become less available with decreasing forest availability.

Carbon sequestration, life provisions, and the abundance of other ecosystem services provided by tropical forests are largely dependent on biodiversity, such that a loss of biodiversity negatively impacts the quantity and quality of ecosystem services (Losos & Leigh 2004; FAO 2010). For example, large mammals disperse seeds of tropical hard wood trees (Almeida-neto et al. 2008), which are themselves responsible for removing large quantities of carbon from the atmosphere. The absence of large mammals to disperse seeds and aid in the generation of these tree species results in forests that takes up less carbon when compared to forests with greater large mammal diversity (Bello et al. 2015; Deere et al. 2018; Goetz et al. 2018).

Because of the importance of biodiversity in maintaining tropical forest ecosystem services, many conservation efforts to date have justifiably focused on preserving biodiversity by, for example, conserving large tracts of land that act as biological reserves (Tilman et al. 2017). These types of conservation approaches are sometimes made under the assumption that simply designating an area as protected and limiting human interference will maintain the area's biodiversity. However, as biodiversity is influenced by a set of interactions between species or between biotic and abiotic factors (Hagen et al. 2012), this approach neglects to account for the dynamic intricacies of an ecosystem. For example, lowland tapirs (*Tapirus terrestris*) are largely frugivorous, consuming fruits in one portion of the forest and traveling long distances to defecate or extirpate the seeds in another location (Bueno et al. 2013). Therefore, interactions associated with tapir diet and movement influence the quantity and locations of future trees, in turn impacting overall forest diversity. As tapirs are not functionally redundant (Bueno et al. 2013), a conservation plan that does not consider this interaction, and the land use needs essential to maintaining this interaction, may result in preserving a portion of forest that is not sustainable in

the long-term.

This research describes a different approach to tropical forest conservation. Rather than employing methods that simply quantify biodiversity, I approach tropical forest conservation by determining and conserving species habitat use patterns and the interactions that shape them. The benefit of this approach is that it assesses an ecosystem as a whole, by the multiple interactions that shape it, rather than by a single factor, such as the number of species in a given location. I focus my work on interactions involving large mammals, as they play a key role in maintaining tropical forest ecosystems by predating and dispersing seed (Ripple et al. 2015), creating habitat for other organisms (Beck et al. 2010), acting as top down regulators of prey populations (Galetti & Dirzo 2013; Galetti et al. 2015a), and influencing geologic processes such as sedimentation, erosion, and climate regulation (Estes et al. 2011). Large mammals interact with their environment in two main ways, through their diet and their movement. Therefore, I evaluate how patterns associated with large mammal diet and movement are altered with anthropogenically-driven climate and land use change.

While this approach to conservation is appropriate for a variety of species and locations, I apply this method of conserving habitat use patterns associated with diet and movement using the white-lipped peccary (*Tayassu pecari*) as a model species. White-lipped peccaries are indicator species of healthy Neotropical forests, as areas where they have gone locally extinct have resulted in drastic changes to forest structure and function, including loss of biodiversity in the ecosystem (Silman et al. 2003; Wyatt and Silman 2004; Altrichter et al. 2012; Galetti et al. 2015a, b). Therefore, white-lipped peccaries are an ideal test subject for evaluating how conserving large mammal interactions and habitat use patterns can inform conservation decisions.

In assessing white-lipped peccary habitat use patterns, I outline the following research objectives:

Objective 1: Evaluate extinct peccary dietary response to past climate change as a proxy for understanding how modern species may respond to current and future climate change

Objective 2: Determine how flexible modern peccary species are in their diet and ability to adapt to anthropogenic land use change

Objective 3: Model how peccary habitat use patterns driven by diet and movement may be altered with land use change

1.2 Organization

I begin this work by diving into the world of paleontology to elucidate how extinct tayassuids altered diet in response to climate change and discuss how this information can be

helpful in looking at how their modern counterparts may respond to current anthropogenic climate change. I employ dental microwear texture analysis and stable isotope analysis from peccary tooth enamel to evaluate whether extinct peccaries consumed food in more open regions (less dense forests or grasslands) during potential times of food shortages (from climate change). I find that extinct peccaries, *Platygonus* and *Mylohyus*, were largely relegated to consuming food in forested environments. However, during the Irvingtonian, a drier and/or colder period during the Pleistocene, *Platygonus* and *Mylohyus* may have somewhat transitioned to mixed feeding. A comparison of stable isotope values from modern white-lipped peccary enamel suggests modern species are relegated to consuming foods in much denser forests than their extinct counterparts. I discuss the caveats of using the fossil record as a proxy for modern species due to time averaging and variations in spatial scales. I conclude that at present, one modern species, the white-lipped peccary, is largely restricted to consuming food items from forested areas, at least during the period over which the analyzed tooth was mineralized (first few months to years of an individual's life).

Chapter 3 explores how current land use change in Brazil influences modern white-lipped peccary diet. Using stable carbon and nitrogen isotopes from white-lipped peccary hair, I quantify the ability of peccaries to alter diet in four regions within three Brazilian biomes, each with varying climate characteristics, degrees of agricultural impact, and forest canopy cover. Results indicate white-lipped peccaries are relegated to consuming food within forests regardless of environmental factors such as climate, or human-modification of the landscape due to agricultural practices. However, some individuals within a population may incorporate crops into their diet during times of food stress. This appears to be a recent phenomenon driven by increased deforestation and agricultural intensification. Regardless, white-lipped peccaries as a species are still highly dependent on forest resources and do not drastically alter diet to include crops, which supports the findings of the previous chapter.

Chapter 4 begins our journey into the emerging field of movement ecology, specifically the novel concept of linking movement ecology with agent-based modelling. In this chapter, I describe an agent-based model created to evaluate how variations in the amount of forest cover, the number of forest fragments, and spatial orientation of those fragments impact large mammal habitat use patterns. Building on the results from chapters 2 and 3, I test this model using movement data from white-lipped peccaries and find that both habitat loss and fragmentation strongly alter peccary habitat use patterns. As the amount of forest cover decreases, peccary habitat use patterns become more disproportionate, such that some portions of suitable habitat are used more intensely while others are completely devoid of peccary interactions. Fragmentation exacerbates these patterns, as an increase in the number of forest fragments on the landscape positively correlates to greater extremes in the disproportionate use of suitable habitat. Therefore, with increasing fragmentation, higher levels of forest cover are needed to maintain peccary habitat use patterns.

However, at 60% forest cover, peccaries can maintain habitat use patterns 93.3% of the time,

regardless of the quantity and spatial orientation of forest fragments, and 100% of the time at 70% forest cover and above. Below this forest cover threshold, the number of fragments and the degree of isolation between those fragments drives habitat use patterns. Collectively, these results suggest that 40% of the forest can be removed (and that land allocated to human agricultural use for example) and still maintain peccary habitat use patterns.
Chapter 5 summarizes all findings from this dissertation and discusses the broader impacts of this work as well as future research directions.

CHAPTER 2

DIETARY VARIABILITY OF EXTINCT TAYASSUIDS AND MODERN WHITE-LIPPED PECCARIES (*TAYASSU PECARI*) AS INFERRED FROM DENTAL MICROWEAR AND STABLE ISOTOPE ANALYSIS

2.1 Introduction

Over time, members of the Tayassuidae (commonly referred to as 'peccaries') have occupied a diverse array of habitats including moist tropical forests, tropical savannas, and closed canopy woodlands in North, South, and Central America (e.g. Altrichter and Boaglio, 2004; Keuroghlian et al., 2009; MacFadden and Cerling, 1996; Wetzel et al., 1975). However, after the end Pleistocene, tayassuid ranges largely became restricted to Mexico, Central America, and South America, with isolated populations of collared peccaries found in the southwestern United States (Altrichter et al., 2001; IUCN, 2017; Torres et al., 2016; Wetzel et al., 1975).
As some extant members of this family, e.g. *Tayassu*, can cause unique top-down effects on their ecosystems through herding behaviors, seed predation and dispersal, and the requirement of large home ranges (Fragoso 1998; Beck 2006; Keuroghlian & Eaton 2008b; Keuroghlian et al. 2009; Reyna-Hurtado et al. 2016), understanding tayassuid ecology both today and in the past can provide information on how dietary preferences have changed both over time and in response to past climate fluctuations. Further, knowledge of how extinct peccary diets compare to those of extant taxa can elucidate the degree to which peccary diet was generalized over time and can provide an understanding of how dietary preferences of modern tayassuids may fluctuate in response to current and future climate change events.

Modern *Tayassu* are highly frugivorous (e.g. Altrichter et al., 2001; Desbiez et al., 2009; Keuroghlian and Eaton, 2008). However, they have also been documented as consuming additional foliage in times of food scarcity (Sowls 1984; Keuroghlian et al. 2009). Further, the amount of fruit in modern *Tayassu* diets varies with geographic location and tracks fruit availability (Beck 2006). However, whether dietary generalism has always been present among tayassuids and the degree to which extinct and extant peccaries share similar dietary patterns remains unclear. Assessing dietary ecology and variability over deep time requires multiple methods capable of capturing different aspects of diet (e.g. textural properties and isotopic composition). Coupling multi-proxy paleoecological information from the fossil record with ecological studies can provide information on dietary ecology over time.
Here, we integrate multiple paleoecological methods including morphological data, dental microwear texture analysis (DMTA), and geochemical analyses to clarify the ecology of fossil peccaries as well as modern *Tayassu* peccaries at a variety of spatial and temporal scales, including since the Plio-Pleistocene and between North and South America. Specifically, we test the following hypotheses:

i) Tayassuids from the late Miocene throughout the Pleistocene were dietary generalists,

consuming browse and mixed vegetation in Florida.

ii) Extinct sympatric genera were able to coexist because they consumed disparate diets and hence represent different dietary niches, as inferred from stable isotopes and DMTA.

iii) When compared to their extinct counterparts, extant tayassuids exhibit similar degrees of dietary variability, as inferred from stable isotopes and DMTA.

2.2 Background

2.2.1 Evolutionary history of the Tayassuidae

Tayassuids, suiform artiodactyls, are distantly related to pigs, hogs, and boars (Wright, 1998). Three species of extant tayassuids currently exist: the white-lipped peccary (*Tayassu pecari* Link 1795), the collared peccary (*Pecari tajacu* Linnaeus 1758), and the chacoan peccary (*Catagonus wagneri* Rusconi 1930). The majority of evidence suggests that tayassuids first appeared during the late Eocene of North America (Wright 1998). While some suggest tayassuids are represented in South America during the late Miocene (e.g. Campbell et al., 2010 and sources therein), unequivocal skeletal evidence indicates that tayassuids are definitively recorded in South America by the late Pliocene (Cione et al., 2015; Gasparini et al., 2013).

Phylogeny between extinct and extant tayassuids remains unresolved; however, it is a topic of active research (Parisi Dutra et al., 2017; Prothero, 2015). To date, the most complete assessments of peccary relationships comes from Wright (1989) and Parisi Dutra et al. (2017). Using morphological data, Wright (1989) separated the tayassuids into two monophyletic clades, one composed of *Platygonus*, *Mylohyus*, and *Tayassu*, and the second comprised of *Catagonus* and *Pecari*. Through genetic and morphological analyses, Parisi Dutra et al. (2017) suggested the genus *Catagonus* is polyphyletic, such that *Catagonus brachydontus* is the sister group to *Platygonus*, and *Mylohyus*, while *Catagonus wagneri* is most closely related to *Tayassu*. Due to the paraphyletic nature of the genus *Catagonus*, we hereafter refer to *Catagonus brachydontus* with the newly designated nomenclature of *Protherohyus brachydontus* (Parisi Dutra et al., 2017). Other research based on dentition posits *Protherohyus* and *Catagonus* may be most closely related to *Platygonus* (Wetzel et al. 1975). A genetic assessment consisting solely of extant species concluded *Tayassu pecari* and *Pecari tajacu* form a monophyletic clade, with *Catagonus wagneri* equally related to both (Gongora and Moran, 2005). If the phylogeny of Wright (1989) is correct, peccaries likely underwent multiple separate migrations from North America to South America since the Pliocene, as Miocene representatives of *Platygonus* and Pleistocene *Pecari* are preserved in North American deposits (Hulbert et al., 2009; Wright, 1998). Perhaps the best-known and well-described fossil peccaries are those from the late Miocene through the Pleistocene, *Protherohyus*, *Mylohyus*, and *Platygonus*, and as such will be the focus of this study. Further, the extant genus, *Tayassu* (commonly referred to as the white-lipped peccary), is included as a modern taxon with a potential generalized diet based on

observational data and fecal analyses (e.g. Altrichter et al., 2001; Keuroghlian and Eaton, 2008).

2.2.2 Paleoecology of extinct peccaries

Although many tayassuid fossil remains have been described, limited studies have undertaken paleoecological assessments of extinct peccaries. Those that have, center on morphological information (e.g. Hulbert, 2001) with some additional studies using geochemical data to infer tayassuid paleoecology (MacFadden & Cerling 1996; Koch et al. 1998; Feranec & MacFadden 2000; D'Amo 2001; Feranec 2005; DeSantis et al. 2009; Feranec & DeSantis 2014; Yann & DeSantis 2014; Trayler et al. 2015; Yann et al. 2016). Additionally, there is only one dental microwear study of tayassuid fossil remains, *Platygonus compressus* from southern Indiana (Schmidt, 2008). Through a two-dimensional dental microwear analysis, the author concluded that the species' diet was similar to those of browsers or mixed-feeders, consuming both hard and soft food materials as well as abrasive and non-abrasive foods (Schmidt 2008). Cheek teeth of *Protherohyus* and *Platygonus* are zygodont, having sharply angular crests associated with primary cusps, with those of *Platygonus* being more hypsodont than the former (Wright, 1989). In contrast, *Mylohyus* has bunodont teeth, those with rounded cusps (Wright, 1998). General morphological interpretations of diet based on dentition suggest *Platygonus* may have consumed cactus and coarse-vegetation, while *Mylohyus* preferred fruit, nuts, and softer vegetation or were browse/browse-dominated mixed feeders (Hulbert, 2001; Webb, 1974; Webb et al., 2008; Wright, 1998). This would largely restrict *Mylohyus* to being a forest-dwelling taxon and suggests that *Platygonus* occupied more open environments, such as prairies (Webb, 1974).

Most stable isotope analyses of extinct peccaries in North America center around sites in Florida, where they are abundant and well preserved (MacFadden & Cerling 1996; Koch et al. 1998; Feranec & MacFadden 2000; D'Amo 2001; Feranec 2005; DeSantis et al. 2009; Yann et al. 2013; Feranec & DeSantis 2014; Yann & DeSantis 2014). Stable isotope analyses of *Platygonus* and *Mylohyus* enamel from Pleistocene glacial and interglacial localities of Florida indicate *Platygonus* was a C_3 browser during a glacial period (Inglis 1A, FL), even though C_4 grasses were present (DeSantis et al. 2009). However, *Platygonus* transitioned to mixed feeding during an early Irvingtonian (~1.6 to 1 Ma) interglacial period (Leisy Shell Pit 1A) and consumed both C_3 browse and C_4 grass (DeSantis et al. 2009). DeSantis and colleagues (2009) did not analyze *Mylohyus* during known glacial periods due to lack of specimens at Inglis 1A but note that the genus consumed a mixture of C_3 and C_4 vegetation during interglacial times. *Mylohyus* consistently consumed C_3 vegetation during the latest Pleistocene in Florida, as evidenced by isotopic analysis of specimens from Vero Beach 2 ($\delta^{13}C$ values of –10.8 ‰ and –10.9 ‰) and Cutler Hammock ($\delta^{13}C$ values of –11.4 ‰, –10.0 ‰, and –8.0 ‰; Koch et al., 1998). Additional isotopic studies categorize *Platygonus* as a mixed feeder during the first half of the Pleistocene and then strict browser starting in the middle Irvingtonian (~1.0 to 0.6 Ma; Feranec and MacFadden, 2000). Feranec and MacFadden (2000) and DeSantis and colleagues (2009) suggested this shift occurred in response to the appearance of a second mixed-feeding

peccary, *Mylohyus*, or a shift in flora; yet, morphological interpretations suggest that *Mylohyus* was likely a browser (Webb et al., 2008). Work by Yann and DeSantis (2014) indicate that both *Platygonus* and *Mylohyus* were browsing or mixed feeding at additional Pleistocene sites (Haile 8A and Tri-Britton) in Florida. Based on carbon isotopes of tayassuids from Florida throughout the Pleistocene, the consumption of moderate amounts of CAM plants or C_3 grasses by *Platygonus* and *Mylohyus* was possible (MacFadden & Cerling 1996), although unlikely due to the rarity of CAM plants and C_3 grasses in Florida (Teeri & Stowe 1976; Stowe & Teeri 1978; Koch et al. 1998). *Platygonus compressus* from Ingleside (Texas) has carbon isotope values consistent with the consumption of C_3 browse in more open environments and/or mixed feeding of both C_3 browse and C_4 grass (values of –9.1 ‰ and –8.8 ‰; Yann et al., 2016). Further, Trayler and colleagues (2015) report one stable carbon isotope value of –13.5 ‰ for *Platygonus vetus* at a mid-Irvingtonian aged site in California, Fairmead Landfill. With the exception of one specimen from the Love Bone Bed of Florida (MacFadden & Cerling 1996), the dietary ecology of extinct *Protherohyus* specimens in North America have not yet been extensively studied using geochemical techniques.

2.2.3 Ecology of extant peccaries

Modern *Tayassu* cheek teeth are bunodont and clear correlations between tooth morphology and diet have not been demonstrated in extant tayassuids (Wright 1998), suggesting additional methods are needed to fully correlate diet between extinct and extant taxa. While *Tayassu* have been recorded in seasonally inundated wetlands, dry tropical forests, and tropical savannas, (e.g. Keuroghlian and Eaton, 2008; Keuroghlian et al., 2009), they are found primarily in moist, tropical forests from southern Mexico to Argentina. They are considered largely frugivorous, and often consume palm fruits and seeds (Altrichter et al., 2001; Keuroghlian and Eaton, 2008; Keuroghlian et al., 2009; Kiltie, 1981a, 1981b; Wright, 1998) with analyses from stomach contents suggesting that palm seeds alone can account for over 60 % of *Tayassu* diet (Kiltie 1981b; Bodmer 1990; Beck 2006). Additionally, *Tayassu* consume a greater diversity of fruits during the wet season, when more fruits are available (Keuroghlian et al. 2009). During periods of low fruit availability or food scarcity, vegetative plant parts including stems, leaves, and roots have been documented as constituting up to 39 % of stomach contents (Kiltie 1981b; Barreto et al. 1996; Desbiez et al. 2009). A small portion of stomach contents (< 1 %) even consisted of consumed animal materials (Kiltie, 1981a) and additional studies have noted a preference of seeds infected with bruchid beetle larvae (Kiltie 1981b; Fragoso 1994; Silvius 2002; Jansen 2003).

2.2.4 Dental Microwear Texture Analysis (DMTA)

Dental microwear texture analysis quantifies microscopic features via scale-sensitive fractal analysis on the chewing surface of teeth that have resulted from food processing (e.g.,

Scott et al., 2005, 2006; Ungar et al., 2003). DMTA reflects the textural properties of an organism's diet within the last few days to weeks of an animal's life (Grine 1986) and can distinguish between consumption of foods that are soft and tough compared to those that are hard and brittle (Calandra and Merceron, 2016; DeSantis, 2016; Scott et al., 2005, 2006; Ungar et al., 2003). Tough foods, such as grasses and some leaves, are resistant to crack propagation and are therefore best broken down by blade-like structures and shearing motions (e.g. shearing cusps; Strait, 1997). Hard foods are those that break or crack such as seeds, nuts, and woody browse, such that the harder the food, the more resistant it is to cracking (Strait, 1997). An additional descriptive term, abrasiveness, describes a food's ability to create abrasions on the wear surface of the tooth (Calandra and Merceron, 2016).

Resulting scale-sensitive fractal analyses from DMTA generate the following informative parameters: anisotropy (*epLsar*), complexity (*Asfc*), heterogeneity of complexity (*HAsfc*), and textural fill volume (*Tfv*; Scott et al., 2005, 2006). Greater anisotropy values in herbivores result from the consumption of tougher food items like leaves or grass, while greater complexity values indicate consumption of harder and/or more brittle food items like woody browse, seeds, or fruit pits (e.g. DeSantis et al., 2017; DeSantis, 2016; Hedberg and DeSantis, 2016; Jones and DeSantis, 2017; Scott, 2012). Heterogeneity of complexity (*HAsfc*) measures the variation among textural features across a surface, while textural fill volume (*Tfv*) numerically reflects both the shape and texture of the surface, specifically the concavity and convexity (Scott et al., 2006). A surface with greater concavity or convexity will have a greater *Tfv* value as compared to a more planar surface (Scott et al. 2006).

Initial analyses of microscopic wear features in mammals used scanning electron microscopes or optical microscopes to quantify the relative number of pits and scratches, with increased pits indicative of the consumption of hard food items and a high proportion of scratches demonstrating a diet rich in abrasive food items, such as grass consumption for herbivores (e.g. Semprebon et al., 2004; Solounias and Semprebon, 2002; Walker et al., 1978). However, at times, these methods can be subject to observer error and inconsistent in data replication (DeSantis et al., 2013; Grine et al., 2002; Mihlbachler and Beatty, 2012). While these initial dental microwear studies were seminal in our understanding of ancient diets via microscopic wear patterns on teeth, the 3D analysis of wear features, as demonstrated with DMTA, is better able to distinguish between disparate dietary niches, reduce observer bias, and improve reproducibility (DeSantis et al., 2013). Further, assessment of microscopic wear features through DMTA has been successfully employed to evaluate the textural properties of diet in a diverse assemblage of mammals (e.g. DeSantis, 2016 and references therein).

2.2.5 Geochemical data

Whereas dental microwear reflects diet over the last few days to weeks of an organism's life, stable carbon isotopes in tooth enamel reflect diet during the time over which enamel was mineralized, on the order of weeks to months, a time period much earlier in life than that

reflected by microwear analysis (Hoppe et al. 2004). Stable carbon isotopes recovered from enamel hydroxyapatite can aid in assessing the proportion of C_3 or C_4 plants consumed, as well as clarifying relative forest density (van der Merwe & Medina 1989, 1991; Cerling et al. 2004a; DeSantis & Wallace 2008). Carbon values from diet are recorded in mammalian enamel with a fractionation factor of –14.1 ‰ for moderately sized herbivores (Cerling & Harris 1999). When comparing with modern taxa, there is an additional 1.5 ‰ subtracted from each stable carbon isotope value for extinct specimens to account for increased CO_2 emissions since the industrial revolution, the Suess Effect (Cerling et al. 1997; Cerling & Harris 1999; Passey et al. 2005). Stable carbon isotope values of below – 9 ‰ indicate a diet primarily composed of C_3 plant material, while values greater than – 2 ‰ indicate a diet primarily composed of C_4 plants, in extinct peccaries (Cerling et al. 1997; Kohn 2010). Values falling between those two end members reflect a mixed-feeding diet in extinct taxa (Cerling et al., 1997; Cerling and Harris, 1999; Kohn, 2010). Likewise, stable isotope values below – 10.5 ‰ or above – 3.5 ‰ indicate a predominantly C_3 or C_4 diet, respectively, in modern taxa.

When coupled, stable isotopes and DMTA have the ability to distinguish between C_3 and C_4 browsing and grazing diets (e.g. Prideaux et al., 2009; DeSantis et al., 2017), as well as document changes in textural properties of food consumed, even when isotopic breadth is similar (e.g. Jones and DeSantis, 2017).

2.3 Materials and Methods

2.3.1 Sample Collection

Specimens of extinct taxa, *Protherohyus*, *Platygonus*, and *Mylohyus*, were sampled for DMTA and geochemical analysis from the vertebrate paleontology collections at the University of Florida (Supplementary Tables 1 and 2). For stable isotope analysis of extinct genera, we analyzed a total of 115 teeth including 8 *Protherohyus*, 58 *Platygonus*, and 49 *Mylohyus*. We sampled 126 specimens for DMTA including 22 *Protherohyus*, 72 *Platygonus*, and 32 *Mylohyus* (Table S2). In Florida, *Mylohyus* specimens spanned the late Miocene (Hemphillian) to late Pleistocene (Rancholabrean), while *Platygonus* specimens have been recovered from the Pliocene (Blancan) to Pleistocene (Rancholabrean; Hulbert, 2001). In Florida, *Protherohyus* is known only from the Hemphillian.

Extant *Tayassu* specimens were sampled from collections at the Museu de Zoologia da Universidade de São Paulo (MZUSP) as well as skulls donated for use by the Wildlife Conservation Society, Brazil (WCS, Brazil) and Dr. Sandra Calvacanti from the Brazilian Institute for the Conservation of Neotropical Carnivores (CENAP, Brazil). We analyzed 14 *Tayassu* microwear samples from MZUSP and 9 samples from WCS and CENAP (Supplementary Tables 1 and 2). No isotope samples were taken from specimens at MZUSP. Rather, 35 teeth were drilled from the WCS and CENAP collections. Because of this, all *Tayassu* specimens drilled for isotopic analysis are primarily from more open-canopy biomes of central Brazil (Pantanal and Cerrado), whereas *Tayassu* specimens evaluated for microwear analysis

also included specimens from closed-canopy biomes (Amazonian and Atlantic forests; Olson et al., 2001).

2.3.2 DMTA

Microwear analyses followed procedures outlined in Scott et al. (2006). Molars, M/m1 or M/m2, were cleaned and molded with a polyvinylsiloxane dental material. After drying, molds were taken back to Vanderbilt University and each sample was puttied to form a stable basin from which to create a cast. Tooth replicates were then made using epoxy (Epotek 301) and examined at Vanderbilt University on a Plu Neox Profiler with white light at 100x magnification. Specifically, we scanned a 276-micrometer x 204-micrometer area of enamel on the occlusal surface of the protocone (-id). When the protocone (-id) was not preserved or did not exhibit a testable wear stage, the hypocone (-id) was scanned. Only on a few instances were alternate areas of a molar scanned. The scanned area was then divided into a 2 x 2 grid, representing a total of four scans. The median value between the four scans was used to analyze surficial wear features using Toothfrax and Sfrax software packages, software designed specifically for analyzing three-dimensional microscopic wear patterns on teeth.

2.3.3 Geochemical Analysis

To sample and chemically prepare specimens for stable isotope analysis, we followed similar procedures to DeSantis et al. (2009). We selectively bulk sampled (drilled a line of enamel perpendicular to the growth axis of the tooth) M/m1 or P/p4 with a low-powered drill and collected the resulting enamel powder, approximately 2 mg. Chemical preparation of samples occurred at Vanderbilt University where enamel powder was reacted with 30 % hydrogen peroxide for at least 24 hours, facilitating the removal of organic material. After removing hydrogen peroxide, samples were rinsed with distilled water to remove any remaining hydrogen peroxide residue. We then placed 0.1 N acetic acid in each vial for 18 hours to remove diagenetic carbonates, after which the samples were rinsed with distilled water again, dried, and subsequently mailed to the University of Florida Stable Isotope Facility in the Department of Geological Sciences. There, the processed enamel powders were analyzed within ± 0.1 ‰ analytical precision using a VG Prism stable isotope mass spectrometer with an in-line ISOCARB automatic sampler. All samples were normalized to the laboratory standard (NBS-19 with a $\delta^{13}C$ value of 1.95 ‰ vs. PDB) and are reported in traditional delta notation $\delta^{13}C = [(^{13}C/^{12}C_{sample}) / (^{13}C/^{12}C_{standard}) - 1] \times 1000$ using the V-PDB standard (Coplen 1994). An additional 1.5 ‰ has been subtracted from carbon isotope values of extinct fossil taxa to account for increased emissions since the industrial revolution and facilitate comparison to modern *Tayassu* specimens (e.g. an isotope value of –12.0 ‰ for an extinct specimen becomes –13.5 ‰ to facilitate comparison to its modern counterpart).

We also compiled published data on tayassuid stable carbon isotopes in enamel from

peccaries in Florida and incorporated those into our analyses (Table S1; D'Amo, 2001; DeSantis et al., 2009; Feranec, 2005; Feranec and DeSantis, 2014; Feranec and MacFadden, 2000; Koch et al. 1998; MacFadden and Cerling, 1996; Yann and DeSantis, 2014).

2.3.4 Statistical Methods

With the exception of isotopic data from *Protherohyus*, results from DMTA and isotopic analyses were confirmed by a Shapiro-Wilk test to follow a non-normal distribution (Supplementary Table 3). However, given the small sample size of *Protherohyus* and the need to compare the genus with other genera, we used non-parametric statistical tests for all analyses. All statistical analyses were done in R, version 3.31 (R Core team, 2013) using Mann-Whitney U test when comparing two taxa and Dunn's procedure (Dunn 1964) when comparing more than two groups. P-values < 0.05 were considered significant. We also calculated summary statistics including mean, median, standard deviation, maximum value, minimum value, and range. We compared each of the DMTA variables (*Asfc*, *epLsar*, *Tfv*, $HAsfc_{3x3}$, and $HAsfc_{9x9}$) and stable carbon isotope values between Florida peccaries exclusive of North American Land Mammal Age (NALMA), among co-occurring genera within a single NALMA, for a single genus over multiple NALMAs, and between extinct and modern peccaries.

2.4 Results

2.4.1 DMTA

Dental microwear texture analysis summary statistics are outlined in Tables 1-2 and Figure 1, with all temporal and taxonomic comparisons noted in Table 3 and Supplemental Tables 4 and 5.

Table 1: Summary statistics of DMTA attributes per taxonomic group. *Asfc*, area-scale fractal complexity; *epLsar*, anisotropy; *Tfv*, textural fill volume; $HAsfc_{3x3}$, $HAsfc_{9x9}$, Heterogeneity of complexity in a 3 x 3 and 9 x 9 grid, respectively; SD, standard deviation (n – 1); Range, total range of all samples examined.

Genus	Statistic	n	*Asfc*	*epLsar*	*Tfv*	$HAsfc_{3x3}$	$HAsfc_{9x9}$
Mylohyus	Mean	32	6.666	0.0022	13603	0.512	0.957
	Median		4.716	0.0020	13394	0.482	0.825
	SD		5.279	0.0010	2176	0.248	0.444
	Maximum		24.085	0.0038	17918	1.424	2.263
	Minimum		0.933	0.0007	7699	0.160	0.296
	Range		23.152	0.0032	10219	1.264	1.967
Platygonus	Mean	72	4.816	0.0029	12612	0.445	0.847
	Median		2.468	0.0025	13232	0.376	0.764
	SD		5.151	0.0016	3380	0.265	0.485
	Maximum		22.774	0.0073	19873	1.725	3.293
	Minimum		0.447	0.0003	2147	0.181	0.317
	Range		22.327	0.0070	17726	1.544	2.976
Protherohyus	Mean	22	3.306	0.0026	11796	0.641	0.982
	Median		2.577	0.0024	12150	0.567	0.896
	SD		3.046	0.0011	3432	0.448	0.487
	Maximum		13.792	0.0050	16313	2.261	1.929
	Minimum		0.451	0.0006	0	0.203	0.406
	Range		13.341	0.0044	16313	2.058	1.523
Tayassu	Mean	23	4.916	0.0026	13358	0.446	0.789
	Median		2.887	0.0021	13373	0.436	0.718
	SD		4.347	0.0013	1745	0.221	0.368
	Maximum		16.800	0.0061	15964	0.882	1.504
	Minimum		1.681	0.0008	9081	0.124	0.254
	Range		15.118	0.0053	6884	0.759	1.249

Table 2: Statistical comparisons (P-values) for all DMTA attributes between taxa. *Asfc*, area-scale fractal complexity; *epLsar*, anisotropy; *Tfv*, textural fill volume; *HAsfc*$_{3x3}$, *HAsfc*$_{9x9}$, Heterogeneity of complexity in a 3 x 3 and 9 x 9 grid respectively. Bold denotes significance ($p < 0.05$).

		Mylohyus	*Platygonus*	*Protherohyus*
Asfc	*Platygonus*	**0.003**		
	Protherohyus	**0.002**	0.175	
	Tayassu	0.104	0.168	0.063
epLsar	*Platygonus*	**0.018**		
	Protherohyus	0.067	0.455	
	Tayassu	0.159	0.239	0.317
Tfv	*Platygonus*	0.074		
	Protherohyus	**0.020**	0.143	
	Tayassu	0.367	0.186	0.056
Hasfc$_{3x3}$	*Platygonus*	**0.027**		
	Protherohyus	0.224	**0.005**	
	Tayassu	0.144	0.309	**0.047**
Hasfc$_{9x9}$	*Platygonus*	0.070		
	Protherohyus	0.483	0.091	
	Tayassu	0.074	0.364	0.086

Collectively, excluding NALMA subsampling, *Mylohyus* yields the largest mean complexity value (6.666) and has a complexity range of 23.152, while *Protherohyus* has the smallest mean complexity value (3.306) and a complexity range of 13.341 (Table 1). *Mylohyus* has significantly higher complexity than both *Platygonus* ($p = 0.0034$) and *Protherohyus* ($p = 0.002$; Table 2). In contrast, *Mylohyus* has significantly lower anisotropy than *Platygonus* ($p = 0.044$), but not *Protherohyus* (Table 2). *Platygonus* has lower heterogeneity of complexity than both *Mylohyus* ($p = 0.040$) and *Protherohyus* ($p = 0.012$) at the 3 x 3 scale; yet, there are no significant differences between genera in heterogeneity of complexity at the 9 x 9 scale (Table 2). *Mylohyus* has a higher mean texture fill volume than *Protherohyus* ($p = 0.020$) but does not differ from *Platygonus* (Table 2).

A comparison between DMTA features for *Tayassu* and each extinct taxon reveals there are no significant differences in any DMTA features between *Tayassu* and any of the extinct genera with the exception of *HAsfc*$_{3x3}$, where *Tayassu* demonstrates lower mean values than those of *Protherohyus* ($p = 0.047$; Tables 1-2).

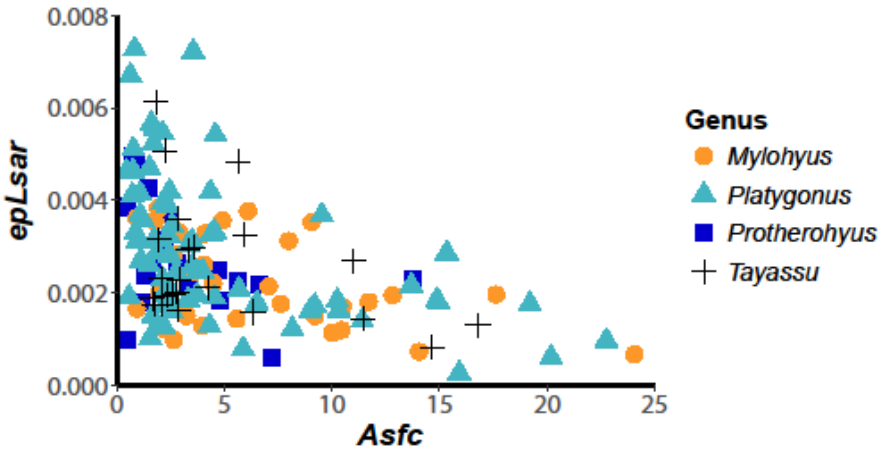

Figure 1: Scatterplot comparing the DMTA parameters of complexity (*Asfc*) and anisotropy (*epLsar*) for *Protherohyus*, *Mylohyus*, *Platygonus*, and *Tayassu*.

DMTA variables of extinct peccaries were also compared among genera, through time. Mean complexity values for *Mylohyus* appear to generally increase over time from the Hemphillian to the Rancholabrean (Table 3). During the Hemphillian, *Myloyhus* complexity values were lower than during the Blancan ($p = 0.013$) and Rancholabrean ($p = 0.007$) (Table S4). Texture fill volume values in the Hemphillian were lower in the Irvingtonian ($p = 0.047$) and the Blancan ($p = 0.016$), but not the Rancholabrean (Table S4). *Mylohyus* does not exhibit any other textural differences in dental microwear attributes between the Hemphillian and Rancholabrean (Table S4). There are no significant differences in any dental microwear feature over time for *Platygonus* (Table S5). As *Protherohyus* fossils in Florida are only recorded from the early Pliocene (Hemphillian), temporal comparisons for this genus were not possible. Summary statistics of DMTA attributes of co-occurring genera in each NALMA can be found in Table 3. *Mylohyus* and *Protherohyus* co-occur during the Hemphillian and do not significantly differ in any DMTA attribute during this time period (Table S6); *Platygonus* fossils are not present in high enough densities during the Hemphillian in Florida to facilitate inclusion into this analysis. *Mylohyus* and *Platygonus* co-occur during the Irvingtonian, Blancan, and Rancholabrean NALMAs (Table 3). During the Irvingtonian and Blancan, *Mylohyus* and *Platygonus* have indistinguishable DMTA attribute values with the exception of *Mylohyus* having higher mean $HAsfc_{3x3}$ values than *Platygonus* during the Irvingtonian ($p = 0.028$; Table S7). During the Rancholabrean, *Platygonus* had a lower mean complexity value (4.349) than *Mylohyus* (8.348; $p = 0.025$).

Table 3: Summary statistics of all DMTA attributes separated by taxonomic group and North American Land Mammal Age (NALMA). *Asfc*, area-scale fractal complexity; *epLsar*, anisotropy; *Tfv*, textural fill volume; $HAsfc_{3x3}$, $HAsfc_{9x9}$, Heterogeneity of complexity in a 3 x 3 and 9 x 9 grid respectively; SD, standard deviation (n – 1). Range, total range of all samples examined.

		Hemphillian		Blancan		Irvingtonian		Rancholabrean		Modern
		Mylohyus	*Protherohyus*	*Mylohyus*	*Platygonus*	*Mylohyus*	*Platygonus*	*Mylohyus*	*Platygonus*	*Tayassu*
Asfc	Mean	3.045	3.306	7.901	3.445	6.053	5.072	8.348	4.349	4.916
	Median	2.786	2.577	10.454	1.690	4.284	2.497	7.645	2.898	2.887
	Standard Deviation	1.834	3.046	4.170	3.917	4.572	5.304	6.277	5.210	4.347
	Maximum	7.087	13.792	11.734	10.322	12.827	22.774	24.085	20.200	16.800
	Minimum	0.941	0.451	2.673	0.447	2.815	0.578	0.933	0.724	1.681
	Total Range	6.146	13.341	9.060	9.874	10.012	22.196	23.152	19.476	15.118
epLsar	Mean	0.0023	0.0026	0.0018	0.0031	0.0021	0.0028	0.0023	0.0032	0.0026
	Median	0.0023	0.0024	0.0017	0.0026	0.0021	0.0025	0.0020	0.0025	0.0021
	Standard Deviation	0.0009	0.0011	0.0009	0.0023	0.0004	0.0014	0.0012	0.0020	0.0013
	Maximum	0.0036	0.0050	0.0033	0.0067	0.0026	0.0073	0.0038	0.0072	0.0061
	Minimum	0.0012	0.0006	0.0010	0.0008	0.0016	0.0003	0.0007	0.0006	0.0008
	Total Range	0.0023	0.0044	0.0023	0.0059	0.0010	0.0070	0.0032	0.0066	0.0053
Tfv	Mean	12482	11796	14757	11209	14545	12948	13566	11802	13358
	Median	12572	12150	14855	11292	14806	13367	13297	11481	13373
	Standard Deviation	2186	3432	1218	3663	1666	3287	2371	3639	1745
	Maximum	16781	16313	16447	15669	16145	19873	17918	19021	15964
	Minimum	9421	0	13026	5109	12422	2147	7699	5028	9081
	Total Range	7360	16313	3421	10559	3723	17726	10219	13993	6884
$HAsfc_{3x3}$	Mean	0.551	0.641	0.501	0.686	0.593	0.428	0.474	0.399	0.446
	Median	0.422	0.567	0.422	0.366	0.580	0.379	0.479	0.344	0.436
	Standard Deviation	0.403	0.448	0.131	0.619	0.032	0.209	0.215	0.180	0.221
	Maximum	1.424	2.261	0.649	1.725	0.639	1.129	0.987	0.884	0.882
	Minimum	0.160	0.203	0.393	0.234	0.572	0.181	0.229	0.233	0.124
	Total Range	1.264	2.058	0.255	1.492	0.067	0.948	0.758	0.651	0.759
$HAsfc_{9x9}$	Mean	1.108	0.982	0.832	1.379	1.049	0.797	0.895	0.802	0.789
	Median	0.806	0.896	0.800	0.788	1.048	0.773	0.777	0.738	0.718
	Standard Deviation	0.740	0.487	0.089	1.245	0.213	0.319	0.356	0.388	0.368
	Maximum	2.263	1.929	0.942	3.293	1.283	1.680	1.605	1.872	1.504
	Minimum	0.296	0.406	0.722	0.364	0.815	0.317	0.397	0.400	0.254
	Total Range	1.967	1.523	0.220	2.929	0.468	1.363	1.209	1.472	1.249

2.4.2 Stable carbon isotopes

Results from carbon isotope analyses are found in Tables 4-6, and Figure 2. When all isotopic values are pooled together (regardless of NALMA), *Mylohyus*, *Platygonus*, and *Protherohyus* all demonstrated similar mean $\delta^{13}C$ values that are indistinguishable from one another (Tables 4-5). *Mylohyus* had a range of 12.0 ‰, while *Protherohyus* and *Platygonus* had ranges of 6.3 ‰ and 10.6 ‰, respectively (Table 4). However, when comparing co-occurring genera in each NALMA, $\delta^{13}C$ values were not always indistinguishable (Figure 2, Table 6). During the Hemphillian, *Mylohyus* had a lower mean $\delta^{13}C$ value (–13.5 ‰) than *Protherohyus* (–10.6 ‰; $p = 0.032$). During the Blancan, both *Platygonus* and *Mylohyus* had similar $\delta^{13}C$ values (–12.8 ‰ and –13.9 ‰, respectively; Table S4). While $\delta^{13}C$ values for *Platygonus* and *Mylohyus* in the Irvingtonian are indistinguishable ($p = 0.518$), *Platygonus* had a lower mean $\delta^{13}C$ value (-13.0 ‰) than *Mylohyus* (-11.0 ‰) during the Rancholabrean ($p = 0.002$; Table 6).

Table 4: Summary statistics for stable carbon isotope analysis (V-PDB, ‰) between genera. Data summarized here include both newly collected data as well as data from MacFadden and Cerling (1996), Koch et al. (1998), Feranec and MacFadden (2000), D'Amo (2001), Feranec (2005), DeSantis et al. (2009), Feranec and DeSantis (2014), and Yann and DeSantis (2014). n is sample size; SD, standard deviation (n – 1). Values have been corrected for the Suess effect (–1.5 ‰ in extinct taxa as compared to modern taxa).

	Protherohyus	Mylohyus	Platygonus	Tayassu
n	8	49	58	35
Mean	-10.6	-11.4	-11.3	-14.4
Median	-11.1	-12.0	-12.0	-14.5
SD	2.5	2.5	2.7	0.7
Maximum	-7.3	-3.8	-4.8	-12.7
Minimum	-13.6	-15.8	-15.4	-15.5
Total Range	6.3	12.0	10.6	2.8

Table 5: Statistical comparisons (P-values) for stable carbon isotope analysis between all studied taxa. Values from extinct genera accounted for the Suess effect (-1.5 ‰) prior to comparison. P-values less than 0.05 are considered significant and noted here in bold.

	Mylohyus	Platygonus	Protherohyus
Platygonus	0.467		
Protherohyus	0.213	0.198	
Tayassu	<0.0001	<0.0001	<0.0001

An evaluation of *Mylohyus* through time reveals that during the Hemphillian and Blancan *Mylohyus* had similar mean $\delta^{13}C$ values (–13.5 ‰ and –13.9 ‰, respectively; Table S8). Yet, mean $\delta^{13}C$ values from *Mylohyus* in the Hemphillian are lower than those of *Mylohyus* in the Irvingtonian ($p = 0.003$) and Rancholabrean ($p = 0.003$). Similarly, mean $\delta^{13}C$ values in the Blancan were also lower than the Irvingtonian ($p = 0.006$) and the Rancholabrean ($p = 0.009$). However, *Mylohyus* stable carbon isotope values during the Rancholabrean and the Irvingtonian do not differ from each other, nor do they differ between the Hemphillian and the Blancan (Table S8). *Platygonus* has lower mean $\delta^{13}C$ values during the Blancan, as compared to the Irvingtonian ($p = 0.011$), yet not the Rancholabrean ($p = 0.355$), as Rancholabrean values are lower than those of the Irvingtonian ($p = 0.0002$).

Table 6: Summary statistics of stable carbon isotope values (V-PDB, ‰) of all extinct taxa during different NALMA (North American Land Mammal Age). n is sample size; SD, standard deviation (n – 1); Range, total range of all samples examined. Values have been corrected for the Suess effect (–1.5 ‰ in extinct taxa as compared to modern taxa).

	Hemphillian		**Blancan**		**Irvingtonian**		**Rancholabrean**	
	Mylohyus	*Protherohyus*	*Mylohyus*	*Platygonus*	*Mylohyus*	*Platygonus*	*Mylohyus*	*Platygonus*
n	7	8	3	8	10	33	29	17
Mean	-13.5	-10.6	-13.9	-12.8	-10.6	-10.0	-11.0	-13.0
Median	-13.8	-11.1	-14.0	-12.9	-11.6	-10.1	-11.5	-13.1
SD	2.4	2.5	1.0	0.9	2.4	2.8	2.2	1.7
Maximum	-8.6	-7.3	-12.9	-11.5	-6.4	-4.8	-3.8	-9.4
Minimum	-15.8	-13.6	-14.9	-14.6	-13.7	-14.2	-13.6	-15.4
Range	7.2	6.3	2.0	3.1	7.3	9.4	9.8	6.0

While all extinct peccaries evaluated have similar mean $\delta^{13}C$ values exclusive of NALMA, *Tayassu* has a lower mean $\delta^{13}C$ value than any of the extinct genera (after accounting for the Suess effect, see Materials and Methods; Tables 4-5).

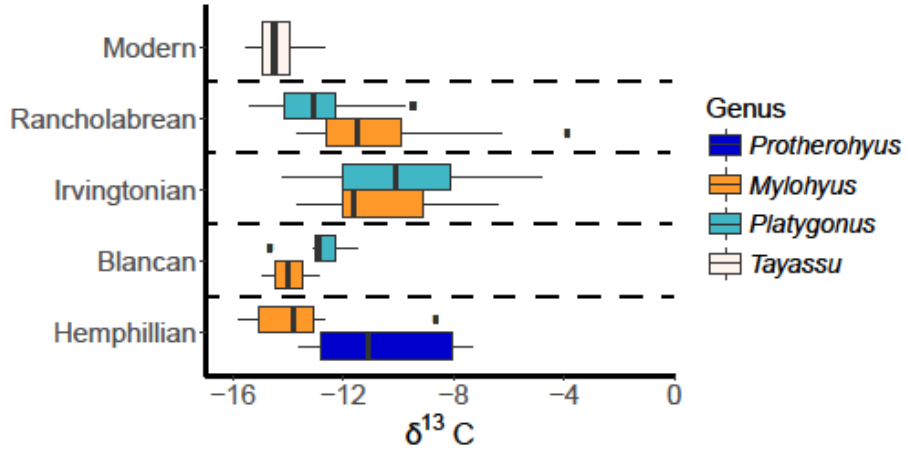

Figure 2: Boxplot of stable carbon isotope values separated by NALMA for co-occurring Tayassuidae genera. All stable carbon values for extinct genera have been adjusted by –1.5 ‰ to account for increased emissions since the industrial revolution (Cerling et al., 1997; Cerling and Harris, 1999; Passey et al., 2005). The single line within each box represents the median value, while the left and right boundaries of the box represent the first and third quartiles, respectively. Lines extending perpendicularly from the outer boundaries of the box encompass data falling outside of the first and third quartiles, with the end points of these lines not exceeding 1.5 * inner quartile range (distance between lower and upper quartile). Isolated black dots are outliers.

2.5 Discussion

2.5.1 Extinct Peccaries

Of the tayassuids sampled, only *Protherohyus* and *Mylohyus* were evaluated during the Hemphillian NALMA due to the limited availability of specimens for study. As indicated by lower $\delta^{13}C$ values, *Mylohyus* consumed food items from a more closed environment than *Protherohyus* (van der Merwe & Medina 1989, 1991). Further, higher mean *Asfc* values indicate *Mylohyus* also consumed harder food items than *Protherohyus* (Ungar et al. 2003; Scott et al. 2005, 2006). Collectively, these results suggest *Mylohyus* may have been a C_3 frugivore and/or consumed a greater proportion of woody browse (including hard twigs), consistent with morphological interpretations (Hulbert, 2001; Webb et al., 2008). The wide range of $\delta^{13}C$ values for *Protherohyus* (–13.6 ‰ to –7.3 ‰) suggests that *Protherohyus* consumed both C_3 and C_4 material. As C_3 grasses and C_4 shrubs are rare in Florida (Koch et al., 1998; Stowe and Teeri, 1978; Teeri and Stowe, 1976;), these data suggest that *Protherohyus* consumed both browse and grass.

While *Protherohyus* fossils are not recorded in Florida after the Hemphillian, *Mylohyus* persists in Floridian deposits throughout the Pleistocene (Hulbert, 2001). During the Hemphillian, *Mylohyus* consumed softer food items than during the Rancholabrean ($p = 0.007$) and Blancan ($p = 0.013$) as evidenced by lower mean *Asfc* values in the Hemphillian. *Mylohyus* also exhibited lower *Tfv* values ($p = 0.016$) during the Hemphillian as compared to the Blancan, indicating that microwear features had lower volumes during the Hemphillian. Stable carbon values from *Mylohyus* in the Hemphillian and Blancan are significantly lower than those of the Irvingtonian and Rancholabrean, indicating *Mylohyus* was foraging in more open environments in the Pleistocene as compared to the late Miocene or Pliocene. Collectively, these results suggest *Mylohyus* had a diet comprised of primarily C_3 browse and/or fruit and consumed hard objects throughout the late Miocene to early Pliocene. As complexity values for *Mylohyus* are higher in the Rancholabrean and the genus is potentially consuming food items in more open environments, increased complexity values may also be indicative of increased grit consumption (Janis et al. 2002; Kaiser & Schulz 2006). However, recent research has shown that the dietary signal overwhelms any signal created by dust or phytoliths (Merceron et al. 2016), so these changes in complexity are most likely indicative of dietary differences.

After the disappearance of *Protherohyus* at the end of the Pliocene, *Platygonus* becomes more prominent and coexists with *Mylohyus* in Florida throughout the Pleistocene (Hulbert, 2001). When comparing the two genera independent of NALMA, higher *epLsar* values suggest *Platygonus* was consuming tougher food items than *Mylohyus* ($p = 0.044$), potentially tough leaves and/or grass. The higher complexity values seen in *Mylohyus* suggest the genus consumed harder food items than *Platygonus* ($p = 0.009$, Table 2). These results are consistent with morphological differences between these taxa. *Mylohyus* has more bunodont teeth, which are well suited for crushing and grinding, while *Platygonus* has sheering crests on their teeth, which suggest a more folivorous or tough-food diet (Webb, 1974). Overall, isotopic ranges for both

genera suggest both *Platygonus* and *Mylohyus* consumed C_3 and C_4 plant material in Florida (Table 4; Cerling et al., 1997; Cerling and Harris, 1999).

Stable carbon isotope values from both genera become significantly higher and indistinguishable from one another during the Irvingtonian (Table S8), suggesting both *Platygonus* and *Mylohyus* shifted their diet from primarily C_3 browse towards more of a mixed diet. Further, isotope values for the two genera were indistinguishable from one another, indicating both genera potentially foraged in similar habitats. During the Rancholabrean, *Mylohyus* continued to consume harder food items in more open environments than *Platygonus*, as evidenced by higher *Asfc* values and greater stable carbon isotope values for *Mylohyus*. (Figure 2).

Throughout the Pleistocene, *Platygonus* does not alter the textural properties of food items consumed and during all times is consuming tough foods (e.g., tough leaves and/or grass). However, *Platygonus* is interpreted as a C_3 browser in the early and late Pleistocene but a mixed C_3/C_4 feeder in the mid Pleistocene (Irvingtonian), demonstrating variability in dietary behavior including potential food or habitat preferences. The environment during the Irvingtonian may have been more open than the earlier or later Pleistocene as indicated by higher $\delta^{13}C$ values from both *Platygonus* and *Mylohyus* during this time period, and previous studies (DeSantis et al., 2009). This may suggest that *Platygonus* was primarily a C_3 browser but was able to fluctuate diet during times of increased aridity.

All tayassuid mean isotope values are below –9 ‰ suggesting that none of the peccaries in this study had a primarily C_4 grazing diet; however, higher isotopic values indicate at least some C_4 resources were consumed by *Platygonus* and *Mylohyus*. Further, *Mylohyus* was not restricted to the forest in terms of food consumption during the Irvingtonian and Rancholabrean NALMAs, as $\delta^{13}C$ values are representative of a broader diet including both C_3 and C_4 resources during these time periods. With the exception of the Irvingtonian, when *Platygonus* and *Mylohyus* are eating both C_3 and C_4 food sources, $\delta^{13}C$ values for *Platygonus* are consistent with those of a predominantly C_3 browser. Over the past 2.5 million years, the paleoclimate of Florida has been consistently somewhat warm and humid, as evidenced by the consistent presence of alligators and land tortoises (Hulbert 2001), though some periods reflect glacial times when climates were dryer and/or cooler with associated sea level fluctuations (DeSantis et al., 2009; Hulbert, 2001; Yann and DeSantis, 2014). The transition from lower $\delta^{13}C$ values in the Hemphillian and Blancan to higher values in the Irvingtonian is consistent with prior studies documenting that some Irvingtonian sites occurred during interglacial periods and were subjected to increased evapotranspiration (DeSantis et al., 2009; Yann et al., 2013). Lower $\delta^{13}C$ values in the Rancholabrean suggest a return to consuming vegetation in more closed environments, despite some sites occurring during times with increased evapotranspiration (Yann and DeSantis, 2014).

Previous studies have hypothesized that more generalized dietary behavior may have been key to surviving the end Pleistocene extinction (e.g. DeSantis and Haupt, 2014). Therefore,

it is also interesting to note that both *Mylohyus* and *Platygonus,* taxa that have demonstrated the ability to alter diet in response to changing climate, become extinct at the end Pleistocene. Thus, perhaps the ability to alter diet was not a sufficient survival mechanism for tayassuids and additional selective pressures, such as increased predation (e.g. Surovell and Waguespack, 2009), were driving factors in their extinction.

2.5.2 Modern peccaries

All three genera of extinct peccaries exhibit higher mean isotopic values as compared to modern *Tayassu* (Tables 4-5). This may be due either to the extinct peccaries having more generalized diets or an impact of canopy-cover, which can be greater in tropical as compared to temperate latitudes (Canham et al., 1990). Further, there are no differences in the textural properties of food items consumed between *Tayassu* and any of their extinct relatives (Table 2, Figure 1), suggesting that *Tayassu* consume similar food items in terms of texture (i.e. abrasiveness and hardness). Low mean carbon isotope values and relatively high complexity values similar to those of the extinct peccaries, indicate modern *Tayassu* exhibit similar diets to their extinct counterparts and are primarily C_3 frugivores/folivores/browsers, consistent with modern ecological studies evaluating diet (e.g. Altrichter et al., 2001; Beck, 2005; Keuroghlian and Eaton, 2008). A narrow range of *Tayassu* carbon isotope values (Table 4) may insinuate that modern tayassuids have a more restrictive diet, isotopically, or potentially have a large range of food items available within a narrow range of isotopic values. As modern ecological studies note, *Tayassu* consume a wide variety of food items based on seasonal availability (Keuroghlian et al. 2009). Based on isotopic data here discussed, variations in diet during times of food scarcity likely do not include C_4 plant material as a food source, thus limiting total isotopic variability.

It is important to note that our results may be a conservative estimate of stable carbon isotope values for *Tayassu*. All specimens analyzed here were recovered from central Brazil, and all but five occurred in the Cerrado and Pantanal biomes, an interior tropical forest and seasonally inundated wetland, respectively (Olson et al., 2001). We anticipate, however, that stable carbon values from the enamel of peccaries in a denser tropical rainforest, such as the Atlantic Forest or the Amazon (Olson et al. 2001), would result in more negative values than are indicated here. Therefore, the carbon values from modern *Tayassu* enamel as noted in this study may be interpreted as a minimum estimate of differences between extant and extinct peccaries. In addition, comparisons between extinct and extant peccaries may also be somewhat reflective of the time averaging, as extant samples are from a more temporarily narrow time frame. Future work that assesses how extinct peccaries compare to the extant collared peccary (*Pecari tajacu*) and the chacoan peccary (*Catagonus wagneri*) can help clarify if and how dietary variability as inferred from stable isotopes and dental microwear has changed for the Tayassuidae as a whole, as opposed to one specific genus.

2.6 Conclusions

Here, we assessed the degree of dietary variability among extinct peccaries in Florida to understand whether extinct peccaries were able to fluctuate diet in times of changing climate and to use this information as a proxy for understanding how modern taxa may respond to climate changes. In Florida, both *Mylohyus* and *Platygonus* shift from consuming predominantly C_3 vegetation to a mixed diet of C_3 and C_4 vegetation over time, while *Protherohyus* consumed vegetation in more open areas during the Hemphillian when C_4 grasses were beginning to expand globally (Cerling et al., 1997). In contrast, modern *Tayassu* show no indication of mixed-feeding and instead consume primarily C_3 resources in more closed environments, even in more open biomes such as the Cerrado and the Pantanal. The diet of *Tayassu* may be a function of a shift in dietary preferences in the present day, as compared to their extinct counterparts. While it is unclear if and how *Tayassu* will alter diets with changing climates, like their extinct predecessors, tayassuids did fluctuate their diet over time and may be more adaptable than other co-occurring taxa.

CHAPTER 3

SPATIAL ISOTOPIC DIETARY PLASTICITY OF A NEOTROPICAL FOREST UNGULATE: THE WHITE-LIPPED PECCARY (*TAYASSU PECARI*)

3.1 Introduction

White-lipped peccaries (*Tayassu pecari*, Tayassuidae, Cetartiodactyla) are social, forest ungulates, ranging from southern Mexico to northern Argentina (Reyna-Hurtado et al. 2009; Altrichter et al. 2012; Keuroghlian et al. 2013; Jorge et al. 2019). By traveling in herds as large as 200 individuals, white-lipped peccaries (WLPs) often constitute the largest proportion of terrestrial biomass in pristine Neotropical forests (Kiltie and Terborgh 1983; Reyna-Hurtado et al. 2016). WLPs are predominantly frugivorous, a trait partially responsible for their large daily displacement (Kiltie 1981; Beck 2005; Keuroghlian and Eaton 2008b; Keuroghlian et al. 2009; Jorge et al. 2019). The percentage of fruit composition in the diet of WLPs ranges from 60 to 80%, depending upon season and biome, and includes fruits from a variety of families such as Arecaceae, Fabaceae, Moraceae, Sapotaceae, and Chrysobalanaceae (Kiltie 1981b; Bodmer 1989; Altrichter et al. 2001; Beck 2005; Keuroghlian & Eaton 2008b; Desbiez et al. 2009; Keuroghlian et al. 2009).

Through their dietary preferences and large home ranges (Fragoso 1998; Reyna-Hurtado et al. 2009; Keuroghlian et al. 2015), WLPs play a key role in seed dispersal and seed predation (Altrichter et al. 2001; Keuroghlian & Eaton 2008b), and have unique top-down effects on Neotropical forest ecosystems (Beck 2005; Keuroghlian & Eaton 2008b; Keuroghlian et al. 2009; Beck et al. 2010). For example, WLPs are the primary predators of palm seeds, destroying 73% of all palm seeds they consume and as a result directly modulating the demography and spatiotemporal distribution of palms in Neotropical forests (Beck 2005, 2006; Keuroghlian & Eaton 2009).

White-lipped peccary habitats are currently threatened because of increased land-use change and deforestation, resulting in the species being listed as “vulnerable” by the International Union for Conservation of Nature (IUCN— (Altrichter et al. 2012; Keuroghlian et al. 2013). Areas where WLPs have become locally extinct resulted in drastic changes to forest structure and loss of biodiversity (Silman et al. 2003; Wyatt and Silman 2004; Altrichter et al. 2012; Galetti et al. 2015a, b). As a result, WLPs serve as indicator species of healthy Neotropical forest ecosystems, making their conservation a high priority (Eaton et al. 2017). While it is understood their ability to physically navigate fragmented and agriculturally modified ecosystems is dependent on the presence of large, continuous tracts of forest (Altrichter et al. 2001; Jácomo et al. 2013; Keuroghlian et al. 2015; Jorge et al. 2019), it remains unclear if the diet of WLPs is also altered in response to human-driven land-use changes.

Here, we used stable carbon and nitrogen isotopes from WLP hair and food resources from four regions in three Brazilian biomes with differing climactic characteristics, native forest

cover, levels of fragmentation, and availability of agriculture crops to investigate whether WLPs alter their diet spatially and in conjunction with increased agricultural impacts and decreased native forest cover. While individual plant species consumed by WLPs have been documented (Altrichter et al. 2001; Beck 2005; Keuroghlian and Eaton 2008a, 2008b; Desbiez et al. 2009), stable isotopes can often reflect a much broader picture of diet, including seasonal variations in diet, relative trophic position, or environmental and habitat preferences (van der Merwe & Medina 1991; Cerling et al. 2004b; Loudon et al. 2007; Ben-David & Flaherty 2012). Stable carbon isotopes ($\delta^{13}C$) from mammal hair can determine whether an organism's diet consisted predominately of plants employing the C_4 photosynthetic pathway or those using a C_3 pathway (Bender 1971; Sponheimer et al. 2003a; Ayliffe et al. 2004). Plants using the C_4 photosynthetic pathway are common in warm environments with high light conditions and limited water availability such as deserts, grasslands, and some subtropical and tropical regions (Teeri & Stowe 1976; Stowe & Teeri 1978; Ehleringer et al. 1991). Examples of common C_4 plants include warm season grasses, sugarcane, and corn (Ehleringer & Bjorkman 1977; Klink & Joly 1989; Martinelli et al. 1999). The majority of plants on the planet are C_3 plants (Still et al. 2003). Plants using the C_3 photosynthetic pathway are more common in cooler, more temperate, or wetter climates and include trees, shrubs, herbs, cool-season grasses, rice, and soybeans. Isotopically, C_4 plants will have higher $\delta^{13}C$ values than C_3 plants, as the C_3 photosynthetic pathway discriminates more against the heavy ^{13}C isotope (Bender 1971; Ehleringer et al. 1991). In addition to distinguishing between C_4 and C_3 plant consumption, stable carbon isotopes can also reflect canopy density, as vegetation growing in denser forests will have lower $\delta^{13}C$ values than vegetation from less-dense forests (van der Merwe & Medina 1989, 1991).

Stable nitrogen isotopes ($\delta^{15}N$) from hair can provide specific information regarding the trophic level at which a species is eating, where higher $\delta^{15}N$ values can indicate consumption at a higher trophic level. This phenomenon occurs due to discrimination against the lighter ^{14}N isotope during excretion (e.g., Loudon et al. 2007; Ben-David and Flaherty 2012). Collectively, $\delta^{13}C$ and $\delta^{15}N$ can describe the type of food resource consumed, including engagement in more omnivorous diets, more herbivorous diet with emphasis in C_3 or C_4 plants, and information regarding forest canopy cover and climatic characteristics (e.g., humidity; Madhavan et al. 1991) from areas where the animals are consuming resources.

Given WLPs are largely restricted to forested environments (Fragoso 1998; Altrichter et al. 2001; Reyna-Hurtado et al. 2009; Keuroghlian et al. 2015), even in agriculturally dominated landscapes (Jorge et al. 2019), we hypothesize that WLPs will primarily consume resources within the forest and thus diet would vary in accordance with forest type and density. Specifically, we anticipate diet to remain within the C_3 range but to vary in relation to the environmental characteristics of each region including floral and seasonal characteristics, such that consumption from more dense, wet tropical forests (e.g., ombrophilous Atlantic Forest) would be isotopically distinguished (via more negative $\delta^{13}C$ values) from consumption in less dense, dryer forests with more severe seasonal patterns (e.g., semi-deciduous Atlantic Forest,

Cerrado, and Pantanal, in that order). As each of the regions in this study area have varied histories of human occupancy, we expect the diet of WLPs in regions devoid of heavy human influences (e.g., deforestation and agricultural development) to be reflective of the underlying stable carbon and nitrogen isotopic signatures of the native plants, as these would be the primary components of the diet of WLPs.

3.2 Materials and Methods

3.2.1 Field Sites

All WLP hair and resource samples used in this study originated from four regions in three Brazilian biomes (Figure 3): Pantanal (n = 5 sites, 61 hairs), Cerrado (n = 4 sites, 56 hairs), semi-deciduous Atlantic Forest (n = 4 sites, 47 hairs), and ombrophilous Atlantic Forest (n = 3 sites, 68 hairs). The Pantanal is a seasonally inundated inland savanna wetland, dotted with naturally occurring salt and freshwater ponds and spans Brazil, Bolivia, and Paraguay (Olson et al. 2001; Alho 2008). The Pantanal experiences extreme seasonal variation between the wet and dry seasons with approximately 80% of the Pantanal completely inundated during the wet season (Alho 2008). While the Pantanal floodplain is threatened because of deforestation and land-use change (Parente & Ferreira 2018), the Brazilian portion retains greater than 80% of the native forest (Machado et al. 2011). The land that has been deforested in the Pantanal is allocated mostly to cattle production (Seidl et al. 2001). The Cerrado contains the headwaters for the Pantanal and is predominantly savanna shrubland, with forest and wooded grasslands (Olson et al. 2001). While the Cerrado experiences both a wet and a dry season, it does not become inundated in the wet season, as does the Pantanal. Because of extensive cattle ranching and agricultural expansion, only about 50% of the native Cerrado landscape remains and less than 3% of that is federally protected (Klink & Machado 2005; Arantes et al. 2016). Some areas of the southwestern Cerrado, which border the Pantanal, maintain only about 30% of native forests, as the surrounding areas are dedicated to cattle production (Santana 2015; Jorge et al. 2019).

The Atlantic Forest biome consists of tropical broadleaf forest and extends along the eastern coast of Brazil and northern Argentina. Because of an extensive history of development and deforestation, less than 12% of the total Atlantic Forest remains and even less so in the interior portions of the biome, as deforestation varies greatly depending on the region (Ribeiro et al. 2009). Forest density also varies spatially throughout the biome, with densely forested coastal regions receiving more rain and experiencing less seasonal shifts compared to the less dense forests in the interior portion of the biome (Câmara 2003). The ombrophilous Atlantic Forest refers to the portion of the Atlantic Forest that is closest to the ocean and receives more rain. Much of the area is federally or state protected and consists of large, continuous tracts of native forest vegetation. While there are some instances of poaching (Galetti et al. 1997; Cullen et al. 2000), these areas are free from agricultural development and heavy land use interference. Sites in the semi-deciduous Atlantic Forest occur in the landlocked interior of southeastern Brazil and experience more seasonality in weather patterns. Sites within this region of the biome also occur

predominantly on private land and exist as pockets of native forest cover surrounded by agricultural fields predominantly growing soy, sugarcane, coffee, and corn.

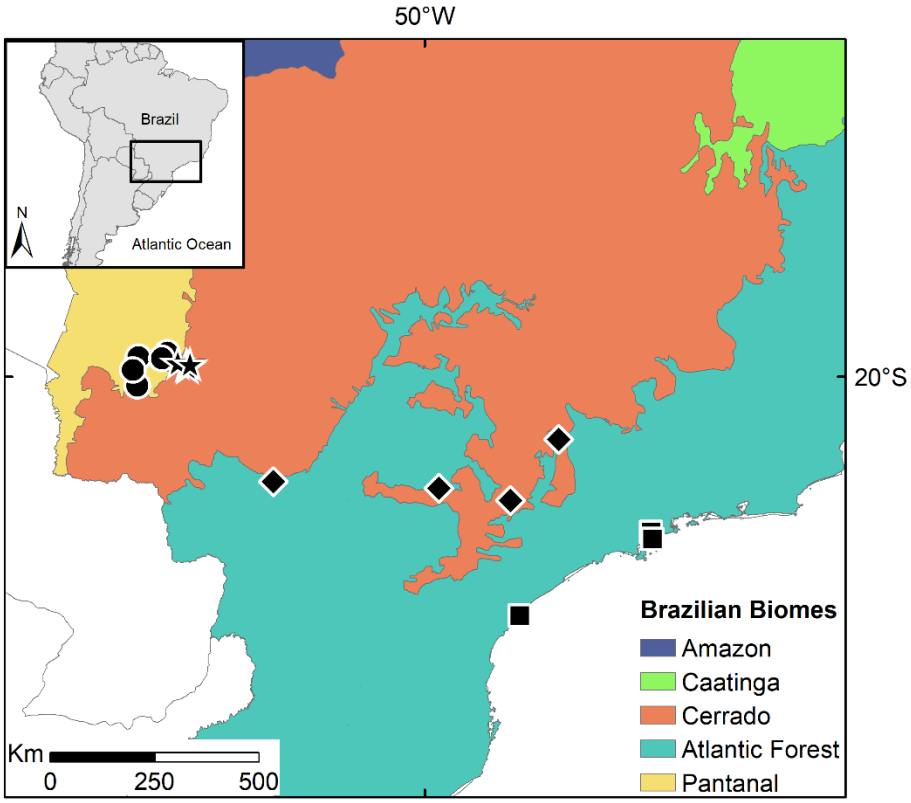

Figure 3: Map of Brazil showing the six biomes in the country. Black points indicate sites where white-lipped peccary (*Tayassu pecari*) hair samples originated. Hair samples were collected from four regions in three biomes: 1) the Pantanal, circles; 2) the Cerrado, stars; 3) the semi-deciduous Atlantic Forest, diamonds; and 4) the ombrophilous Atlantic Forest, squares. The semi-deciduous Atlantic Forest is a transitional region between the Atlantic Forest and the Cerrado biomes, consisting of localities containing flora indicative of the Atlantic Forest biome and localities containing flora from the Cerrado biome (Ribeiro et al. 2009). All samples collected from the semi-deciduous Atlantic Forest were directly collected from sites containing Atlantic Forest flora.

3.2.2 Sample collection

White-lipped peccary hair was collected from specimens at the Museu de Zoologia da Universidade de São Paulo (MZUSP), via hair traps, or from live captures (ICMBio -Instituto Chico Mendes de Conservação da Biodiversidade – SISBIO license n. 31088 and n. 46131). Hair from MZUSP was collected between 1955 and 1992 (n = 9 samples, 2 from the ombrophilous Atlantic Forest and 7 from the semi-deciduous Atlantic Forest), while hair collected from hair traps occurred between 1990 and 2016 and live captures occurred between 2014 and 2016. Hair collection from live captures followed ASM guidelines as outlined in Sikes et al. (2016).

Food resources were opportunistically collected from each region between 2009 and 2016 and are reflective of potential dietary items for WLPs including multiple plant parts (e.g., leaf, fruit, root) as well as animal prey and fungi. Animal prey (e.g., small invertebrates such as

beetles, gastropods, and chilopods) were collected from the topsoil in known WLP foraging areas, mimicking prey that are possibly consumed during bioturbation as WLPs search for food.

3.2.3 Sample processing and isotope analysis

Hair was cut just above the root, placed in a glass vial, and rinsed three times with a 2:1 chloroform:ethanol solution to remove all potential contaminants. Hair was then thoroughly rinsed with DI water and put into a drying oven at 55ºC for 48 hours. Individual hairs were placed in envelopes, catalogued with a unique identification number, and sent to the University of Wyoming Stable Isotope Facility (UW SIF) for processing. There, each hair was homogenized, weighed, and placed in a tin capsule for processing. At UW SIF, hair was analyzed on the continuous flow isotope ratio mass spectrometer (CF-IRMS; Thermo Finnigan Delta Plus XP Isotope Ratio MS; Thermo Finnigan LLC, Somerset, New Jersey) by an elemental analyzer (Costech 4010 Elemental Analyzer; Costech Analytical Technologies Inc., Valencia, California) and interface (Finnigan Conflo III Universal Interface). Standard uncertainties were 0.1‰ for carbon and 0.04‰ for nitrogen. All $\delta^{13}C$ values are reported with reference to the Vienna Pee Dee Belemnite (V-PDB) and $\delta^{15}N$ to atmospheric air.

Resources were washed with distilled water, dried, and crushed with a mortar and pestle. The resulting crumbles were placed in a microcentrifuge 1.5 mL tube, labeled with a unique identification number, and sent to the Stable Isotope Center (CIE) at the São Paulo State University (UNESP) for analysis. At CIE, resources were pulverized using a cryogenic grinder (Spex Sample - Geno Grinder 2010; Spex SamplePrep LLC, Metuchen, New Jersey). Each powdered sample was then weighed and placed in a tin capsule for isotopic analysis. At CIE, resources were analyzed on a CF-IRMS (Delta V Advantage Isotope Ratio MS; Thermo Scientific, Karlsruhe, Germany) with an elemental analyzer (Flash 2000 Organic Elemental Analyzer; Thermo Scientific, Germany) and interface (Conflo V Universal Interface; Thermo Scientific, Germany). Standard uncertainties were 0.2‰ and 0.3‰ for carbon and nitrogen, respectively.

Results of stable isotope analyses for both hair and resources are expressed through standard delta notation such that $\delta^{13}C = [(^{13}C/^{12}C_{sample}) / (^{13}C/^{12}C_{standard}) - 1] \times 1000$ and similar for $\delta^{15}N$. Trophic discrimination factors (TDF) between diet and hair were specifically calculated for WLP using the SIDER package in R (Healy et al. 2017) and found to have a mean TDF of – 3.1‰ for carbon and – 3.8‰ for nitrogen. We considered stable carbon isotope plant values between – 9‰ and – 20‰ indicative of plants using a C_4 photosynthetic pathway, while $\delta^{13}C$ values between – 20‰ and – 34‰ indicated plants using the C_3 photosynthetic pathway (Bender 1971; Cerling et al. 1997; Kohn 2010).

As hair is composed of hydrophobic proteins that are not easily degraded (Lubec et al. 1987), stable carbon and nitrogen isotope composition from hair are reliable indicators of diet (Macko et al. 1999; Sponheimer et al. 2003a; Ayliffe et al. 2004; Cerling et al. 2009) because dietary signals are incorporated into hair at the time of growth and remain stable unless altered

by certain species of parasitic and saprotrophic fungi or thermophilic anaerobic bacteria (Böckle et al. 1995; Friedrich and Antranikian 1996). As hair collected in this study was not exposed to conditions favored by these parasitic species, authors do not anticipate the age of the hair or the source location (i.e., museum-collected or field-collected) would affect the isotopic signal.

3.2.4 Statistical analysis

All statistical analyses were performed using R software, version 3.5 (R Core Team 2018). A Shapiro-Wilk test for stable carbon and nitrogen values from peccary hair confirmed both were non-normally distributed ($P < 0.0001$ and $P = 0.014$, respectively). Therefore, when comparing peccary hair and resources among locations and through time, we used a Kruskal-Wallis test with a Dunn post hoc test for significant Kruskal-Wallis results and employed a Bonferroni correction to increase the robustness of resulting relationships by controlling for the family-wise error rate (Dunn 1964; Cabin & Mitchell 2000). Adjusted *P*-values reference this correction. We used a Wilcoxon rank-sum test to discern whether hair and resources from the same location were selected from populations having the same distribution. In all analyses, we considered *P*-values less than 0.05 to be significant.

3.3 Results

Mean $\delta^{13}C_{hair}$ values for all four regions ranged from –28.7‰ to –26.9‰, with the highest and lowest values occurring in the semi-deciduous Atlantic Forest and the ombrophilous Atlantic Forest, respectively (Tables 7 and 8, Figure 4). The Cerrado had higher $\delta^{13}C_{hair}$ than the ombrophilous Atlantic Forest but not the Pantanal, while there were no differences between the Pantanal and ombrophilous Atlantic Forest (Tables 7 and 8). Stable nitrogen isotopes from WLP hair differed among all four regions (Tables 7 and 9), with WLP hair from the semi-deciduous Atlantic Forest having the highest mean $\delta^{15}N$ at 2.6‰, followed by the Pantanal, Cerrado, and the ombrophilous Atlantic Forest having the lowest at 0.1‰ (after the application of a TDF). There were no differences in $\delta^{13}C_{resources}$ among regions ($X^2 = 4.040$, $d.f. = 3$, $P = 0.257$; Table 10). However, stable nitrogen isotope values from resources did vary, with the ombrophilous Atlantic Forest having a lower mean $\delta^{15}N_{resource}$ than both the Cerrado and the Pantanal ($P = 0.018$ and 0.007, respectively; Table 10). Resources from the semi-deciduous Atlantic Forest did not differ in $\delta^{15}N$ compared to the other regions.

Table 7: Summary statistics of stable carbon and nitrogen isotope values (V-PDB, ‰) of white-lipped peccary (*Tayassu pecari*) hair from four regions in central Brazil: Pantanal, Cerrado, semi-deciduous Atlantic Forest, and ombrophilous Atlantic Forest. Values have been adjusted according to trophic discrimination factor of – 3.1‰ for carbon and – 3.8‰ for nitrogen. AF = Atlantic Forest; *n* = sample size; *SD* = standard deviation (*n* – 1); Range = difference between max and min of all samples examined.

Region	*N*	*Isotope*	*Mean*	*Median*	*SD*	*Max*	*Min*	*Range*
AF ombrophilous	68	$\delta^{13}C$	-28.7	-28.7	0.6	-27.3	-30.0	2.7
		$\delta^{15}N$	0.1	0.0	0.9	2.6	-3.1	5.7
AF semi-deciduous	47	$\delta^{13}C$	-26.9	-26.9	2.0	-20.7	-29.6	8.9
		$\delta^{15}N$	2.6	2.2	1.1	6.3	1.0	5.3
Cerrado	56	$\delta^{13}C$	-28.2	-28.4	0.7	-26.7	-29.5	2.8
		$\delta^{15}N$	1.1	1.0	0.6	3.0	-0.6	3.6
Pantanal	61	$\delta^{13}C$	-28.4	-28.7	1.2	-26.0	-30.3	4.3
		$\delta^{15}N$	1.7	1.6	0.8	3.1	0.0	3.1

Table 8: Pairwise statistical comparisons (*P*-values) from Dunn post hoc tests following a Kruskal-Wallis test (overall comparison among all regions: $\chi 2 = 35.288$, $P < 0.0001$) for stable carbon isotope analyses among white-lipped peccary (*Tayassu pecari*) hair from four regions in central Brazil: Pantanal, Cerrado, semi-deciduous Atlantic Forest, and ombrophilous Atlantic Forest. Adjusted *P*-values < 0.05 are considered significant and noted in bold.

Region comparisons	Z	P (adjusted)
AF ombrophilous - AF semi-deciduous	-5.494	**<0.0001**
AF ombrophilous - Cerrado	-2.840	**0.014**
AF semi-deciduous - Cerrado	2.677	**0.022**
AF ombrophilous - Pantanal	-0.720	1
AF semi-deciduous - Pantanal	4.716	**<0.0001**
Cerrado - Pantanal	2.083	0.112

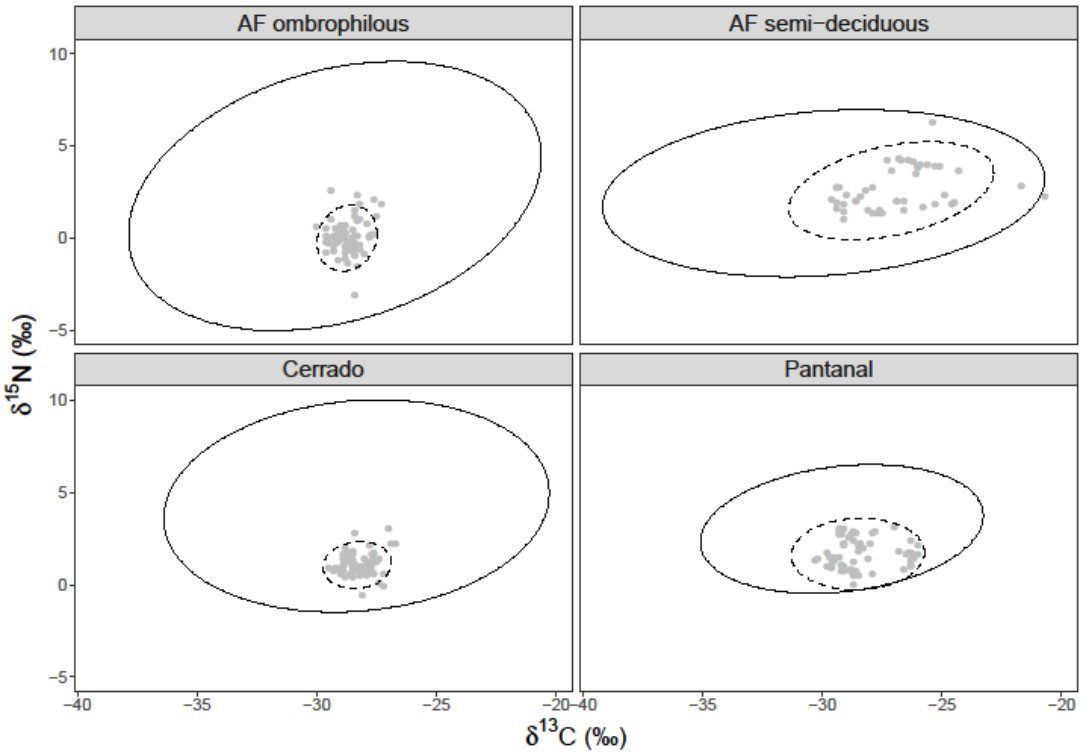

Figure 4: Scatterplots depicting stable carbon and nitrogen isotope values from white-lipped peccary (*Tayassu pecari*) hair and resource samples from the Brazilian Pantanal, Cerrado, semi-deciduous Atlantic Forest, and ombrophilous Atlantic Forest regions. Gray points indicate hair samples of white-lipped peccaries and the dashed-line ellipse shows the associated 95% confidence interval. Solid-line ellipses outline the 95% confidence interval of white-lipped peccary food resources. Resources included here are reflective of potential dietary items including multiple plant parts (e.g., leaves, fruit, roots), animal prey, and fungi, but do not include crops.

Wilcoxon rank-sum tests comparing the distributions of $\delta^{13}C_{hair}$ and $\delta^{13}C_{resources}$ from the same region demonstrated there was no difference between the distributions for hair and resources in the Cerrado or in the ombrophilous Atlantic Forest (after accounting for a TDF of –3.1‰ for carbon and –3.8‰ for nitrogen; Table 11, Figure 4). However, $\delta^{13}C_{hair}$ and $\delta^{13}C_{resources}$ did not show the same distribution in the semi-deciduous Atlantic Forest ($P < 0.0001$) or Pantanal ($P = 0.031$; Table 11, Figure 4). The distribution of stable nitrogen isotopes was not different between hair and resources in the semi-deciduous Atlantic Forest. However, the $\delta^{15}N_{hair}$ and $\delta^{15}N_{resource}$ distributions were different in all other regions (Table 11, Figure 4).

Samples from the semi-deciduous Atlantic Forest allowed for a comparison at two timescales, prior to 2000 and 2016. Prior to 2000, mean $\delta^{13}C_{hair}$ values were lower than those in 2016 ($X^2 = 10.429$, *d.f.* = 1, $P = 0.001$; Figure 5). There were no differences in $\delta^{15}N$ values between hairs sampled prior to 2000 and those from 2016.

Table 9: Pairwise statistical comparisons (*P*-values) from Dunn post hoc tests following a Kruskal-Wallis test (overall comparison among all regions: $\chi 2 = 127.305$, $P < 0.0001$) for stable nitrogen isotope analyses among white-lipped peccary (*Tayassu pecari*) hairs from four regions in central Brazil: Pantanal, Cerrado, semi-deciduous Atlantic Forest, and ombrophilous Atlantic Forest. Adjusted *P*-values < 0.05 are considered significant and noted in bold.

Region comparisons	Z	*P* (adjusted)
AF ombrophilous - AF semi-deciduous	-10.620	<0.0001
AF ombrophilous - Cerrado	-4.800	<0.0001
AF semi-deciduous - Cerrado	5.805	<0.0001
AF ombrophilous - Pantanal	-7.964	<0.0001
AF semi-deciduous - Pantanal	3.143	0.005
Cerrado - Pantanal	-2.909	0.011

Table 10: Summary statistics of stable carbon and nitrogen values (V-PDB, ‰) of white-lipped peccary (*Tayassu pecari*) food resources from four regions in central Brazil: Pantanal, Cerrado, semi-deciduous Atlantic Forest, and ombrophilous Atlantic Forest. AF = Atlantic Forest; *n* = sample size; *SD* = standard deviation; Range = difference between max and min of all samples examined. Resources do not include C_4 crops.

Region	n	Isotope	Mean	Median	SD	Max	Min	Range
AF ombrophilous	267	$\delta^{13}C$	-28.9	-29.0	4.2	-13.1	-38.3	25.2
		$\delta^{15}N$	2.4	2.0	3.7	17.5	-6.3	23.8
AF semi-deciduous	89	$\delta^{13}C$	-29.6	-29.5	4.7	-7.2	-36.9	29.8
		$\delta^{15}N$	2.6	2.3	2.7	20.0	-3.5	23.5
Cerrado	16	$\delta^{13}C$	-27.3	-28.3	5.0	-15.1	-34.7	19.6
		$\delta^{15}N$	4.1	4.2	2.4	7.7	0.3	7.4
Pantanal	59	$\delta^{13}C$	-27.9	-29.1	4.9	-4.9	-33.3	28.4
		$\delta^{15}N$	3.2	3.0	1.8	10.5	-0.5	11.0

3.4 Discussion

Mean $\delta^{13}C_{hair}$ values collected from the Brazilian Pantanal, Cerrado, semi-deciduous Atlantic Forest, and ombrophilous Atlantic Forest regions were all less than – 26‰ (after the application of a TDF), indicating WLPs in all four regions primarily consumed C_3 resources. While the rate of WLP hair growth has not been evaluated, that of the wild boar (*Sus scrofa*), one of the closest living relatives to the Tayassuidae (Chen et al. 2007), has been documented at 1.1 mm/day (Holá et al. 2015). If WLPs have a similar rate of hair growth, then one peccary hair, as sampled here, temporally represented up to a few months. Therefore, bulk sampling an individual hair may have captured a seasonal signal, as the wet or dry seasons in all of the biomes here typically spanned approximately 3 to 6 months (Castro et al. 1994; Alho 2008;

Keuroghlian and Eaton 2008b; Keuroghlian et al. 2009; Ribeiro et al. 2009; Arantes et al. 2016; Jorge et al. 2019). However, as the hairs in this study were collected throughout the year and over multiple years, the seasonal signal was likely averaged out through the analysis of multiple hairs. Thus, while an individual hair might reflect a seasonal dietary preference, the abundance of hairs representing various seasons throughout the year indicated a C_3 diet for WLPs. Further, an isotopic analysis of tooth enamel of WLPs, representing diet during the time of tooth mineralization (e.g., months to years), confirms a C_3 diet over a longer period of time (Bradham et al. 2018).

Table 11: Results of Wilcoxon rank sum test comparing white-lipped peccary (*Tayassu pecari*) hair and resource stable isotopes from the same region (Pantanal, Cerrado, semi-deciduous Atlantic Forest, or ombrophilous Atlantic Forest) in central Brazil. *P*-values < 0.05 are considered significant and noted in bold.

Region	*P*-value ($\delta^{13}C$)	*P*-value ($\delta^{15}N$)
AF ombrophilous	0.543	**<0.0001**
AF semi-deciduous	**<0.0001**	0.306
Cerrado	0.714	**<0.0001**
Pantanal	**0.031**	**<0.0001**

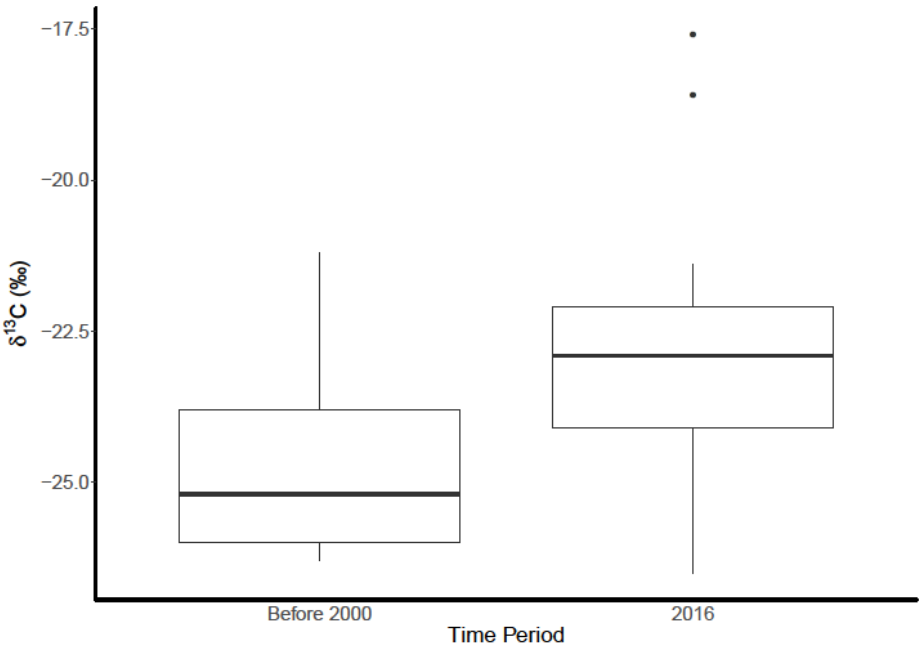

Figure 5: Boxplot of $\delta^{13}C_{hair}$ values from the semi-deciduous Atlantic Forest region for white-lipped peccary (*Tayassu pecari*) hair collected before the year 2000 and hair collected during the year 2016. Values have not been altered in accordance with a fractionation factor. The single line within each box represents the median value, while the upper and lower boundaries of the box represent the first and third quartiles, respectively. Lines extending perpendicularly from the outer boundaries of the box encompass data falling outside of the first and third quartiles, with the end points of these lines not exceeding 1.5 times the inner quartile range (distance between lower and upper quartile). Isolated black dots are outliers.

Because $\delta^{13}C_{resource}$ values did not vary among the regions in this study, any differences in $\delta^{13}C_{hair}$ values between regions were likely indicative of underlying differences in diet and not attributed to differences in the underlying resource isoscapes. While the Cerrado had higher $\delta^{13}C_{hair}$ than the ombrophilous Atlantic Forest (Tables 7 and 8), mean and median $\delta^{13}C_{hair}$ values for both locations were approximately – 28‰, and thus these statistical differences were not ecologically meaningful, as these miniscule changes in carbon were not descriptive of broad dietary variation (Deniro & Schoeniger 1983). Therefore, it can be interpreted that there were no ecologically significant differences in $\delta^{13}C_{hair}$ among the ombrophilous Atlantic Forest, Cerrado, or Pantanal, despite seasonal variations in rainfall and differential degrees of land use by humans among these regions. Therefore, in the ombrophilous Atlantic Forest, Cerrado, and Pantanal, WLP were consuming solely C_3 resources and showed no isotopic evidence of C_4 resource consumption. However, in the semi-deciduous Atlantic Forest, WLP seemed to slightly alter their diet.

In the semi-deciduous Atlantic Forest, mean $\delta^{13}C_{hair}$ value was approximately 2‰ higher than in any of the other ecosystems (Tables 7 and 8, Figure 4), and thus may describe a difference in diet. Stable carbon isotope values comparing the resources from the semi-deciduous Atlantic Forest to the hair from the same region indicated at least some portion of the species'

diet in this region came from material not accounted for in our resource sampling (Table 11, Figure 4), which included only species from the native forest. While this difference was also seen between hair and resources in the Pantanal (Table 11, Figure 4), it was a much weaker relationship and no individual $\delta^{13}C_{hair}$ values indicated consumption of material other than C_3 plants (Figure 4). The food items sampled in this study as "resources" included plants, animals, and fungi, to the exclusion of crops and non-native vegetation. We do not anticipate that the unaccounted resources included native resources that were not seasonally present during the times of sample collection, and thus absent from the analysis, given that the resources sampled span almost the entire range of $\delta^{13}C$ values for C_3 plants. Therefore, WLP in the semi-deciduous Atlantic Forest seemed to be supplementing their primarily C_3 diet with something else that is likely not native.

A higher $\delta^{13}C$ for hair in the semi-deciduous Atlantic Forest may have been driven by the consumption of C_4 resources (Bender 1971; Cerling et al. 1997) or the consumption of resources in a more open, less dense forest than in the other three ecosystems (van der Merwe & Medina 1989, 1991). Further, as dietary protein consumption is routed to collagen, the isotopic composition of hair is also reflective of dietary protein (Ambrose & Norr 1993; Gannes et al. 1998) and thus increased $\delta^{13}C$ values could have resulted from greater protein consumption (e.g., insects— Beck 2005; carcasses— A. Keuroghlian, pers. obs.; fish— (Fernandes et al. 2013); and additional animals— (Perez-Cortez & Reyna-hurtado 2008)).

The main crops grown in the semi-deciduous Atlantic Forest are soybeans, sugarcane, and corn. In addition to agricultural crops, this area has been heavily deforested to account for cattle ranching. Corn and sugarcane are C_4 crops and thus consumption of either would be distinguished isotopically through higher $\delta^{13}C$ values. Previous studies of stable carbon isotope values of Brazilian sugarcane noted a $\delta^{13}C$ range from – 10.2‰ to – 14.3‰ (Bender 1968; Martinelli et al. 2002; Neves et al. 2015; Silva et al. 2015). Two sugarcane samples that we collected from the semi-deciduous Atlantic Forest yielded $\delta^{13}C$ values of – 15.2‰ and – 15.7‰. Corn $\delta^{13}C$ values range from –10.8‰ (Tieszen et al. 1983; Tieszen & Fagre 1993) to – 12.0‰ (Holá et al. 2015). The single corn sample that we collected from one of our semi-deciduous Atlantic Forest study sites (Bacury) yielded a $\delta^{13}C$ of – 15.45‰. Thus, some WLPs may have been consuming either corn or sugarcane to supplement their diet. This could have been in response to seasonal fluctuations in available resources (Keuroghlian & Eaton 2008b; Keuroghlian et al. 2009) or in response to decreased availability of native forest, as the semi-deciduous Atlantic Forest has been heavily deforested over time (Ribeiro et al. 2009), more so than any of the other three regions in this study. As discussed previously, we do not anticipate these changes in diet were recording a purely seasonal signal.

Nitrogen values in hair were also highest in the semi-deciduous Atlantic Forest (Tables 7 and 9), while nitrogen values in resources in the semi-deciduous Atlantic Forest did not differ from those of the other regions (Table 10, Supplementary Table 8). While nitrogen values can be influenced by both biotic and abiotic factors (Ambrose 1991; Craine et al. 2009), increased stable

nitrogen values in hair can indicate consumption of food items at a higher trophic level (Sponheimer et al. 2003b) or can potentially reflect malnutrition (e.g., Loudon et al. 2007). The WLPs that were live-captured as well as those observed in these areas by other researchers showed no indication of malnutrition. Given the slightly higher carbon values and the reflection of dietary protein in collagen in addition to increased stable nitrogen values, it is possible these data indicate WLPs in the semi-deciduous Atlantic Forest were consuming an increased number of insects or other small invertebrates. This would not be uncommon, as WLPs have been known to prefer palm seeds infested with insect larvae such as the bruchid beetle (*Callosobruchus maculatus*— Beck 2005; Reyna-Hurtado et al. 2009), or it may be a reflection that palm seeds were more infested in the semi-deciduous Atlantic forest than in the other three regions (Mendes et al. 2016).

This slight deviation from the traditional C_3 diet to an inclusion of insects or crops as components of diet may have been because of environmental factors (e.g., habitat loss) resulting in a lack of sufficient fruit or seed resources (Terborgh 1986, 1992). Samples from the semi-deciduous Atlantic Forest were collected from either privately owned farm land with isolated patches of native forest or from the Caetetus Ecological Station, a 2,178-ha Atlantic Forest fragment on the inland plateau region of São Paulo state, which is surrounded by farms predominantly growing coffee, soybeans, and maize (Keuroghlian et al. 2004). In the absence of sufficient resources in these small, isolated native forest fragments, WLPs may have been incorporating C_4 crops into their diet.

Soybeans are C_3 crops, and thus WLPs in the semi-deciduous Atlantic Forest may have been consuming soybeans fertilized with organic fertilizer, which would have accounted for a C_3 diet and higher stable nitrogen values (Bateman & Kelly 2007; Choi et al. 2017). However, farmers in this area have confirmed use of mineral fertilizers (NPK) for crops. Soybean $\delta^{13}C$ values range from – 30‰ to – 26‰ (Feng et al. 2003; Yu et al. 2014) and $\delta^{15}N$ values vary from 3.1‰ to 6.6‰, depending on the part of the plant sampled (Amarger et al. 1979). After accounting for a TDF, mean $\delta^{13}C_{hair}$ values in the semi-deciduous Atlantic Forest fell within the range of soybean carbon, but only some nitrogen values did (Figure 4), Therefore, isotopic evidence presented here cannot exclude consumption of soybeans from some sites within this study.

To better understand why WLPs in the semi-deciduous Atlantic Forest may have somewhat altered their diet from traditional C_3 resources, we isotopically analysed the diet of WLPs through time (available samples did not allow for a through-time comparison of diets for other regions in this study). In the semi-deciduous Atlantic Forest, mean $\delta^{13}C$ values from hair collected during 2016 were higher than from those collected prior to the year 2000 (Figure 5). Prior to 2000, mean $\delta^{13}C$ was – 24.8‰ with minimum and maximum values of –26.3‰ and – 21.2‰, respectively. These data indicate that WLPs were consuming primarily C_3 resources with no evidence of C_4 crop consumption. However, in 2016 the mean $\delta^{13}C$ was –23.0‰ and values ranged from –21.2‰ to –17.6‰, suggesting at least some consumption of C_4 resources by

individuals in this area. While the predominant types of crops grown (e.g., sugarcane, coffee, and soybeans) in the semi-deciduous Atlantic Forest have not changed over recent timescales, the quantities of crops grown have varied, with some areas transitioning from a small focus on cattle, cotton, and tobacco production before 2000 to more extensive sugarcane cultivation and cattle ranching recently (C. Leôncio, owner of Fazenda Bacury, pers. comm., April 28, 2018). Others diversified from mainly cattle and coffee production prior to 2000 to extensive soybean cultivation coupled with cattle ranching and coffee production more recently (Marcelo de Rezende Barbosa, owner of Fazenda Torrao de Ouro, pers comm., August 13, 2018). C_4 crops prior to 2000 were not a main component of the diet of WLPs and the highest $\delta^{13}C$ values in the semi-deciduous Atlantic Forest came from 2016. As a result, we posit that the deviation from the traditional C_3 diet is a shift that occurred in the past decade, perhaps in response to land use change in the semi-deciduous Atlantic Forest (Lira et al. 2012).

It is also possible that deviation from a traditional native C_3 diet was seasonal and occurred during the dry season when fruit was scarcest (Keuroghlian & Eaton 2008b; Keuroghlian et al. 2009). The majority of 2016 samples were collected between August and October and older hairs spanned July through December, though not all museum-collected hair samples referenced a specific month of collection. If these dietary changes are reflective of seasonality, fragmentation may be exacerbating the lack of resources in the dry season, potentially causing WLPs to supplement their primarily C_3 diet. Regardless, C_4 resources such as crops did not constitute a large portion of the diet of WLPs and our evidence suggests that only some individuals in a population may have consumed C_4 resources.

The isotopic breadth of the diets of WLPs did not reflect the full isotopic breadth of the potential resources, as seen by the broad range of $\delta^{13}C_{resource}$ values and the small range of WLP $\delta^{13}C_{hair}$ values (Figure 4). Therefore, despite having more resources available, WLPs were somewhat narrow in their dietary choices isotopically. It has been suggested that higher levels of diet plasticity, or a wider range of isotopic dietary options, may translate into a greater ability to persist in changing environments when traditional food items become scarce or unavailable (Keuroghlian & Eaton 2008b; Keuroghlian et al. 2009). Given the somewhat narrow range of the diets of WLPs across regions and biomes and the lack of substantial consumption of dietary resources other than native C_3 resources, peccaries may not be able to alter their diet in rapidly changing conditions to include large portions of C_4 crops.

Most prior data on the diet of WLPs has come from direct observations. Here, we demonstrated geochemically that the main components of the diet of WLPs were C_3 resources, and that worms, fish, and C_4 crops were not a main element of their diet, even though WLPs have been seen consuming these resources at times. Previous studies have confirmed a diet of native fruits and seeds for WLPs (e.g., Beck 2005; Keuroghlian and Eaton 2008a; Desbiez et al. 2009), but those have focused on observing WLPs in their native forested environments and did not evaluate whether and to what degree crops were being consumed. We established that WLPs are likely consuming native C_3 resources in a variety of regions that include open vegetation,

closed vegetation, and more seasonally affected regions. While WLPs may have been able to supplement their traditional diet with insects or crops in areas with a greater history of crop plantations and higher amounts of isolated forest fragments, they did not seem to substantially alter their diet from primarily consuming native C_3 resources. Our results suggest that WLP populations will not be sustained by simply preserving patches of native forests unless those forests contain substantial and sufficient resources to support the dietary needs of WLPs. Therefore, to persist in fragmented landscapes, WLPs are reliant on the presence of native forests.

CHAPTER 4

LINKING AGENT-BASED MODELING AND ANIMAL MOVEMENT TO EVALUATE CHANGES IN HABITAT USE BY MOBILE FOREST-DWELLING SPECIES IN FRAGMENTED LANDSCAPES

4.1 Introduction

Tropical forests regulate global climate, act as carbon sinks, and contain some of the highest levels of biodiversity in the world (Raven 1980; Clark 2007; Bonan 2008; Pan et al. 2011; Anderson-Teixeira et al. 2012). In addition to these global benefits, approximately 1.2 to 1.5 billion people directly rely on tropical forests for food, medicine, and other ecosystems services (FAO 2015b; Vira et al. 2015). However, tropical forests are among the most threatened ecosystems on the planet, with some regions, such as Brazil and Indonesia, experiencing deforestation rates exceeding 500,000 ha/year (FAO 2015b). High rates of tropical deforestation in these regions are largely driven by global demand for palm oil, soy, beef, and wood products (David et al. 2001; Ramankutty et al. 2008; Gibbs et al. 2010; Herold et al. 2015). To compensate for increased global demands, cultivated land area in the tropics is projected to increase by as much as 10 billion ha by the year 2050, more than double the current amount of land dedicated for agricultural purposes (David et al. 2001; Gibbs et al. 2010; Gibbs & Salmon 2015).

Demand for arable land in the tropics has led to increased forest loss and fragmentation, the breaking up of continuous forests into smaller and more isolated units (Fahrig 2003). Loss and fragmentation of tropical forests impact landscape function. For example, forest fragmentation may alter the distribution of fruit-producing tree species (Talora et al. 2016). As a result, forest-dwelling animals that consume fruit may alter their movement and habitat use patterns in order to track these food resources (Baguette et al. 2014; Doherty & Driscoll 2017; Jorge et al. 2019). Animal movement and habitat use play a key role in maintaining functional connectivity, the species-specific interactions with the landscape (Tracey et al. 2013; van Toor et al. 2018), by, for instance, influencing forest structure through seed dispersal or influencing intra-species population dynamics through pathogen transmission (Morales et al. 2010). Therefore, changes in animal habitat use patterns driven by forest fragmentation may alter the functional connectivity of a landscape (van Toor et al. 2018) resulting in loss of biodiversity (Laurance et al. 2002), increased genetic isolation (Hanski 1998), or changes in predator-prey dynamics (Crooks & Soule 2010).

Previous studies have documented the landscape remains structurally connected when suitable habitat is above 60%. Below this threshold, suitable habitat occurs as numerous, small, isolated clusters and functional connectivity is therefore determined by species-specific interactions (Gardner et al. 1991; Pearson et al. 1996). Using both landscape models and biodiversity models, Yin et al. (2017) also concluded between 0% and 40% habitat loss was the

most that could occur and still avoid high rates of biodiversity loss, as that range was the maximum permissible habitat destruction to avoid creating significant landscape fragmentation. With & Crist (1995) used a percolation theory model and also found a fragmentation threshold between 35 and 40% natural habitat loss, below which would result in alterations to population structure.

Other studies have suggested higher amounts of habitat loss are needed before drastic changes in a system occur. The fragmentation threshold hypothesis, as outlined by Andrén (1994) in a meta-analysis, notes that negative effects on species may not be seen until suitable habitat is reduced to between 10% and 30% of the landscape but that for landscapes with less than 30% forest cover remaining, the spatial configuration of the patches is crucial to maintaining species diversity. Fahrig (1998) reached a similar conclusion and suggested that suitable habitat may be reduced by up to 80%, before population persistence would be drastically altered.

These studies have measured or implied species abundance or biodiversity loss as their affected metrics, but information on what happens to key processes before biodiversity is lost may be more important to preventing this loss in the first place. Here, we suggest a new way of determining fragmentation thresholds, by using animal movement and habitat use patterns. We created a spatially explicit agent-based model to assess how the amount of forest cover and the spatial orientation of forest fragments influence animal habitat use patterns and therefore functional connectivity of a landscape. While previous work has investigated how certain species respond to a distinct fragmentation scenario (e.g. De Oliveira Filho & Metzger 2006), how movement (e.g. Vanbianchi et al. 2018) and gene flow (Storfer et al. 2010) are impeded with fragmentation, or whether fragmentation positively or negatively impacts a system (Fahrig 2017), assessing how variations in habitat fragmentation and loss influence the habitat use patterns, such as visitation frequency, remains quantitatively unexplored. Further, our model allows for an evaluation of how habitat use patterns are altered in fragmentation settings that are not necessarily testable in field studies. We explore under what spatial conditions changes in landscape configurations alter animal habitat use patterns and evaluate whether habitat use patterns gradually change with fragmentation or whether thresholds exist at which habitat patterns are drastically altered.

Using habitat use patterns as a metric for informing conservation decisions incorporates empirical animal movement data, which has recently been established as essential information for making effective conservation decisions (Allen & Singh 2016). Knowing how animal behaviors change as the landscape is altered allows for an understanding of the mechanisms by which species may become locally extinct from some fragments. Furthermore, our model also provides insight into how the top-down impacts of a species on its ecosystem will change with fragmentation.

We focus our model simulation on white-lipped peccaries (*Tayassu pecari*) from the Brazilian Cerrado biome but note that this model is relevant to other mobile forest-dwelling

species around the world, such as those in tropical forests of Asia or Africa. White-lipped peccaries are forest-dwelling ecosystem engineers that are not functionally redundant (Keuroghlian & Eaton 2008a; Beck et al. 2010; Jorge et al. 2019). They directly influence ecosystems where they are present by creating habitats for other organisms (Keuroghlian & Eaton 2009; Beck et al. 2010), serving as prey to apex predators (Weckel et al. 2006), and influencing forest structure by traveling in large herds and consuming and dispersing seeds (Kiltie & Terborgh 1983; Bodmer 1989; Fragoso 1998; Keuroghlian & Eaton 2008b). Areas where white-lipped peccaries have gone locally extinct have resulted in dramatic alterations in forest structure and loss of biodiversity (Silman et al. 2003; Wyatt & Silman 2004; Altrichter et al. 2012; Galetti et al. 2015a, 2015b), making white-lipped peccaries an ideal proxy for evaluating how their habitat use patterns, and thus their associated impacts on an ecosystem, are altered with fragmentation.

4.2 Methods

4.2.1 Model Purpose

The purpose of the model is to determine how distinct scenarios of habitat loss and fragmentation affect habitat use patterns by large mobile forest-dwelling species. The model was programmed in R version 3.3 and the code for the model can be found at https://github.com/jlbradha/IBM. A full Overview, Design concepts, and Details (Grimm et al. 2010) for the model can be found in the supplemental material.

4.2.2 Model Description

The model consists of three main steps: (i) creation of a landscape with a specified fragmentation scenario, (ii) animal movement through the landscape; and (iii) analysis of animal habitat use patterns for each fragmentation scenario (Figure 6).

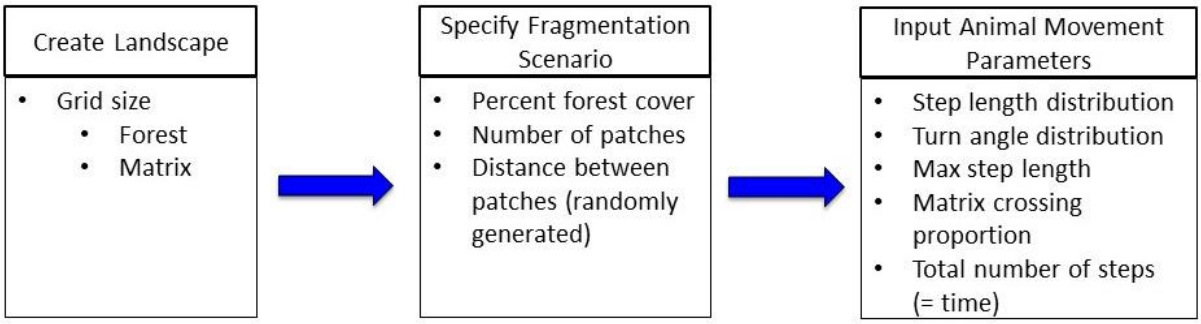

Figure 6: Conceptual model describing the three main steps of the agent-based model

4.2.2.1 Creation of the landscape

The landscape is initialized by creating a grid with a specified length and width, which are determined by the species and landscape of interest. Each cell in the grid is categorized as 'forested' (the cell is composed entirely of forest and is a habitat used by the animal) or 'matrix' (the cell is composed entirely of non-forested habitat and is not used by the animal but can be crossed). The proportion of forested cells to matrix cells is specified by a loss and fragmentation scenario. The loss scenario is determined by the percentage of forest cover and the fragmentation scenario is determined by the number of forest fragments (Figure 7A-B), as studies have documented the importance of these two factors on species persistence and diversity in fragmented landscapes (Lindenmayer et al. 2008; Prugh et al. 2008).

The percent of forest cover can vary between 10% and 100%, where 10% forest cover represents a landscape that is 90% matrix cells and 90% forest cover represent a landscape containing only 10% matrix cells (Figure 7A). The forested area of the landscape is divided into forest fragments, ranging from one to four. When the number of forest fragments is set to one, the forested cells form a single unit, or a single forest fragment (e.g. Figure 7B). A two-fragment simulation divides the forested cells (specified by the percent of forest cover input) into two individual forest fragments. If the number of forest fragments is set to three or four, the predefined amount of forest cover will be divided into three or four individual forest fragments, respectively (Figure 7B). However, the location of the forest fragment(s) on the landscape is randomly generated, such that the distance between the forest fragments varies in scenarios with two or more forest fragments. A distance of zero between two forest fragments indicates that the two randomly generated forest fragments happen to have adjacent/connecting cells and therefore form a single, larger forest fragment. Thus, a setting in which the number of forest fragments is set to 'two' can result in the existence of one single large forest fragment as well as two separate smaller forest fragments, due to the random effect of landscape creation. Therefore, for each specific scenario of percent forest cover and number of forest fragments, the model records the distance between forest fragments and the actual number of fragments present in the landscape regardless of the initial specified fragmentation value (1 to 4 fragments; Figure 7C).

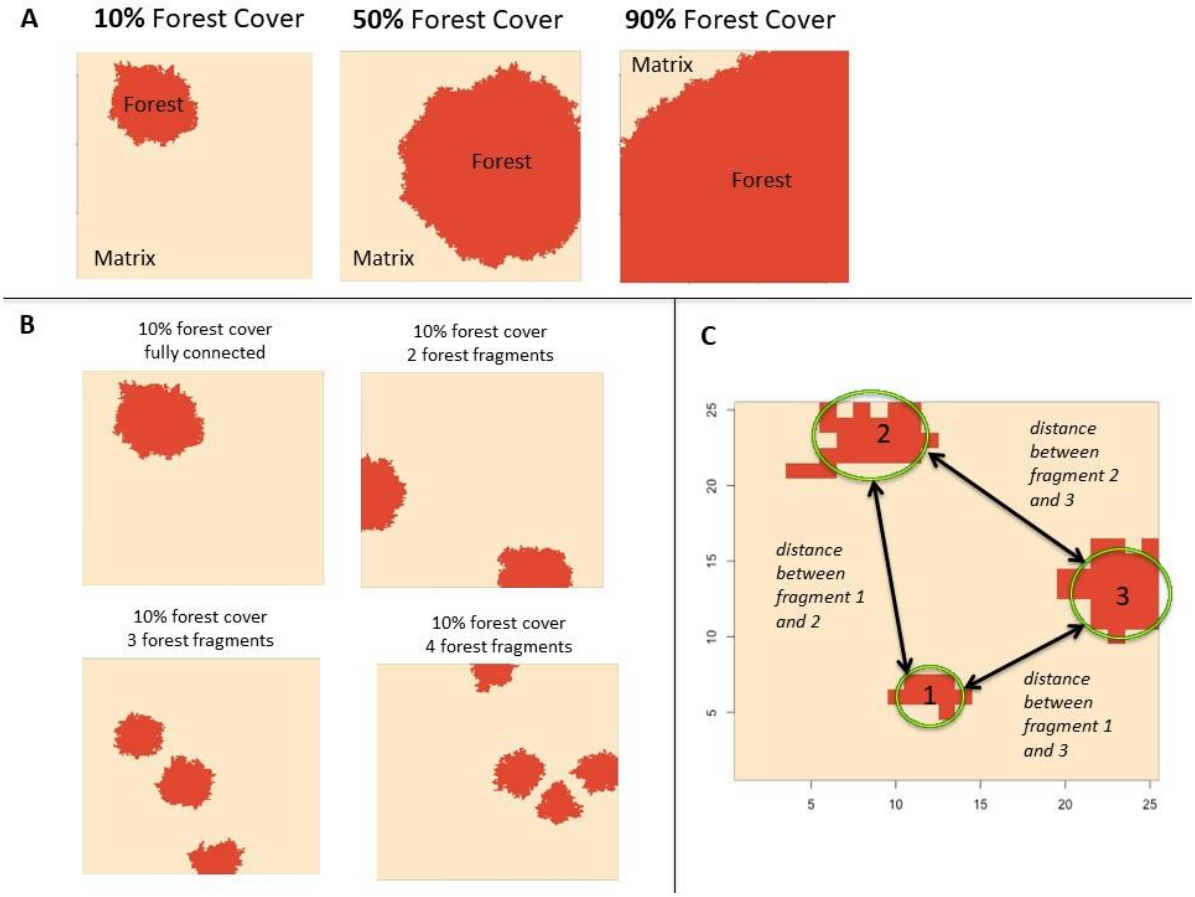

Figure 7: Sample landscape configuration generated by the model: A) one-fragment scenario showing three levels of forest cover: 10%, 50%, and 90%; B) four levels of fragmentation in a 10% forest cover scenario; c) distance between forest fragments quantified as the straight line distance between two fragments. For multi-fragment scenario where n = the number of fragments, the n-1 shortest distances were averaged together to get a distance for the simulation.

4.2.2.2 Animal movement through the landscape

Once fragmentation scenarios are created, the model subjects an individual agent (the forest-dwelling animal species of interest) to move across the landscape and records how habitat use differs for each fragmentation scenario (see Habitat Use Analysis section below). The way the animal moves is governed by the following inputs: an empirical distribution of the step lengths, an empirical distribution of turning angles, the maximum distance that can be taken in a single step, the probability of the agent crossing the matrix, and the maximum distance over which the animal will cross the matrix.

At the beginning of the model simulation, the animal is randomly placed on a forested cell. The model then randomly chooses a step length and a turning angle from the specified distributions to guide animal movement. The step length is the straight-line distance the animal will move, and the turning angle determines in what direction (up, down, left, or right) the animal will complete the step. If a step takes the animal to the middle of the matrix, the model will re-choose a step length and turn angle. If the step takes the animal to another forested

fragment that is separated by matrix from its current forest fragment, the animal decides whether to cross the matrix and make the journey to the next forest fragment based on the following input parameters: probability of matrix crossing and maximum matrix crossing distance. Each forest cell the animal passes over is recorded such that each forested cell has a 'tread count', or the number of times it was used (i.e. visited) by the animal during the simulation. The duration of the simulation is specified through the total number of steps taken. For example, if a single step represents one hour, then 8,760 steps are equivalent to 8,760 hours, or 365 days. This information should be based on the movement data for the species of interest.

4.2.2.3 Habitat use analysis

After the animal has moved over the fragmented landscape, the model quantifies habitat use in two ways: (i) the visitation frequency for each forested cell in the landscape, and (ii) the amount of unused forested cells (cells that were never visited by the animal) in the landscape. In simulations specifying only a single forest fragment (i.e. the landscape is composed of one cluster of forested cells surrounded by matrix cells; Figure 7A), habitat use patterns are reflective of only percent forest cover, as the number of forest fragments is one. However, in simulations with a greater number of fragments, habitat use patterns are reflective of percent forest cover, number of forest fragments, and distance between forest fragments. At the end of all simulations, the model generates a distribution of visitation frequency of forested cells for each combination of forest cover and number of forest fragments, as well as tables recording distances between fragments, and the number of unused forested fragments on the landscape.

4.2.2.4 Model scenario using white-lipped peccaries as an agent

We evaluated the model using white-lipped peccaries (*Tayassu pecari*, Tayassuidae, Cetartiodactyla). White-lipped peccaries are ideal species to use in the simulation as they are restricted to forested environments and rarely utilize agricultural matrices (Keuroghlian et al. 2004; Jorge et al. 2013, 2019). White-lipped peccary movement data came five GPS-tracked herds in an agricultural landscape of the Cerrado biome of central-western Brazil. Location data for the herds was collected every 3 to 6 hours between 2013 and 2016 (Jorge et al. 2019).
In order to have our model landscape reflect the home range of one white-lipped peccary herd (approximately 5 km x 5 km) in the area from which the movement data was collected (Jorge et al. 2019) with a resolution of 30 x 30 m, our model landscape grid measured 167 cells x 167 cells (27,899 cells in total). For each fragmentation scenario, we varied the percent forest cover from 10% to 100% in increments of 10% and specified the number of forest fragments as one to four, in increments of one. Each combination of percent forest cover and number of forest fragments (40 total) was replicated 30 times, comprising a total of 1,200 landscapes and simulation runs. Despite specifying a specific percent forest cover and number of forest fragments combination for each of the 30 iterations, none of the 30 iterations were exactly the

same, as the distance between fragments varied among each of the randomly generated landscapes.

For each fragmentation scenario, a peccary herd moved across the landscape for 14,600 steps. Given that one step in the model represents a three-hour time period (to reflect the temporal resolution of the GPS movement data), 14,600 steps represent 5 years of movement over the landscape. The maximum step distance was specified at 83.33 units, which represents 2,490 m (83.33 units x 30 m / unit). The maximum step length was chosen from the GPS movement data and is the largest distance covered in a three-hour period by any of the white-lipped peccaries studied (Jorge et al. 2019). Step lengths were chosen from an exponential distribution while turning angle was chosen from a circular uniform distribution. These distributions were chosen because they best expressed the GPS collected movement and turning angles (Bradham, unpublished). Given the lack of robust empirical data on matrix crossing, we chose a matrix probability crossing of 50%, as long as the matrix crossing distance was approximately 625 m, the average distance between fragments where empirical movement data was collected.

4.3 Results

The scenario with one fragment and 100% forest cover will be referred to as the control, because there are no barriers for movement and the entire landscape is suitable habitat. In the control, the amount of unvisited forest after five years averaged 1.6%, indicating that peccaries visited 98.4% of forested cells in the landscape at least once during the time period (Figure 8).

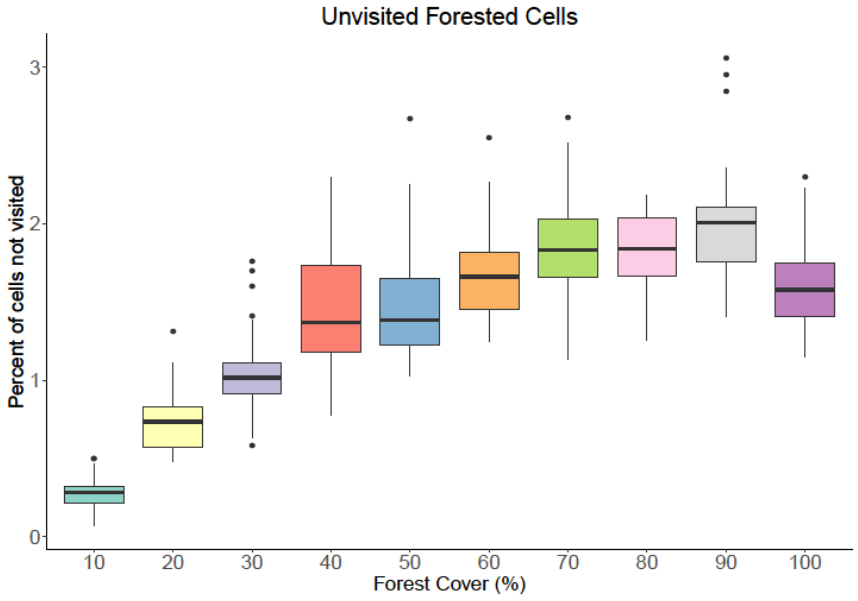

Figure 8: The proportion of unused forested cells for each percent forest cover in one fragment scenarios. As there is no fragmentation, habitat use patterns are reflective of solely variations in forest cover. The single line within each box represents the median value, while the upper and lower boundaries of the box represent the first and third quartiles, respectively. Lines extending perpendicularly from the outer boundaries of the box encompass data falling outside of the first and third quartiles, with the end points of these lines not exceeding 1.5 * inner quartile range (distance between lower and upper quartile). Isolated black dots are outliers.

For all the other simulations where the number of forest fragments was set to one and forest cover was less than 100%, less than 3% of the forest remained unused (i.e. not visited by peccaries), independent of the amount of forest cover (Figure 8). Therefore, regardless of forest amount, in a non-fragmented landscape, after five years, peccaries visited 97% or more of the forest given their movement patterns and lack of movement barriers (i.e. matrix; Figure 8). However, the visitation frequency distribution of forested cells was driven by the amount of forest cover (Figure 9). As the percent of forest cover decreased, the visitation frequency distribution (i.e. the number of times a forested cell was visited) changed from being highly left skewed (e.g. 100% forest cover; Figure 9A) to less left-skewed (e.g. 50% forest cover; Figure 9B), and finally more uniformly distributed (e.g. 10% forest cover; Figure 9C). Specifically, in 100% forest cover, the mode was at five visits per cell, with a frequency of 3,350 cells, and the maximum number of visits any cell received was 23 (Figure 9A). At 50% forest cover, the mode was 13 visits per cell, with a frequency of 1,061 cells, and the maximum number of times a cell was visited was 38 (Figure 9B). At 10% forest cover the mode was 52 visits per cell with a frequency of 79 cells, and the maximum cell visit was 109 (Figure 9C). Therefore, with decreasing amounts of forest cover, a greater number of cells were visited more frequently.

In the simulations with two or more forest fragments, the percent of unused forest (i.e. non-visited cells) varied drastically depending on the number of fragments and the percentage of forest cover. Below I outline the habitat use patterns for each fragmentation scenario in relation

to both the amount and spatial distribution of available habitat.

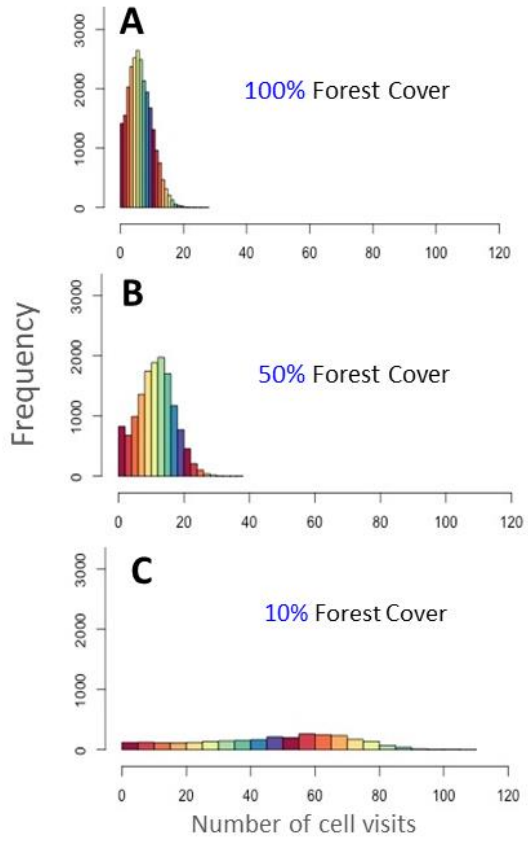

Figure 9: Forest cell visitation frequency for 1-fragment scenario. Therefore, there is no fragmentation, just habitat loss. The figures above are from one (out of thirty total) simulations. However, they are representative of the patterns seen with all simulations of these fragmentation scenarios.

4.3.1 Two-fragment scenario

In the fragmentation scenario where the number of fragments was specified as 2, forest use as a function of forest cover (Figure 10A) was heavily driven by a combination of actual number of fragments generated in the simulation (Table 12, Figure 10B) and average distance between them (Table 13, Figure 10C), which explained the increased number of simulations in which one fragment was not visited at all as the percent of forest cover decreased (Table 12, Figure 10D).

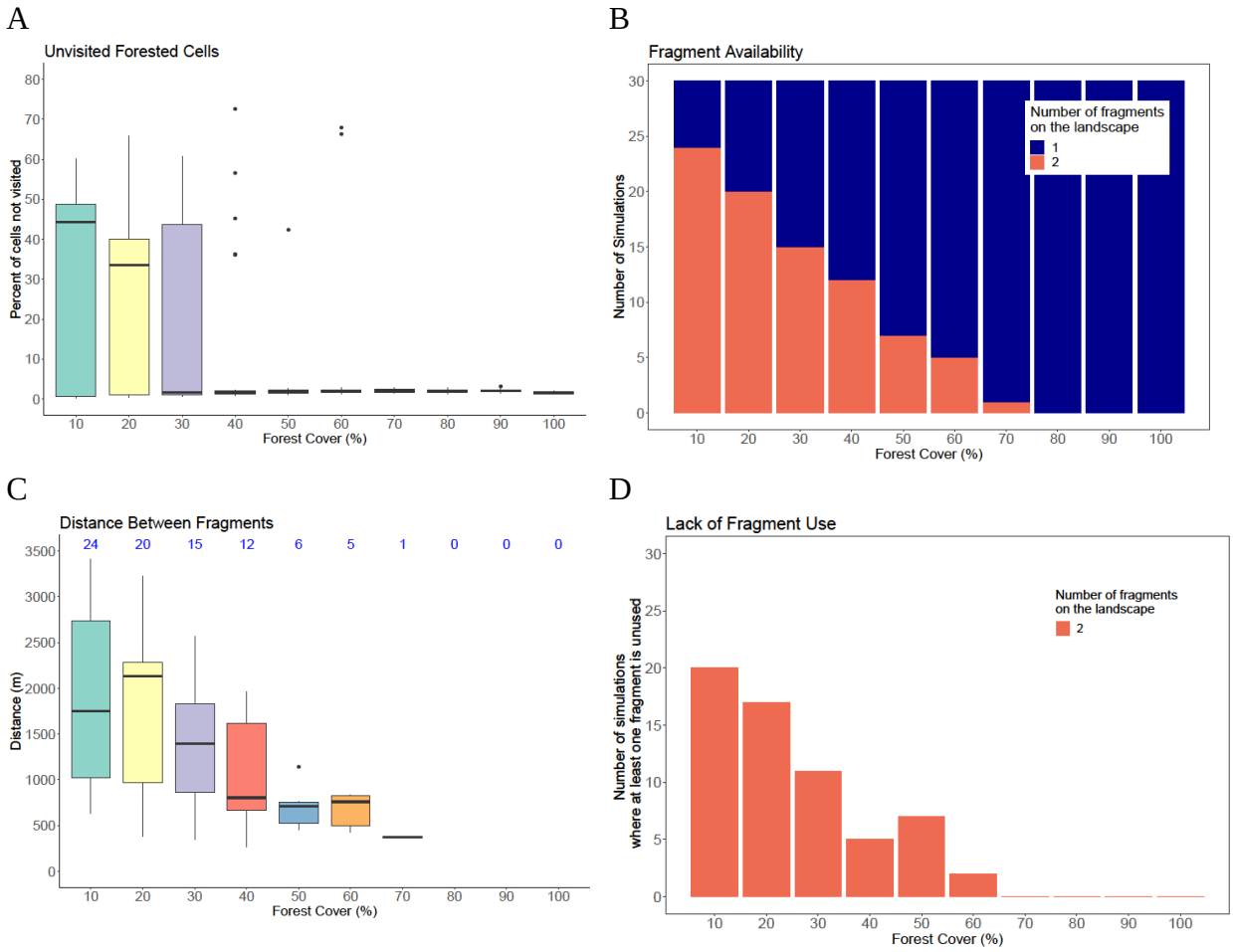

Figure 10: Results from the 2-fragment scenario: A) The percent of forested cells in the landscape that were never visited by peccaries for each habitat loss scenario (i.e. percent of forest cover); B) For each habitat loss scenario, the number of simulations resulting in 1 forest fragment on the landscape and the number of simulations with 2 forest fragments on the landscape; C) Average distance between fragments for each habitat loss scenario. Blue numbers indicate the sample size (n); D) For scenarios where there were two forest fragments on the landscape, bar plot depicting the number of simulations in which one forested fragment was not visited by peccaries. For figures A and C, the single line within each box represents the median value, while the upper and lower boundaries of the box represent the first and third quartiles, respectively. Lines extending perpendicularly from the outer boundaries of the box encompass data falling outside of the first and third quartiles, with the end points of these lines not exceeding 1.5 * inner quartile range (distance between lower and upper quartile). Isolated black dots are outliers.

Table 12: Two-fragment scenario: the amount of forest cover, the number of simulations that resulted in 1 or 2 fragments on the landscape, and the number of simulations in which one of the fragments was not used by the peccaries.

Forest Cover (%)	# of fragments on the landscape	# simulations with 1 or 2 fragments on the landscape	# simulations in which one fragment is not used
10	1	6	0
	2	24	20
20	1	10	0
	2	20	17
30	1	15	0
	2	15	11
40	1	18	0
	2	12	5
50	1	23	0
	2	7	7
60	1	25	0
	2	5	2
70	1	29	0
	2	1	0
80	1	30	0
	2	0	0
90	1	30	0
	2	0	0
100	1	30	0

At or above 70% forest cover, peccaries used almost all forested cells present in the landscape (Figure 10A). This was because at 70% forest cover, ~97% of simulations yielded only one fragment (Table 12, Figure 10B). In the sole simulation where there were two fragments in the landscape (at 70% forest cover), the fragments were only 372 meters apart (Table 13, Figure 10C). Therefore, habitat use patterns mimicked those seen in the one-fragment scenario (i.e. where the forested habitat was fully connected).

Between 60% and 40% of forest cover, an increased number of simulations resulted in scenarios where a greater number of forested cells were not used at all (Figure 10A). This was a consequence of an increased number of simulations generating a landscape with two fragments (Table 12, Figure 10B), where the average distance between them was greater than 600 meters (Figure 10C). As a result, an increased number of simulations resulted in a scenario where one of the two forested fragments were not visited at all (Table 12, Figure 10D). At 60% forest cover, 17% of simulations resulted in a landscape scenario with two fragments. Of those, 40% resulted in peccaries not using one of the fragments. At 50% forest cover, 23% of simulations resulted in a fragmentation scenario with two fragments on the landscape and in all of those scenarios,

peccaries only used one of the two fragments on the landscape. Finally, at 40% forest cover, 40% of the simulations resulted in a fragmentation scenario with two fragments. Of those two-fragment simulations, 42% resulted in landscapes where peccaries used only one fragment.

At 30% forest cover and below, there was a qualitative change in forest habitat use patterns, as there was a wide variation in the number of forested cells that were not used per simulation (Figure 10A). At 30% forest cover, 50% of the simulations resulted in two forest fragments (Table 12, Figure 10B) and the average distance between the two fragments was 1,370 m (Table 13, Figure 10C); therefore, 73% of the simulations with two fragments resulted in peccaries unable to use one of the fragments (Table 12, Figure 10D). At 10% forest cover, 80% of the simulations resulted in two fragments on the landscape (Table 12, Figure 10B) and the average distance between them was 1,842 m (Table 13, Figure 10C). Of those, 83% resulted in peccaries only using one of the forested fragments (Table 12, Figure 10D).

Results from the two-fragment scenario show that below 40% forest cover, the majority of the simulations resulted in a landscape where forest fragments were very isolated from each other, resulting in highly uneven use of the remaining forest.

Table 13: Summary statistics for distances between the fragments (distances between fragments equal to zero were removed). Distances are shown in meters.

		Forest Cover (%)									
Fragmentation Scenario	**Statistic**	**10**	**20**	**30**	**40**	**50**	**60**	**70**	**80**	**90**	**100**
2	mean	1842	1824	1369	1044	709	668	372	*NA*	*NA*	*NA*
	median	1751	2134	1392	804	709	759	372	*NA*	*NA*	*NA*
	min	628	383	343	270	457	429	372	*NA*	*NA*	*NA*
	max	3413	3224	2567	1964	1139	832	372	*NA*	*NA*	*NA*
	n	24	20	15	12	6	5	1	0	0	0
3	mean	1759	1630	1285	1164	1007	708	432	388	*NA*	*NA*
	median	1784	1629	1220	1295	1103	732	432	388	*NA*	*NA*
	min	186	260	397	474	201	405	295	388	*NA*	*NA*
	max	3332	2732	2532	1809	1581	1027	569	388	*NA*	*NA*
	n	28	21	23	21	14	8	2	1	0	0
4	mean	1752	1526	1381	1115	902	751	390	208	*NA*	*NA*
	median	1736	1678	1311	1091	822	719	408	229	*NA*	*NA*
	min	473	367	351	131	350	477	96	42	*NA*	*NA*
	max	2921	2430	2911	2249	1490	1034	665	332	*NA*	*NA*
	n	30	27	26	24	17	11	3	4	0	0

4.3.2 Three-fragment scenario

Like the two-fragment scenario, in the fragmentation scenario where the number of fragments was specified as 3, forest use was a function of forest cover (Figure 11A) and was

driven by the number of individual fragments on the landscape (Table 14, Figure 11B) as well as the distance between them (Table 13, Figure 11C). As a result, the number of simulations in which at least one fragment was not used increased as percent of forest cover decreased (Table 14, Figure 11D).

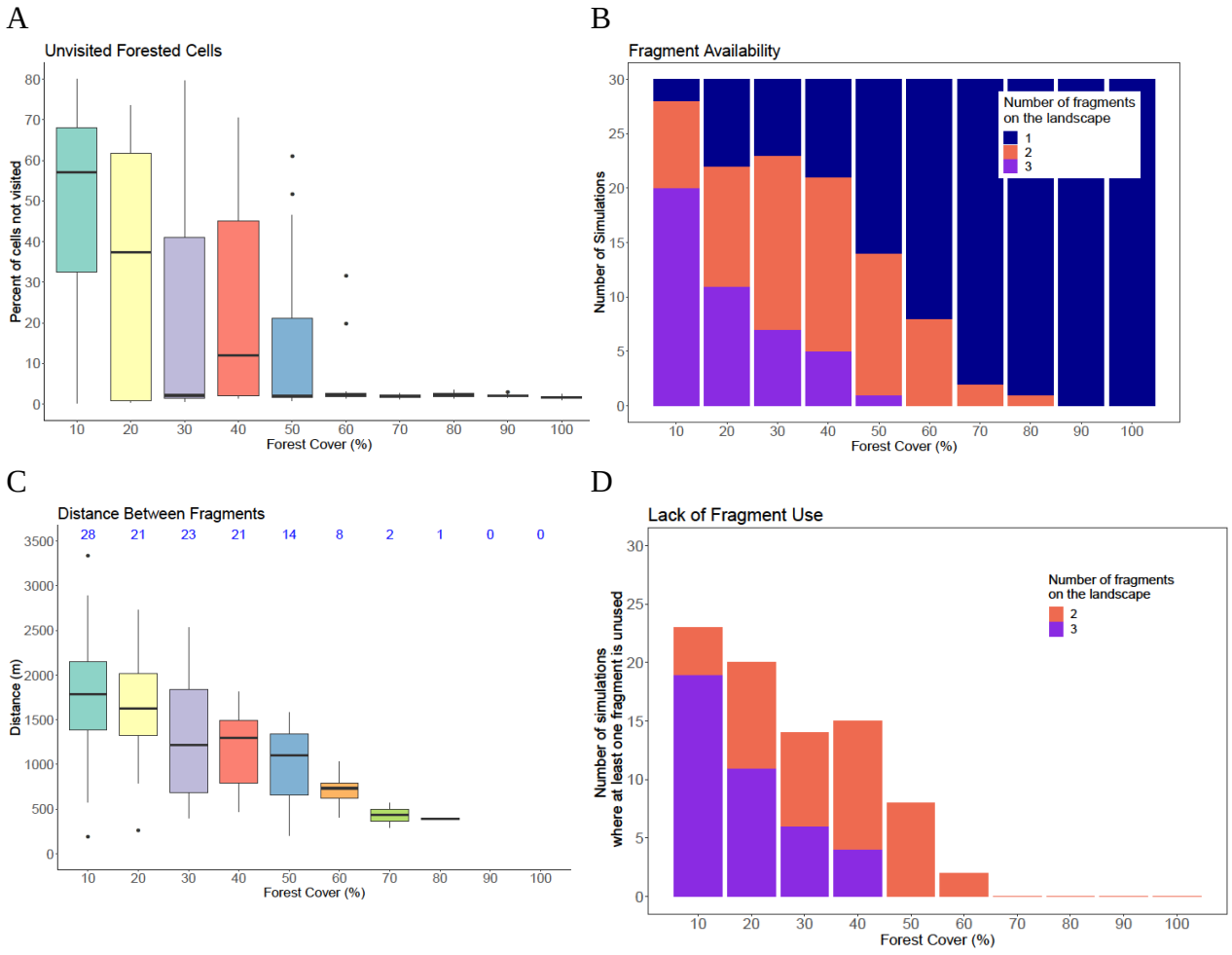

Figure 11: Results 3-fragment scenario: A) The percent of forested cells in the landscape that were never visited by peccaries for each habitat loss scenario (i.e. percent of forest cover); B) For each habitat loss scenario, the number of simulations resulting in 1, 2, or 3 forest fragments on the landscape; C) Average distance between fragments for the two shortest distances in each habitat loss scenario. Blue numbers indicate the sample size (n); D) For scenarios where there were two or three forest fragments on the landscape, bar plot depicting the number of simulations in which at least one forested fragment was not visited by peccaries. For figures A and C, the single line within each box represents the median value, while the upper and lower boundaries of the box represent the first and third quartiles, respectively. Lines extending perpendicularly from the outer boundaries of the box encompass data falling outside of the first and third quartiles, with the end points of these lines not exceeding 1.5 * inner quartile range (distance between lower and upper quartile). Isolated black dots are outliers.

Table 14: Three-fragment scenario: the amount of forest cover, the number of simulations that resulted in 1, 2 or 3 fragments on the landscape, and the number of simulations in which at least one of the fragments was not used by the peccaries.

Forest Cover (%)	# of fragments on the landscape	# simulations 1, 2 or 3 fragments on the landscape	# simulations where at least one fragment is not used
10	1	2	0
	2	8	4
	3	20	19
20	1	8	0
	2	11	9
	3	11	11
30	1	7	0
	2	16	8
	3	7	6
40	1	9	0
	2	16	11
	3	5	4
50	1	16	0
	2	13	8
	3	1	0
60	1	22	0
	2	8	2
	3	0	0
70	1	28	0
	2	2	0
	3	0	0
80	1	29	0
	2	1	0
	3	0	0
90	1	30	0
	2	0	0
	3	0	0
100	1	30	0

In simulations where forest cover was at or above 70%, peccaries used almost all forested cells in the landscape (Figure 11A). Above this forest cover threshold, the landscape never resulted in a scenario with three fragments (Table 14, Figure 11B) and when there were two fragments on the landscape, the average distance between them was less than 430 m (Table 13, Figure 11C). Therefore, habitat use patterns mimicked those seen in the one-fragment simulations where the forested habitat was fully connected.

Between 60% and 50% forest cover, more simulations resulted in a greater number of

forested cells that were not visited (Figure 11A). This was because of an increased number of simulations generated a landscape with two fragments (and one simulation with three fragments; Table 14, Figure 11B), where mean distances between them exceeded 708 m (Table 13, Figure 11C). As a result, more simulations resulted in a scenario where at least one fragment was not visited at all (Table 14, Figure 11D). At 60% forest cover, 27% of simulations resulted in two fragments, and no simulations yielded a landscape with three fragments (Table 14, Figure 11B). Only 25% of the two-fragment scenarios yielded a landscape in which peccaries did not use one of the fragments (Table 14, Figure 11D). At 50% forest cover, 43% of simulations resulted in two fragments and 3% resulted in three fragments (Table 14, Figure 11B). In 62% of the two fragment scenarios, peccaries did not use all fragments on the landscape; yet, peccaries used all forested fragments in the single scenario where there were three fragments on the landscape (Table 14, Figure 11D).

At 40% forest cover and below, there was a qualitative change in forest use patterns, as demonstrated by the wide variation in the number of forested cells that were not used per simulation (Figure 11A). At 40% forest cover, 68% of simulations resulted in more than one forested fragment on the landscape (Table 14, Figure 11B), and the average distance between fragments was 1,164 m (Table 13, Figure 11C). Therefore, at least one fragment was not used by peccaries in 71% of the scenarios with more than one forested fragment on the landscape (Table 14, Figure 11D). At 10% forest cover, 93% of simulations resulted in more than one fragment on the landscape (Figure 11A) and the average distance between them was 1,759 m (Table 13, Figure 11C). Of those, 82% resulted in at least one fragment not used by peccaries (Table 14, Figure 11D).

Results from the three-fragment scenario show that below 50% forest cover, most simulations resulted in a landscape where forest fragments were too isolated to support peccaries using all fragments on the landscape.

4.3.3 Four-fragment scenario

In the fragmentation scenario where the number of fragments was set to 4, forest use as a function of forest cover (Figure 12A) was driven by the combination of actual number of fragments generated in the landscape (Table 15, Figure 12B) and the average distance between them (Table 13, Figure 12C). These patterns explained the increased number of simulations in which at least one fragment was not visited as the percent of forest cover decreased (Table 15, Figure 12D).

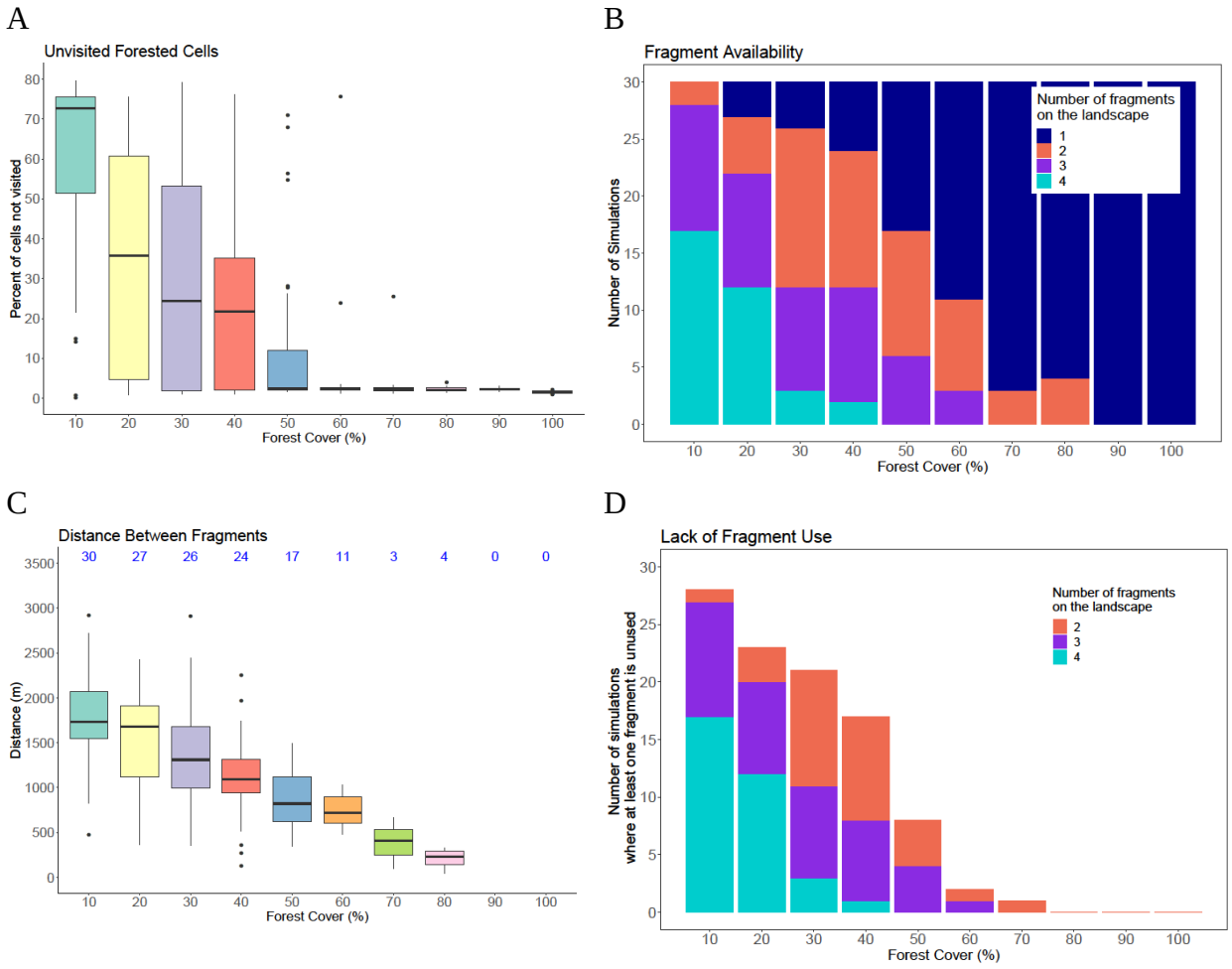

Figure 12: Results 4-fragment scenario: A) The percent of forested cells in the landscape that were never visited by peccaries for each habitat loss scenario (i.e. percent of forest cover); B) For each habitat loss scenario, the number of simulations resulting in 1, 2, 3, or 4 forest fragments on the landscape; C) Average distance between fragments for the three shortest distances in each habitat loss scenario. Blue numbers indicate the sample size (n); D) For scenarios where there were two or more forest fragments on the landscape, bar plot depicting the number of simulations in which at least one forested fragment was not visited by peccaries. For figures A and C, the single line within each box represents the median value, while the upper and lower boundaries of the box represent the first and third quartiles, respectively. Lines extending perpendicularly from the outer boundaries of the box encompass data falling outside of the first and third quartiles, with the end points of these lines not exceeding 1.5 * inner quartile range (distance between lower and upper quartile). Isolated black dots are outliers.

Table 15: Four-fragment scenario: the amount of forest cover, the number of simulations that resulted in 1, 2, 3 or 4 fragments on the landscape, and the number of simulations in which at least one of the fragments was not used by the peccaries.

Forest Cover (%)	# of fragments on the landscape	# simulations with 1, 2, 3 or 4 fragments on the landscape	# simulations where at least one fragment is not used
10	1	0	0
	2	2	1
	3	11	10
	4	17	17
20	1	3	0
	2	5	3
	3	10	8
	4	12	12
30	1	4	0
	2	14	10
	3	9	8
	4	3	3
40	1	6	0
	2	12	9
	3	10	7
	4	2	1
50	1	13	0
	2	11	4
	3	6	4
	4	0	0
60	1	19	0
	2	8	1
	3	3	1
	4	0	0
70	1	27	0
	2	3	1
	3	0	0
	4	0	0
80	1	26	0
	2	4	0
	3	0	0
	4	0	0
90	1	30	0
	2	0	0
	3	0	0
	4	0	0
100	1	30	0

At or above 80% forest cover, peccaries used almost all forested cells present in the landscape (Figure 12A). This was because at 80% forest cover 87% of simulations resulted in one fragment (Figure 12B). When there was more than one fragment on the landscape, the

average distance between them was only 207 m (Table 15, Figure 12C). Therefore, at this forest cover threshold, habitat use patterns mimicked those seen in the one-fragment simulations.

Between 70% and 60% forest cover, an increased number of simulations resulted in scenarios where a greater number of forested cells were not used (Figure 12A). This was a consequence of an increased number of simulations generating a landscape with multiple fragments (Table 15, Figure 12B), where the average distance between fragments ranged from 390 m to 751 m (Table 13, Figure 12C). As a result, an increased number of simulations resulted in a scenario where at least one of the forested fragments was not visited (Table 15, Figure 12D). At 70% forest cover, there were no three-fragment scenarios and only 10% of simulations yielded two fragments (Table 15, Figure 12B). In the two-fragment scenario, only 3% of simulations yielded a landscape where peccaries did not use one of the fragments (Table 15, Figure 12D). At 60% forest cover, 10% of simulations yielded three fragments and 27% yielded two fragments (Table 15, Figure 12B). Of those multi-fragment scenarios, only 18% resulted in at least one fragment not used by peccaries (Table 15, Figure 12D).

At 50% forest cover and below, there is a qualitative change in forest habitat use patterns, resulting in a wide variation in the number of forested cells that were not used (Figure 12A). At 50% forest cover, 57% of simulations resulted in more than one fragment on the landscape (Table 15, Figure 12B) and the average distance between them was 902 m (Table 13, Figure 12C). Therefore, 47% of simulations with multiple fragments resulted in peccaries unable to use at least one of the fragments (Table 15, Figure 12D). At 10% forest cover, all simulations resulted in multiple fragment scenarios (Table 15, Figure 12B) and the average distance between them was 1,752 m (Table 13, Figure 12C). Of those, 93% resulted in scenarios where at least one fragment was never used by peccaries (Table 15, Figure 12D).

Results from the four-fragment scenario show that below 60% forest cover, the majority of simulations resulted in a landscape where forest fragments were too isolated to facilitate peccaries using all forest fragments on the landscape.

4.3.4 All fragment scenarios

In all simulations (one-, two-, three-, and four-fragment), peccaries utilized forest fragments more intensely with decreasing forest cover, as exemplified through higher visitation numbers per cell for more cells (Figure 9). Increased fragmentation of the forest fragments made the pattern of forest use more irregular as percent of forest cover decreased, because the average distance between forest fragments increased (Table 12). With an increased number of forest fragments, more forest cover was needed before peccaries could use all fragments of the landscape. However, regardless of fragmentation level, at or above 70% forest cover peccaries used all fragments of the landscape (Table 12, Tables 14-15, Figures 10-12).

4.4 Discussion

Our results confirm that both fragmentation and habitat loss influence habitat use patterns.

Fragmentation exacerbates the patterns driven by forest loss, as an increase in the number of fragments positively correlated to greater extremes in the disproportionate use of suitable habitat. In addition, the distance between fragments increased with decreasing forest cover. Not surprisingly, forest cover thresholds can be lower with lower levels of fragmentation, as there are less matrix barriers and edge effects.

These results somewhat agree with previous studies noting a 60% forest cover threshold needed to maintain functional connectivity of the landscape. However, Pearson et al. (1996) and Gardner et al. (1991) concluded that at 60% forest cover the structural connectivity of the landscape is maintained. Our results did not show structural connectivity in all simulations with 60% forest cover, but we note that at 60% forest cover, in the majority of the simulations (93.3%) habitat use patterns and therefore functional connectivity of a landscape were maintained. Our results support the importance of spatial configuration in a fragmented landscape, similar to what was specified by Andrén (1994), but we specify that spatial configuration is crucial when suitable remaining habitat is less than 60%, not 30% as suggested by Andrén (1994). Our model results did not support a sustainable landscape at only 10% forest cover regardless of the spatial orientation of the forest fragments, unless those fragments were fully connected. Studies concurring with the lower values of the range proposed by Andrén (1996) may be a result of using species richness as a proxy for evaluating a threshold, whereas we incorporated habitat use patterns. Species richness may generate a lower threshold because it is the ultimate consequence of fragmentation and loss (Radford et al. 2005). However, there may be other ecological patterns prior to local extinction that may trigger downward declines of ecosystem function (Radford et al. 2005).

Additional work specifying critical habitat fragmentation and loss values specific to tropical ecosystems have concluded through different methods similar ranges to what we propose here. Assessing biodiversity conservation in tropical landscapes, Decaëns et al. (2018) concluded the landscape needs to retain over 40% forest in addition to 50% unaffected patches. Assessing different patterns of deforestation, De Oliveira Filho & Metzger (2006) determined that tropical forest-dwelling species needed above 60% forest cover, as below that relationships between key forest components (e.g. edge effects) were abruptly altered. Regarding deforestation in Amazonia specifically, habitat loss greater than ~30 to 50% forest cover acts as a critical threshold beyond which alterations to rainfall patterns negatively impact ecosystem function and structure (Lawrence & Vandecar 2015). Yet, others have suggested a minimum of 50% forest cover is essential to maintaining species richness and abundance of forest-specialist seed dispersers (Morante-Filho et al. 2015; Melito et al. 2018).

Given white-lipped peccaries are a wide-ranging tropical species and can cross the matrix, the threshold values proposed in this study may be considered maximum values, as other species with less dispersal ability may need better connectivity (With & Crist 1995). With and Crist (1995) assessed when isolated populations aggregated in response to fragmentation and found thresholds related to dispersal ability, with habitat generalists needing greater than 40% of

the landscape to have natural habitat and generalists with good dispersal needing only 35% of landscape to have suitable habitat.

Ultimately, thresholds are reflective of individual species preferences and perception of the matrix as connected is a determinant of whether a species will use a fragmented landscape (Andrén & Andren 1994; With & Crist 1995; Prugh et al. 2008; Martin 2018). In general, forest dwelling species, such as white-lipped peccaries, may respond more negatively to fragmentation than habitat generalists who can actively use the matrix instead of just cross through it (With & Crist 1995; Pardini et al. 2010). In addition, fragmentation thresholds may also be habitat dependent. For example, Radford et al. (2005) found that woodland-dependent birds in Australia saw rapid declines in species richness after a threshold of only 10% tree cover was reached. On the other hand, Morante-Filho et al. (2015) concluded less than 50% forest cover impaired species richness for tropical birds. As conclusions on thresholds can vary even between the same taxonomic groups (e.g. birds), it is essential to consider species habitat use patterns, as illustrated with our model, when discussing threshold values for suitable habitat.

In order to maintain white-lipped peccary habitat use patterns seen in the control simulation (i.e. 100% forest cover and no fragmentation) in more than 93% of scenarios, forest cover needed to be at or above 60%, as this resulted in landscape configurations in which the distance between fragments were crossable by peccaries. When forest cover exceeded this threshold, there was unbalanced use of the remaining forest, with some fragments being completely devoid of peccary visitation and others seeing an increase in visitation frequency. Fragmentation exacerbated these patterns. However, in some scenarios, peccary habitat use patterns could be maintained with greater forest loss when the remaining landscape contained fewer fragments. Collectively, these results suggest that in fragmented ecosystems with forest loss exceeding 40%, some forested areas on the landscape may receive an overabundance of mammalian top-down impacts while others may be completely devoid of those impacts. These contrasting habitat use patterns (i.e. over use or no use) will alter ecosystem dynamics including seed dispersal, trampling, and habitat modification (e.g. ecosystem engineering).

Agricultural land currently comprises 38% of earth's land surface and is likely to increase in the future, especially in tropical forests where it is projected to be detrimental to biodiversity conservation (Kehoe et al. 2017). Therefore, pathways that maintain tropical forests while informing landscape planning are essential (Lewis et al. 2015). Further, areas with high deforestation rates such as South America, Southeast Asia, and Africa may already be nearing critical fragmentation thresholds (Saravia et al. 2018). Therefore, models, such as this one, that propose solutions for maintaining tropical forests while also accounting for human land use needs are essential.

We have focused our model on evaluating habitat use patterns in varying fragmentation scenarios, where the quality of all forest fragments is equal, such that all forest fragments have the same diversity and frequency of endless resources. In future iterations, this model could be enhanced to distinguish between the quality and quantity of different forested cells to see how

habitat use patterns vary with fragment quality.

In addition, it should be noted that when applying the model results to conservation decisions, it is important to consider scale (Fahrig 1998), such as the minimum amount of forest cover needed to maintain a population. Here, we did not specify a minimum fragment size to sustain populations, rather we investigated how the fragment size would influence habitat use patterns should peccaries be able to survive in a patch that size. Nonetheless, the fragment size in our model should be scaled up to reflect the minimum fragment size necessary for peccary populations to persist (see Jorge et al. 2013, 2019).

4.5 Conclusion

Our model showed that habitat use patterns by a forest-dwelling mobile species can be used to determine fragmentation thresholds beyond which ecosystem structure and function may become impaired. When the amount of forest cover was less than 60%, maintenance of normal habitat use patterns was dependent on the quantity, spatial configuration, and distance between forest fragments. Below 40% forest cover, connectivity of the landscape was highly impaired as most of the matrix was not crossable. This greatly affected patterns of habitat use, irrespective of spatial configuration of forest fragments. Future work will assess whether this relationship is true for less mobile or non-forest dwelling species as well as the repercussions on ecosystem function related to alterations in habitat use patterns.

CHAPTER 5

SYNTHESIS AND OUTLOOK

5.1 Synthesis

Tropical regions have undergone recurrent deforestation since the 1990s. Continuation of this trend will severely impair tropical forest ecosystem services, the consequences of which could be dire for human well-being. Therefore, it is urgent to establish guidelines and approaches that conserve the natural landscape while also accounting for human land use needs. The research outlined in this dissertation contributed to this effort by describing an approach for evaluating tropical forest conservation using animal interactions and habitat use patterns as conservation proxies. In this work, I described ecological interactions associated with large mammal movement and diet and evaluated how conserving these interactions could provide information on how to balance land use for both human and wildlife needs.

In chapters two and three, I focused on interactions involving large mammal diet. In chapter two, I took a deep time approach and evaluated how extinct peccaries altered diet with climate change. A comparison between extinct peccary dietary plasticity and modern white-lipped peccary dietary plasticity indicated extinct peccaries may have shifted diet during times of colder and or drier climate, while modern peccaries did not show the same dietary flexibility. However, the time over which extinct peccaries altered diet (e.g. on a scale of thousands of years) was vastly more expansive than the brief snapshot in time for which modern peccary diet was analyzed. Therefore, although extinct peccaries may have had the ability to alter diet, it cannot be assumed that modern peccaries will do the same in response to current anthropogenic climate change. Chapter three discussed modern peccary dietary plasticity as related to climate and land use change in central Brazil. Based on stable isotope analysis of white-lipped peccary hair, I concluded that white-lipped peccaries were largely restricted to consuming food in natural forested environments, even though some individuals may have consumed small portions of crops during times of food stress.

Where chapters two and three focused on animal interactions as related to animal diet, chapter four looked at interactions related to animal movement. Using movement data from GPS-collared white-lipped peccaries and the conclusions from chapters two and three noting that peccaries are restricted to the forest for food, I created an agent-based model to evaluate how habitat loss and fragmentation alter white-lipped peccary habitat use patterns. With decreasing forest availability and increasing fragmentation, peccaries used suitable habitat areas more intensely, meaning these areas were subjected to an overabundance of peccary interactions (e.g. trampling, seed predation), while other areas of suitable habitat were completely devoid of peccary interactions. However, when forest loss was less than 40%, functional connectivity (as measured through habitat use patterns) was maintained in more than 93% of simulations. As

disparities in peccary habitat use patterns and associated landscape interactions may alter forest structure, the size and spatial orientation of forest fragments are key to maintaining habitat use patterns when forest loss exceeds 40%.

5.2 Outlook

My work to date has focused on the ways in which mammals respond to changing conditions. Building on this work, I have recently begun field experiments to understand how fragmentation and seasonality exacerbate these responses. Through international collaborations with colleagues at the Universidade Federal do Mato Grosso do Sul and the Projecto Queixada grass roots environmental group in Brazil, we have recently constructed exclosure (fenced) plots in ecosystems with varying levels of fragmentation. These plots exclude large mammals and provide an opportunity to investigate the impacts of land use change on plant-animal interactions by assessing the cascading effects on plant and invertebrate biodiversity, forest regeneration, and soil nitrogen cycling resulting from the absence or over-presence of large mammals. I hope to incorporate the results of this study in a future iteration of the agent-based model simulation described in chapter 4 to better understand the ecological repercussions of habitat use pattern alterations.

I also plan to begin research at the intersection of wildlife conservation and human well-being. I am working with colleagues at Utah State University and the University of Colorado to understand how human land use decisions impact forest structure and function and how changes in forest factors ultimately impact subsequent land use decisions. At the local scale, we will investigate how species-level biological interactions (*e.g.* predator-prey interactions) determine ecosystem services and how these relationships may be altered because of climate and land use change. At a larger scale we will determine the relationship between quantity and quality of forest on agricultural and cattle ranching ecosystem services to evaluate under what conditions sustainable landscapes exist that benefit both humans and wildlife.

WORKS CITED

Alho C. 2008. Biodiversity of the Pantanal: response to seasonal flooding regime and to environmental degradation. Brazilian Journal of Biology **68**:957–966. Available from http://www.scielo.br/pdf/bjb/v68n4s0/a05v684s.pdf (accessed June 11, 2018).

Allen AM, Singh NJ. 2016. Linking Movement Ecology with Wildlife Management and Conservation. Frontiers in Ecology and Evolution **3**:1–13. Available from http://journal.frontiersin.org/article/10.3389/fevo.2015.00155.

Almeida-neto M, Campassi F, Galetti M, Jordano P, Oliveira-filho A. 2008. Vertebrate dispersal syndromes along the Atlantic forest: Broad-scale patterns and macroecological correlates. Global Ecology and Biogeography **17**:503–513.

Altrichter M, Carrillo E, Sáenz J, Fuller TK. 2001. White-lipped peccary (*Tayassu pecari*, Artiodactyla: Tayassuidae) diet and fruit availability in a Costa Rican rain forest. Revista de Biologia Tropical **49**:1183–1192.

Altrichter M, Taber A, Beck H, Reyna-Hurtado R, Lizarraga L, Keuroghlian A, Sanderson EW. 2012. Range-wide declines of a key Neotropical ecosystem architect, the near threatened white-lipped peccary (*Tayassu pecari*). Oryx **46**:87–98.

Amarger N, Mariotti A, Mariotti F, Durr JC, Bourguignon C, Lagacherie B. 1979. Estimate of symbiotically fixed nitrogen in field grown soybeans using variations in 15N natural abundance. Plant and Soil **52**:269–280.

Ambrose S, Norr L. 1993. Carbon isotopic evidence for routing of dietary protein to bone collagen, and whole diet to bone apatite carbonate: purified diet growth experiments. Pages 1–37 Molecular archaeology of prehistoric human bone. Springer Berlin Heidelberg, New York.

Ambrose SH. 1991. Effects of diet, climate and physiology on nitrogen isotope abundances in terrestrial foodwebs. Journal of Archaeological Science **18**:293–317.

Anderson-Teixeira KJ, Snyder PK, Twine TE, Cuadra S V., Costa MH, Delucia EH. 2012. Climate-regulation services of natural and agricultural ecoregions of the Americas. Nature Climate Change **2**:177–181. Nature Publishing Group. Available from http://dx.doi.org/10.1038/nclimate1346.

Andrén H, Andren H. 1994. Effects of Habitat Fragmentation on Birds and Mammals in Landscapes with Different Proportions of Suitable Habitat: A Review. Oikos **71**:355. Available from http://www.jstor.org/stable/3545823?origin=crossref.

Arantes AE, Ferreira LG, Coe MT. 2016. The seasonal carbon and water balances of the Cerrado environment of Brazil: Past, present, and future influences of land cover and land use. ISPRS Journal of Photogrammetry and Remote Sensing **117**:66–78. Available from https://ac-els-cdn-com.proxy.library.vanderbilt.edu/S0924271616000514/1-s2.0-S0924271616000514-main.pdf?_tid=291a812d-fd36-4acb-b9b6-af04f5ccb0ed&acdnat=1528685097_32ca5e18b09db2e48b5a2c576da1d763 (accessed June 10, 2018).

Ayliffe LK, Cerling TE, Robinson T, West AG, Sponheimer M, Passey BH, Hammer J, Roeder B, Dearing MD, Ehleringer JR. 2004. Turnover of carbon isotopes in tail hair and breath CO_2 of horses fed an isotopically varied diet. Oecologia **139**:11–22.

Baccini A, Walker W, Carvalho L, Farina M, Sulla-Menashe D, Houghton RA. 2017. Tropical forests are a net carbon source based on aboveground measurements of gain and loss. Science **358**:230–234.

Baguette M, Stevens VM, Clobert J. 2014. The pros and cons of applying the movement ecology paradigm for studying animal dispersal. Movement Ecology **2**:1–13.

Barreto G, Hernandez O, Ojasti J. 1996. Diet of peccaries (Tayassu tajacu and T. pecari) in a dry forest of Venezuela. Journal of the Zoological Society of London **241**:279–284.

Bateman A, Kelly S. 2007. Fertilizer nitrogen isotope signatures. Isotopes in Environmental and Health Studies **43**:237–247.

Beck H. 2005. Seed predation and dispersal by peccaries throughout the Neotropics and its consequences: a review and synthesis. Pages 77–115 Seed Fate: predation, dispersal and seedling establishment. CABI Publishing, Wallingford, UK.
Beck H. 2006. A review of peccary–palm interactions and their ecological ramifications across the Neotropics. Journal of Mammalogy **87**:519–530.
Beck H, Thebpanya P, Filiaggi M. 2010. Do Neotropical peccary species (Tayassuidae) function as ecosystem engineers for anurans? Journal of Tropical Ecology **26**:407–414.
Bello C, Galetti M, Pizo M, Magnago LFS, Rocha M, Lima R, Peres C, Ovaskainen O, Jordano P. 2015. Defaunation affects carbon storage in tropical forests. Science Advances **1**:1–11. Available from http://advances.sciencemag.org/content/1/11/e1501105.abstract.
Ben-David M, Flaherty EA. 2012. Stable isotopes in mammalian research: a beginner's guide. Journal of Mammalogy **93**:312–328.
Bender M. 1971. Variations in the 13C/12C ratios of plants in relation to the pathway of photosynthetic carbon dioxide fixation. Phytochemistry **10**:1239–1244.
Bender MM. 1968. Mass spectrometric studies of carbon 13 variations in corn and other grasses. Radiocarbon **10**:468–472.
Böckle B, Galunsky B, Muller R. 1995. Characterization of a keratinolytic serine proteinase from *Streptomyces pactum* DSM 40530. Applied and Environmental Microbiology **61**:3705–3710.
Bodmer RE. 1989. Strategies of Seed Dispersal and Seed Predation in Amazonian Ungulates. Biotropica **23**:255–261. Association for Tropical Biology and Conservation. Available from https://www.jstor.org/stable/2388202?origin=crossref (accessed June 27, 2018).
Bodmer RE. 1990. Ungulate frugivores and the browser-grazer continuum. Oikos **57**:319–325.
Bonan G. 2008. Forests and climate change: Forcings, feedbacks, and the climate benefits of forests. Science **320**:1444–1449.
Bradham JL, DeSantis LRG, Jorge MLSP, Keuroghlian A. 2018. Dietary variability of extinct tayassuids and modern white-lipped peccaries (*Tayassu pecari*) as inferred from dental microwear and stable isotope analysis. Palaeogeography, Palaeoclimatology, Palaeoecology **499**:93–101. Elsevier. Available from https://doi.org/10.1016/j.palaeo.2018.03.020.
Bueno RS, Guevara R, Ribeiro MC, Culot L, Bufalo FS, Galetti M. 2013. Functional Redundancy and Complementarities of Seed Dispersal by the Last Neotropical Megafrugivores. PLoS ONE **8**.
Cabin RJ, Mitchell RJ. 2000. To Bonferonni or not to Bonferonni: When and how are the questions. Bulletin of the Ecoloical Society of America:246–248.
Câmara I. 2003. Brief history of conservation in the Atlantic Forest. Pages 31–42 in C. Galindo- Leal and I. Câmara, editors. The Atlantic Forest of South America: Biodiversity Status, Threats, and Outlook. CABS and Island Press, Washington.
Campbell K, Portero D, Romero-Pittman L, Hertel F, Rivera N. 2010. Amazonian magnetostratigraphy: dating the first pulse of the Great American Faunal Interchange. Journal of South American Earth Sciences **29**:619–626.
Canham CD, Denslow JS, Platt WJ, Runkle JR, Spies T a., White PS. 1990. Light regimes beneath closed canopies and tree-fall gaps in temperate and tropical forests. Canadian Journal of Forest Research **20**:620–631.
Castro L, Moreira A, Assad E. 1994. Definition and regionalization of pulviometric patterns in the Brazilian Cerrado. Pages 13–23 in E. Assad, editor. Chuva nos Cerrados: Análise e espacializção. Brasília: Embrapa Cerrados.
Cerling TE, Harris JM. 1999. Carbon isotope fractionation between diet and bioapatite in ungulate mammals and implications for ecological and paleoecological studies. Oecologia **120**:347–363.
Cerling TE, Harris JM, Macfadden BJ, Leakey MG, Quadek J, Eisenmann V, Ehleringer JR. 1997. Global vegetation change through the Miocene / Pliocene boundary. Nature **389**:153–158.
Cerling TE, Hart J a., Hart TB. 2004a. Stable isotope ecology in the Ituri Forest. Oecologia **138**:5–12.

Cerling TE, Passey BH, Ayliffe LK, Cook CS, Ehleringer JR, Harris JM, Dhidha MB, Kasiki SM. 2004b. Orphans' tales: Seasonal dietary changes in elephants from Tsavo National Park, Kenya. Palaeogeography, Palaeoclimatology, Palaeoecology **206**:367–376.

Cerling TE, Wittemyer G, Ehleringer JR, Remien CH, Douglas-Hamilton I. 2009. History of Animals using Isotope Records (HAIR): a 6-year dietary history of one family of African elephants. Proceedings of the National Academy of Sciences of the United States of America **106**:8093–8100.

Chen K, Baxter T, Muir WM, Groenen MA, Schook LB. 2007. Genetic resources, genome mapping and evolutionary genomics of the pig (*Sus scrofa*). International Journal of Biological Sciences **3**:153–165.

Choi WJ, Kwak JH, Lim SS, Park HJ, Chang SX, Lee SM, Arshad MA, Yun SI, Kim HY. 2017. Synthetic fertilizer and livestock manure differently affect $\delta^{15}N$ in the agricultural landscape: A review. Agriculture, Ecosystems and Environment **237**:1–15. Elsevier B.V. Available from http://dx.doi.org/10.1016/j.agee.2016.12.020.

Clark DA. 2007. Detecting tropical forests' responses to global climatic and atmospheric change: Current challenges and a way forward. Biotropica **39**:4–19.

Coplen TB. 1994. Reporting of stable hydrogen, carbon, and oxygen isotopic abundances. Pure and Applied Chemistry **66**:273–276.

Craine JM et al. 2009. Global patterns of foliar nitrogen isotopes and their relationships with climate, mycorrhizal fungi, foliar nutrient concentrations, and nitrogen availability. New Phytologist **183**:980–992.

Crooks KR, Soule ME. 2010. Crooks and Soule 1999.pdf:563–566.

Cullen L, Bodmer RE, Valladares Pádua C. 2000. Effects of hunting in habitat fragments of the Atlantic forests, Brazil. Biological Conservation **95**:49–56.

D'Amo P. 2001. Paleofaunal, paleodietary and paleoenvironmental study of Cutler Hammock: a cave deposit from the late Pleistocene of Florida. University of Florida.

David T, Joseph F, Brian W, Carla D, Andrew D, Robert H, David S, William HS, Daniel S, and Deborah S. 2001. Forecasting Agriculturally Driven Global Environmental Change. Science **292**:281. Available from http://www.sciencemag.org/cgi/content/abstract/sci;292/5515/281?maxtoshow=&hits=10&RESULTFORMAT=&fulltext=soil+carbon+tropical+wetland&searchid=1&FIRSTINDEX=000021&resourcetype=HWCIT.

De Oliveira Filho FJB, Metzger JP. 2006. Thresholds in landscape structure for three common deforestation patterns in the Brazilian Amazon. Landscape Ecology **21**:1061–1073.

Deere NJ, Guillera-Arroita G, Baking EL, Bernard H, Pfeifer M, Reynolds G, Wearn OR, Davies ZG, Struebig MJ. 2018. High Carbon Stock forests provide co-benefits for tropical biodiversity. Journal of Applied Ecology **55**:997–1008.

Deniro MJ, Schoeniger MJ. 1983. Stable carbon and nitrogen isotope ratios of bone collagen: Variations within individuals, between sexes, and within populations raised on monotonous diets. Journal of Archaeological Science **10**:199–203.

DeSantis L, Field J, Wroe S, Dodson J. 2017a. Dietary response of Sahul (Pleistocene Australia-New Guinea) megafauna to climate and environmental change. Paleobiology **43**:181–195.

DeSantis L, Patterson B. 2017. Dietary behaviour of man-eating lions as revelaed by dental microwear textures. Scientific Reports **7.1**:904.

DeSantis L, Schubert B, Schmitt-Linville E, Ungar P, Donohue S, Haupt R. 2015. Dental microwear textures of carnivorans from the La Brea Tar Pits, California and potential extinction implications. Contributions to Science, Los Angeles County Museum of Natural History **42**:37–52.

DeSantis L, Tseng Z, Liu J, Hurst A, Schubert B, Jiangzuo Q. 2017b. Asessing niche conservatism using a multiproxy approach: dietary ecology of extinct and extant spotted hyenas. Paleobiology **43**:286–303.

Desantis LG, Scott JR, Schubert BW, Donohue SL, McCray B, Van Stolk C, Winburn A, Greschko M, O'Hara M. 2013. Direct comparisons of 2D and 3D dental microwear proxies in extant herbivores and carnivorous mammals. PLoS ONE **8**:e71428.

DeSantis LRG. 2016. Dental microwear textures: reconstructing diets of fossil mammals. Surface Topography: Metrology and Properties **4**. IOP Publishing. Available from http://stacks.iop.org/2051-672X/4/i=2/a=023002?key=crossref.44a0dbe573fdfff601c279ca8e7700e0.

DeSantis LRG, Feranec RS, MacFadden BJ. 2009. Effects of global warming on ancient mammalian communities and their environments. PLoS ONE **4**:2–8.

DeSantis LRG, Haupt RJ. 2014. Cougars' key to survival through the Late Pleistocene extinction : insights from dental microwear texture analysis. Biology letters **10**.

DeSantis LRG, Schubert BW, Scott JR, Ungar PS. 2012. Implications of Diet for the Extinction of Saber-Toothed Cats and American Lions. PLoS ONE **7**.

DeSantis LRG, Wallace SC. 2008. Neogene forests from the Appalachians of Tennessee, USA: Geochemical evidence from fossil mammal teeth. Palaeogeography, Palaeoclimatology, Palaeoecology **266**:59–68.

Desbiez ALJ, Santos SA, Keuroghlian A, Bodmer RE. 2009. Niche partitioning among white-lipped peccaries (*Tayassu pecari*), collared peccaries (*Pecari tajacu*), and feral pigs (*Sus Scrofa*). Journal of Mammalogy **90**:119–128.

Doherty TS, Driscoll DA. 2017. Coupling landscape and movement ecology for species conservation in production landscapes. Proceedings of the Royal Society B **285**:20172272.

Dunn O. 1964. Multiple comparisons using rank sums. Technometrics **6**:241–252.

Eaton DP, Keuroghlian A, Santos M do CA. 2017. Citizen scientists help unravel the nature of cattle impacts on native mammals and birds visiting fruiting trees in Brazil's southern Pantanal. Biological Conservation **208**:29–39. Elsevier Ltd. Available from http://dx.doi.org/10.1016/j.biocon.2016.09.010.

Ehleringer J, Bjorkman O. 1977. Quantum Yields for CO_2 Uptake in C_3 and C_4 Plants: Dependence on Temperature, CO_2, and O_2 Concentration. Plant Physiology **59**:86–90. Available from http://www.plantphysiol.org/cgi/doi/10.1104/pp.59.1.86.

Ehleringer J, Sage R, Flanagan L, Pearcy R. 1991. Climate change and the evolution of C_4 photosynthesis. Trends in Ecology and Evolution **6**:95–99.

Estes J a et al. 2011. Trophic downgrading of planet Earth. Science **333**:301–306.

Fahrig L. 1998. When does fragmentation of breeding habitat affect population survival? Ecological Modelling **105**:273–292.

Fahrig L. 2003. Effects of habitat fragmentation on biodiversity. Annual Review of Ecology Evolution and Systematics **34**:487–515. Available from http://arjournals.annualreviews.org/doi/abs/10.1146%2Fannurev.ecolsys.34.011802.132419.

Fahrig L. 2017. Fahrig L. 2017 (in press). **2017**:1–45.

FAO. 2010. Global Forest Resources Assessment 2010.

FAO. 2015a. Global Forest Resources Assessment 2015. Page Forest Ecology and Management. Available from http://www.fao.org/forestry/fra2005/en/.

FAO. 2015b. Global Forest Resources Assessment 2015: How are the world's forests changing? Rome.

Feng H, An L, Chen T, Qiang W, Xu S, Zhang M, Wang X, Cheng G. 2003. The effect of enhanced ultraviolet-B radiation on growth, photosynthesis and stable carbon isotope composition ($\delta^{13}C$) of two soybean cultivars (Glycine max) under field conditions. Environmental and Experimental Botany **49**:1–8. Elsevier. Available from https://www.sciencedirect.com/science/article/pii/S0098847202000436 (accessed June 11, 2018).

Feranec RS. 2005. Growth rate and duration of growth in the adult canine of Smilodon gracilis, and inferences on diet through stable isotope analysis. Bulletin of the Florida Museum of Natural

History **45**:369–377.
Feranec RS, DeSantis LRG. 2014. Understanding specifics in generalist diets of carnivorans by analyzing stable carbon isotope values in Pleistocene mammals of Florida. Paleobiology **40**:477–493. Available from http://www.bioone.org/doi/abs/10.1666/13055.
Feranec RS, MacFadden BJ. 2000. Evolution of the grazing niche in Pleistocene mammals from Florida: Evidence from stable isotopes. Palaeogeography, Palaeoclimatology, Palaeoecology **162**:155–169.
Fernandes D, Keuroghlian A, Eaton DP, Desbiez A. 2013. When there are no fruits for white-lipped peccaries, how about Sushi? Suiform Surroundings **12**:51–54.
Fragoso J. 1998. Home range and movement patterns of white-lipped peccary (*Tayassu pecari*) herds in the northern Brazilian Amazon. Biotropica **30**:458–469. Available from http://onlinelibrary.wiley.com/doi/10.1111/j.1744-7429.1998.tb00080.x/abstract%5Cnhttp://doi.wiley.com/10.1111/j.1744-7429.1998.tb00080.x.
Fragoso M. 1994. Large mammals and the community dynamics of an Amazonian rain forest. University of Florida, Gainesville.
Friedrich A, Antranikian G. 1996. Keratin degradation by Fervidobacterium pennavorans, a novel thermophilic anaerobic species of the order Thermotogales. Applied and Environmental Microbiology **62**:2875–2882.
Galetti M, Bovendorp RS, Guevara R. 2015a. Defaunation of large mammals leads to an increase in seed predation in the Atlantic forests. Global Ecology and Conservation **3**:824–830. Elsevier B.V. Available from www.elsevier.com/locate/gecco (accessed June 10, 2018).
Galetti M, Dirzo R. 2013. Ecological and evolutionary consequences of living in a defaunated world. Biological Conservation **163**:1–6. Elsevier Ltd. Available from http://dx.doi.org/10.1016/j.biocon.2013.04.020.
Galetti M, Guevara R, Neves CL, Rodarte RR, Bovendorp RS, Moreira M, Hopkins Iii JB, Yeakel JD. 2015b. Defaunation affect population and diet of rodents in Neotropical rainforests. Biological Conservation **190**:2–7. Available from https://s3.amazonaws.com/academia.edu.documents/38864752/Biological_Conservation_2015_Galetti.pdf?AWSAccessKeyId=AKIAIWOWYYGZ2Y53UL3A&Expires=1530150833&Signature=y37ChAN341REaPbHeFcjzN5U9gU%3D&response-content-disposition=inline%3B filename%3DDefaunation (accessed June 27, 2018).
Galetti M, Martuscelli P, Olmos F, Aleixo A. 1997. Ecology and conservation of the Jacutinga *Pipile jacutinga* in the Atlantic Forest of Brazil. Biological Conservation **82**:31–39.
Gannes LZ, Martınez del Rio C, Koch P. 1998. Natural abundance variations in stable isotopes and their use in animal physiological ecology. Comparative Biochemistry and Physiology **119**:725–737.
Gardner R, Turner M, O'Neill R, Lavorel S. 1991. Simulation of the scale-dependent effects of landscape boundaries on species persistence and dispersal. Ecotones:76–89.
Gibbs HK, Ruesch AS, Clayton MK, Holmgren P, Foley JA, Ramankutty N, Achard F. 2010. Tropical forests were the primary sources of new agricultural land in the 1980s and 1990s. Proceedings of the National Academy of Sciences **107**:16732–16737.
Gibbs HK, Salmon JM. 2015. Mapping the world's degraded lands. Applied Geography **57**:12–21. Elsevier Ltd. Available from http://dx.doi.org/10.1016/j.apgeog.2014.11.024.
Goetz SJ, Schmitz OJ, Atwood TB, Galetti M, Leroux SJ, Doughty CE, Wilmers CC, Davies AB. 2018. Animals and the zoogeochemistry of the carbon cycle. Science **362**:eaar3213.
Green J, DeSantis L, Smith G. 2017. Regional variation in the browsing diet of Pleistocene Mammut americanum (Mammalie, Proboscidea) as recorded by dental microwear textures. Palaeogeography, Palaeoclimatology, Palaeoecology.
Grimm V, Berger U, DeAngelis DL, Polhill JG, Giske J, Railsback SF. 2010. The ODD protocol: A review and first update. Ecological Modelling **221**:2760–2768. Elsevier B.V. Available from http://dx.doi.org/10.1016/j.ecolmodel.2010.08.019.

Grine F, Ungar P, Teaford M. 2002. Error rates in dental microwear quantification using scanning electron microscopy. Scanning **24**:144–153.
Grine FE. 1986. Dental evidence for dietary differences in Australopithecus and Paranthropus: a quantitative analysis of permanent molar microwear. Journal of Human Evolution **15**:783–822.
Hagen M et al. 2012. Biodiversity, Species Interactions and Ecological Networks in a Fragmented World. Page Advances in Ecological Research, 1st edition. Elsevier Ltd. Available from http://dx.doi.org/10.1016/B978-0-12-396992-7.00002-2.
Hanski I. 1998. Metapolulation dynamics. Nature **396**:41–49.
Haupt R, Desantis LG, Green J, Ungar PS. 2013. Dental microwear texture as a proxy for diet in xenarthrans. Journal of Mammalogy **94**:856–866.
Healy K, Guillerme T, Kelly SBA, Inger R, Bearhop S, Jackson AL. 2017. SIDER: An R package for predicting trophic discrimination factors of consumers based on their ecology and phylogenetic relatedness. Ecography:1–7.
Hedberg C, DeSantis L. 2016. Dental microwear texture analysis of extant koalas: clarifying causal agents of microwear. Journal of Zoology.
Herold M, Clevers JGPW, Beuchle R, Sy V De, Lindquist E, Verchot L, Achard F. 2015. Land use patterns and related carbon losses following deforestation in South America. Environmental Research Letters **10**:124004.
Holá M, Ježek M, Kušta T, Košatová M. 2015. Trophic discrimination factors of stable carbon and nitrogen isotopes in hair of corn fed wild boar. PLoS ONE **10**:1–12.
Hoppe KA, Stover SM, Pascoe JR, Amundson R. 2004. Tooth enamel biomineralization in extant horses: Implications for isotopic microsampling. Palaeogeography, Palaeoclimatology, Palaeoecology **206**:355–365.
Hulbert R. 2001. The Fossil Vertebrates of Florida. University Press of Florida.
Hulbert RC, Morgan GS, Kerner A. 2009. Collared peccary (Mammalia, Artiodactyla, Tayassuidae, Pecari) from the Late Pleistocene of Florida. Papers on Geology, Vertebrate Paleontology, and Biostratigraphy in Honor of Michael O. Woodburne. Museum of Northern Arizona Bulletin 65, Flagstaff, Arizona.:543–556.
IUCN, the IUCN Red List of Threatened Species. 2016.
Jácomo AT de A, Furtado MM, Kashivakura CK, Marinho-Filho J, Sollmann R, Tôrres NM, Silveira L. 2013. White-lipped peccary home-range size in a protected area and farmland in the central Brazilian grasslands. Journal of Mammalogy **94**:137–145. Available from https://academic.oup.com/jmammal/article-lookup/doi/10.1644/11-MAMM-A-411.1.
Janis CM, Damuth J, Theodor JM. 2002. The origins and evolution of the North American grassland biome: The story from the hoofed mammals. Palaeogeography, Palaeoclimatology, Palaeoecology **177**:183–198.
Jansen P. 2003. Scatterhoarding and tree regeneration: ecology of nut dispersal in a neotropical rainforest. Wageningen University, Wageningen, The Netherlands.
Jones DB, DeSantis L. 2016. Dietary ecology of the extinct cave bear: evidence of omnivory as inferred from dental microwear textures. Acta Palaeontologica Polonica **61**:735–741.
Jones DB, DeSantis L. 2017. Dietary ecology of ungulates from the La Brea tar pits in southern California: a multi-proxy approach. Palaeogeography, Palaeoclimatology, Palaeoecology:110–127.
Jorge MLSP, Galetti M, Ribeiro MC, Ferraz KMPMB. 2013. Mammal defaunation as surrogate of trophic cascades in a biodiversity hotspot. Biological Conservation **163**:49–57.
Jorge MLSP, Keuroghlian A, Bradham J, Oshima J, Ribeiro M. 2019. White-lipped peccary movement and range in agricultural lands of Central Brazil. Page in R. Reyna-Hurtado and C. A. Chapman, editors. Movement Ecology of Neotropical Forest Mammals.
Kaiser TM, Schulz E. 2006. Tooth wear gradients in zebras as an environmental proxy - A pilot study. Mitt. hamb. zool. Mus. Inst.:187–211.

Kehoe L, Romero-Muñoz A, Polaina E, Estes L, Kreft H, Kuemmerle T. 2017. Biodiversity at risk under future cropland expansion and intensification. Nature Ecology and Evolution **1**:1129–1135.
Keuroghlian a., Eaton DP. 2008a. Importance of rare habitats and riparian zones in a tropical forest fragment: Preferential use by *Tayassu pecari*, a wide-ranging frugivore. Journal of Zoology **275**:283–293.
Keuroghlian A, Andrade Santos MDC, Eaton DP. 2015. The effects of deforestation on white-lipped peccary (*Tayassu pecari*) home range in the southern Pantanal. Mammalia **79**:491–497.
Keuroghlian A, Desbiez ALJ, Reyna-Hurtado R, Altrichter M, Beck H, Taber A, Fragoso M. 2013. Tayassu pecari. Available from www.iucnredlist.org (accessed June 5, 2017).
Keuroghlian A, Eaton DP. 2008b. Fruit availability and peccary frugivory in an isolated Atlantic forest fragment: Effects on peccary ranging behavior and habitat use. Biotropica **40**:62–70.
Keuroghlian A, Eaton DP. 2009. Removal of palm fruits and ecosystem engineering in palm stands by white-lipped peccaries (*Tayassu pecari*) and other frugivores in an isolated Atlantic Forest fragment. Biodiversity and Conservation **18**:1733–1750.
Keuroghlian A, Eaton DP, Desbiez A. 2009. The response of a landscape species, white-lipped peccaries, to seasonal resource fluctuations in a tropical wetland, the Brazilian Pantanal. International Journal of Biodiversity and Conservation **1**:87–97. Available from http://www.researchgate.net/publication/228854256_The_response_of_a_landscape_species_white-lipped_peccaries_to_seasonal_resource_fluctuations_in_a_tropical_wetland_the_Brazilian_pantanal/file/79e41512fea705d23d.pdf.
Keuroghlian A, Eaton DP, Longland WS. 2004. Area use by white-lipped and collared peccaries (*Tayassu pecari* and *Tayassu tajacu*) in a tropical forest fragment. Biological Conservation **120**:411–425. Available from http://library.bfreebz.org/Mammals/Alexine Keuroghlian%2C et al. Area Use by White-Lipped and Collared Peccaries %28Tayassu pecari and Tayassu tajacu%29 in a Tropical Forest Fragment%2C 2004.pdf (accessed June 27, 2018).
Kiltie R. 1981a. Distribution of palm fruits on a rain forest floor: why white-lipped peccaries forage near objects. Biotropica:141–145.
Kiltie R. 1981b. Stomach contents of rain forest peccaries (*Tayassu tajacu* and *T. pecari*). Biotropica **13**:234–236.
Kiltie R, Terborgh J. 1983. Observations on the behavior of rain forest peccaries in Peru: why do white-lipped peccaries form herds? Zeitschrift für Tierpsychologie **62**:241–255.
Klink C, Joly C. 1989. Identiication and distribution of C3 and C4 grasses in open and shaded habitats in Sao Paulo State Brazil. Biotropica **21**:30–34.
Klink CA, Machado RB. 2005. Conservation of the Brazilian Cerrado **19**:707–713.
Koch PL, Hoppe KA, Webb SD. 1998. The isotopic ecology of late Pleistocene mammals in North America Part 1. Florida. Chemical Geology **152**:119–138.
Kohn M. 2010. Carbon isotope compositions of terrestrial C3 plants as indicators of (paleo) ecology and (paleo) climate. Proceedings of the National Academy of Sciences **107**:19691–19695.
LAURANCE WF., LOVEJOY TE., VASCONCELOS HL., BRUNA EM., DIDHAM RK., STOUFFER PC., GASCON C., BIERREGAARD RO., LAURANCE SG., SAMPAIO E. 2002. Ecosystem Decay of Amazonian Forest Fragments: a 22- year investigation. Conservation Biology **16**:606–618.
Lawrence D, Vandecar K. 2015. Effects of tropical deforestation on climate and agriculture. Nature Climate Change **5**:27–36.
Lewis SL, Edwards DP, Galbraith D. 2015. Increasing human dominance of tropical forests. Science **349**:827–832.
Lindenmayer D et al. 2008. A checklist for ecological management of landscapes for conservation. Ecology Letters **11**:78–91.
Lira PK, Tambosi LR, Ewers RM, Metzger JP. 2012. Land-use and land-cover change in Atlantic Forest landscapes. Forest Ecology and Management **278**:80–89. Available from

http://dx.doi.org/10.1016/j.foreco.2012.05.008.
Losos E, Leigh E. 2004. Tropical forest diversity and dynamism. University of Chicago Press.
Loudon JE, Sponheimer M, Sauther M, Cuozzo F. 2007. Intraspecific variation in hair $\delta^{13}C$ and $\delta^{15}N$ values of ring-tailed lemurs (Lemur catta) with known individual histories, behaviors, and feeding ecology. American journal of physical anthropology **133**:978–985.
Lubec G, Nauer G, Seifert K, Strouhal E, Porteder H, Szilvassy J, Teschler M. 1987. Structural stability of hair over three thousand years. Journal of Archaeological Science **14**:113–120.
MacFadden BJ, Cerling TE. 1996. Mammalian herbivore communities, ancient feeding ecology, and carbon isotopes: A 10 million-year sequence from the Neogene of Florida. Journal of Vertebrate Paleontology **16**:103–115.
Machado RB, Barcellos Harris M, Silva SM, Neto MBR. 2011. Human impacts and environmental problems in the Brazilian Pantanal. Pages 719–739 in W. Junk, editor. The Pantanal: Ecology, Biodiversity and Sustainable Management of a Large Neotropical Seasonal Wetland. Sofia: Pensoft, eBook Collection (EBSCOhost), EBSCOhost (accessed June 10, 2018).
Macko SA, Lubec G, Teschler-Nicola M, Andrusevich V, Engel MH. 1999. The Ice Man's diet as reflected by the stable nitrogen and carbon isotopic composition of his hair. The FASEB Journal **13**:559–562. Available from http://www.fasebj.org/content/13/3/559.abstract%5Cnhttp://www.fasebj.org/content/13/3/559.full.pdf%5Cnhttp://www.fasebj.org/content/13/3/559.short.
Madhavan S, Treichel I, O'Leary MH. 1991. Effects of relative humidity on carbon isotope fractionation in plants. Botanica Acta **104**:292–294.
Martin CA. 2018. An early synthesis of the habitat amount hypothesis. Landscape Ecology **33**:1831–1835. Springer Netherlands. Available from https://doi.org/10.1007/s10980-018-0716-y.
Martinelli LA, Ballester MV, Krusche A V., Victoria RL, De Camargo PB, Bernardes M, Ometto JPHB. 1999. Landcover changes and $\delta^{13}C$ composition of riverine particulate organic matter in the Piracicaba River Basin (southeast region of Brazil). Limnology and Oceanography **44**:1826–1833.
Martinelli LA, Camargo PB, Lara LBLS, Victoria RL, Artaxo P. 2002. Stable carbon and nitrogen isotopic composition of bulk aerosol particles in a C4 plant landscape of southeast Brazil. Atmospheric Environment **36**:2427–2432.
Melito M, Metzger JP, de Oliveira AA. 2018. Landscape-level effects on aboveground biomass of tropical forests: A conceptual framework. Global Change Biology **24**:597–607.
Mendes CP, Ribeiro MC, Galetti M. 2016. Patch size, shape and edge distance influence seed predation on a palm species in the Atlantic forest. Ecography **39**:465–475.
Merceron G, Ramdarshan A, Francisco A, Gautier D, Boisserie J, Milhet X, Novello A, Pret D. 2016. Untangling the environmental from the dietary: dust does not matter. Proceedings of the Royal Society B: Biological Sciences **283**:20161032.
Mihlbachler MC, Beatty BL. 2012. Magnification and resolution in dental microwear analysis using light microscopy. Palaeontologia Electronica **15**:1–15.
Morales JM, Moorcroft PR, Matthiopoulos J, Frair JL, Kie JG, Powell RA, Merrill EH, Haydon DT. 2010. Building the bridge between animal movement and population dynamics. Philosophical Transactions of the Royal Society B: Biological Sciences **365**:2289–2301.
Morante-Filho JC, Faria D, Mariano-Neto E, Rhodes J. 2015. Birds in anthropogenic landscapes: The responses of ecological groups to forest loss in the Brazilian Atlantic forest. PLoS ONE **10**:1–18. Available from http://dx.doi.org/10.1371/journal.pone.0128923.
Neves LA, Sarmanho GF, Cunha VS, Daroda RJ, Aranda DAG, Eberlin MN, Fasciotti M. 2015. The carbon isotopic ($^{13}C/\ ^{12}C$) signature of sugarcane bioethanol: certifying the major source of renewable fuel from Brazil. Anal. Methods **7**:4780–4785. Available from http://xlink.rsc.org/?DOI=C5AY00272A.
Olson DM et al. 2001. Terrestrial Ecoregions of the World: A New Map of Life on Earth. BioScience

51:933. Available from http://www.bioone.org.proxy.library.vanderbilt.edu/doi/pdf/10.1641/0006-3568%282001%29051%5B0933%3ATEOTWA%5D2.0.CO%3B2 (accessed June 10, 2018).
Pan Y et al. 2011. A large and persistent carbon sink in the world's forests. Science **333**:988–93. Available from http://www.scopus.com/inward/record.url?eid=2-s2.0-80051879083&partnerID=tZOtx3y1.
Pardini R, de Bueno AA, Gardner TA, Prado PI, Metzger JP. 2010. Beyond the fragmentation threshold hypothesis: Regime shifts in biodiversity across fragmented landscapes. PLoS ONE **5**.
Parente L, Ferreira L. 2018. Assessing the spatial and occupation dynamics of the Brazilian pasturelands based on the automated classification of MODIS images from 2000 to 2016. Remote Sensing **10**:606. Multidisciplinary Digital Publishing Institute. Available from http://www.mdpi.com/2072-4292/10/4/606 (accessed June 10, 2018).
Passey BH, Robinson TF, Ayliffe LK, Cerling TE, Sphonheimer M, Dearing MD, Roeder BL, Ehleringer JR. 2005. Carbon isotope fractionation between diet, breath CO2, and bioapatite in different mammals. Journal of Archaeological Science **32**:1459–1470.
Pearson SM, Turner M, Gardner RH, O'Neill R V. 1996. An organism-based perspective of habitat fragmentation. Biodiversity in managed landscapes: theory and practice. Oxford University Press, New York:77–95.
Perez-Cortez S, Reyna-hurtado R. 2008. La dieta de los pecaries (*Pecari tajacu* y *Tayassu pecari*) en la región de Calakmul, Campeche, México. Revista Mexicana de Mastozoología **12**:17–42.
Prideaux GJ, Ayliffe LK, DeSantis LRG, Schubert BW, Murray PF, Gagan MK, Cerling TE. 2009. Extinction implications of a chenopod browse diet for a giant Pleistocene kangaroo. Proceedings of the National Academy of Sciences of the United States of America **106**:11646–11650.
Prugh L, Hodges K, Sinclair A, Brashares J. 2008. Effect of habitat area and isolation on fragmented animal populations. Proceedings of the National Academy of Sciences **105**:20770–20775.
R Core Team. 2018. R: A Language and Environment for Statistical Computing. Vienna, Austria. Available from www.r-project.org.
Radford JQ, Bennett AF, Cheers GJ. 2005. Landscape-level thresholds of habitat cover for woodland-dependent birds. Biological Conservation **124**:317–337.
Ramankutty N, Evan AT, Monfreda C, Foley JA. 2008. Farming the planet: 1. Geographic distribution of global agricultural lands in the year 2000. Global Biogeochemical Cycles **22**:1–19.
Ramdarshan A, Blondel C, Brunetiere N, Francisco A, Gautier D, Surault J, Merceron G. 2016. Seeds, browse, and tooth wear: a sheep perspective. Ecology and Evolution **6**:5559–5569.
Raven P. 1980. Research priorities in tropical biology. National Academy of Sciences, Washington, D.C.
Reyna-Hurtado R, Beck H, Altrichter M, Chapman CA, Bonnell TR, Keuroghlian A. 2016. What ecological and anthropogenic factors affect group size in white-lipped peccaries (Tayassu pecari)? Biotropica **48**:246–254.
Reyna-Hurtado R, Rojas-Flores E and, Tanner GW. 2009. Home range and habitat preferences of white-lipped peccaries (*Tayassu pecari*) in Calakmul, Campeche, Mexico. Journal of Mammalogy **90**:1199–1209.
Ribeiro MC, Metzger JP, Martensen AC, Ponzoni FJ, Hirota MM. 2009. The Brazilian Atlantic Forest: How much is left, and how is the remaining forest distributed? Implications for conservation. Biological Conservation **142**:1141–1153.
Ripple WJ et al. 2015. Collapse of the world's larges herbivores. Scientific Advances **1**:e1400103.
Santana WSC. 2015. Análise-multitemporal da paisagem, potencialidades e fragilidades sob a ótica do uso e ocupação: destaque para as terras da Alta Bacia do Rio Taboco-MS. Universidade Estadual Paulista.
Saravia LA, Doyle SR, Bond-Lamberty B. 2018. Power laws and critical fragmentation in global forests. Scientific Reports **8**:1–12. Springer US. Available from http://dx.doi.org/10.1038/s41598-018-36120-w.

Schmidt CW. 2008. Dental microwear analysis of extinct flat-deaded peccary (Platygonus compressus) from southern Indiana. Proceedings of Indiana Academy of Science **117**:95–106.
Schubert B, Ungar P, DeSantis L. 2010. Carnassial microwear and dietary behavior in large carnivorans. Journal of Zoology **280**:257–263.
Scott RS, Teaford MF, Ungar PS. 2012. Dental microwear texture and anthropoid diets. American Journal of Physical Anthropology **147**:551–579.
Scott RS, Ungar PS, Bergstrom TS, Brown CA, Childs BE, Teaford MF, Walker A. 2006. Dental microwear texture analysis: technical considerations. Journal of Human Evolution **51**:339–349.
Scott RS, Ungar PS, Bergstrom TS, Brown CA, Grine FE, Teaford MF, Walker A. 2005. Dental microwear texture analysis shows within-species diet variability in fossil hominins. Nature **436**:693–695.
Seidl AF, De Silva JDSV, Moraes AS. 2001. Cattle ranching and deforestation in the Brazilian Pantanal. Ecological Economics **36**:413–425.
Semprebon GM, Godfrey LR, Solounias N, Sutherland MR, Jungers WL. 2004. Can low-magnification stereomicroscopy reveal diet? Journal of Human Evolution **47**:115–144.
Sikes RS, Gannon W, Mammalogists the AC and UC of the AS of. 2011. Guidelines of the American Society of Mammalogists for the use of wild mammals in research and education. Journal of Mammalogy **92**:235–253.
Silman MR, Terborgh JW, Kiltie R. 2003. Population regulation of a dominant rain forest tree by a major seed predator. Ecology **84**:431–438.
Silva GC, Moreira MZ, Scofield AL, Godoy JMO, Almeida LF, Wagener ALR. 2015. Mapping ethanol production sources in Brazil through stable isotopes. Journal of the Brazilian Chemical Society **26**:1283–1296.
Silvius KM. 2002. Spatio-temporal patterns of palm endocarp use by three Amazonian forest mammals: granivory or 'grubivory'? Journal of Tropical Ecology **18**:707–723.
Soepadmo E. 1993. Tropical rain forests as carbon sinks. Chemosphere **27**:1025–1039.
Solounias N, Semprebon G. 2002. Advances in the Reconstruction of Ungulate Ecomorphology with Application to Early Fossil Equids. American Museum Novitates **3366**:1–49.
Sowls L. 1984. The Peccaries. University of Arizona Press, Tucson.
Sponheimer M, Robinson T, Ayliffe L, Passey B, Roeder B, Shipley L, Lopez E, Cerling T, Dearing D, Ehleringer J. 2003a. An experimental study of carbon-isotope fractionation between diet, hair, and feces of mammalian herbivores. Canadian Journal of Zoology **81**:871–876.
Sponheimer M, Robinson T, Ayliffe L, Roeder B, Hammer J, Passey B, West A, Cerling T, Dearing D, Ehleringer J. 2003b. Nitrogen isotopes in mammalian herbivores: Hair $\delta^{15}N$ values from a controlled feeding study. International Journal of Osteoarchaeology **13**:80–87.
Still CJ, Berry JA, Collatz GJ, DeFries RS. 2003. Global distribution of C_3 and C_4 vegetation: Carbon cycle implications. Global Biogeochemical Cycles **17**:6-1-6–14. Available from http://doi.wiley.com/10.1029/2001GB001807.
Storfer A, Murphy MA, Spear SF, Holderegger R, Waits LP. 2010. Landscape genetics: Where are we now? Molecular Ecology **19**:3496–3514.
Stowe T, Teeri J. 1978. Geographic distribution of C4 species of the Dicotyledonae in relation to climate. American Naturalist **112**:609–623.
Talora DC, Faria D, Cazetta E, Rocha-Santos L, Mariano-Neto E, Pessoa MS, Hambuckers A. 2016. Fruit biomass availability along a forest cover gradient. Biotropica **49**:45–55.
Teeri JA, Stowe LG. 1976. Climactic patterns and the distribution of C4 grasses in North America. Oecologia **23**:1–12.
Terborgh J. 1986. Keystone plant resources in the tropical forest. Pages 330–344 in M. E. Soule, editor. Conservation biology, the science of scarcity and diversity. Sinauer Associates, Inc., Sunderland,Massachusetts.

Terborgh J. 1992. Maintenance of diversity in tropical forests. Biotropica **24**:283. Association for Tropical Biology and Conservation. Available from https://www.jstor.org/stable/2388523?origin=crossref (accessed June 27, 2018).
Tieszen LL, Boutton TW, Tesdahl KG, Slade NA. 1983. Fractionation and turnover of stable carbon isotopes in animal tissues: Implications for $\delta^{13}C$ analysis of diet. Oecologia **57**:32–37.
Tieszen LL, Fagre T. 1993. Carbon isotopic variability in modern and archaeological maize. Journal of Archaeological Science **20**:25–40.
Tilman D, Clark M, Williams D, Kimmel K, Polasky S, Packer, C. 2017. Future threats to biodiversity and pathways to their prevention. Nature - in review.
Tracey JA, Boydston E, Lyren L, Crooks KR. 2013. Mapping behavioral landscapes for animal movement: a finite mixture modeling approach. Ecological Applications **23**:654–669.
Trayler RB, Dundas RG, Fox-Dobbs K, Van De Water PK. 2015. Inland California during the Pleistocene-Megafaunal stable isotope records reveal new paleoecological and paleoenvironmental insights. Palaeogeography, Palaeoclimatology, Palaeoecology **437**:132–140. Elsevier B.V. Available from http://dx.doi.org/10.1016/j.palaeo.2015.07.034.
Ungar PS, Brown C a., Bergstrom TS, Walker SA. 2003. Quantification of dental microwear by tandemscanning confocalmicroscopy and scale-sensitive fractal analyses. Scanning **25**:185–193.
van der Merwe NJ, Medina E. 1989. Photosynthesis and ratios in Amazonian rain forests. Geochimica et Cosmochimica Acta **53**:1091–1094.
van der Merwe NJ, Medina E. 1991. The canopy effect, carbon isotope ratios and foodwebs in Amazonia. Journal of Archaeological Science **18**:249–259.
van Toor ML, Kranstauber B, Newman SH, Prosser DJ, Takekawa JY, Technitis G, Weibel R, Wikelski M, Safi K. 2018. Integrating animal movement with habitat suitability for estimating dynamic migratory connectivity. Landscape Ecology **33**:879–893.
Vanbianchi C, Gaines WL, Murphy MA, Hodges KE. 2018. Navigating fragmented landscapes: Canada lynx brave poor quality habitats while traveling. Ecology and Evolution **8**:11293–11308.
Vira B, Wildburger C, Mansourian S. 2015. Forests, trees and landscapes for food security and nutrition: A global assessment report. IUFRO World Series Volume 33.
Walker A, Hoeck H, Perez L. 1978. Microwear of Mammalian Teeth as an Indicator of Diet. Science **201**:908–910.
Weckel M, Giuliano W, Silver S. 2006. Jaguar (Panthera onca) feeding ecology: Distribution of predator and prey through time and space. Journal of Zoology **270**:25–30.
Wetzel RM, Dubos RE, Martin RL, Myers P, Ward WR. 1975. *Catagonus*, an "extinct" peccary, alive in Paraguay. Science **189**:379–381.
With K, Crist T. 1995. Critical thresholds in species' responses to landscape structure. Ecology **76**:2446–2459.
Wright D. 1989. Phylogenetic relationships of Catagonus wagneri: sister taxa from the tertiary of North America. Pages 281–308 in K. Redford, editor. Advances in Neotropical Mammalogy. Sandhill Crane Press, Gainesville.
Wright D. 1998. Tayassuidae. Pages 389–401 in C. M. Janis, K. Scott, and L. Jacobs, editors. Evolution of Tertiary Mammals of North America Volume 1: Terrestrial Carnivores, Ungulates, and Ungulatelike Mammals. Cambridge University Press, Cambridge.
Wyatt JL, Silman MR. 2004. Distance-dependence in two Amazonian palms: Effects of spatial and temporal variation in seed predator communities. Oecologia **140**:26–35.
Yann L, DeSantis L, Koch PL, Lundelius E. 2016. Dietary ecology of Pleistocene camelids: Influences of climate, environment, and sympatric taxa. Palaeogeography, Palaeoclimatology, Palaeoecology **461**:400.
Yann LT, DeSantis LRG. 2014. Effects of Pleistocene climates on local environments and dietary behavior of mammals in Florida. Palaeogeography, Palaeoclimatology, Palaeoecology **414**:370–381.

Available from http://linkinghub.elsevier.com/retrieve/pii/S0031018214004751.
Yann LT, DeSantis LRG, Haupt RJ, Romer JL, Corapi SE, Ettenson DJ. 2013. The application of an oxygen isotope aridity index to terrestrial paleoenvironmental reconstructions in Pleistocene North America. Paleobiology **39**:576–590. Available from http://www.bioone.org/doi/abs/10.1666/12059.
Yin D, Leroux SJ, He F. 2017. Methods and models for identifying thresholds of habitat loss. Ecography **40**:131–143.
Yu H-B, Gao Q-F, Dong S-L, Wen B, Hou Y-R, Ning L-G. 2014. Utilization of corn meal and extruded soybean meal by sea cucumber *Apostichopus japonicus* (Selenka): Insights from carbon stable isotope analysis. Aquaculture **435**:106–110. Available from http://or.nsfc.gov.cn/bitstream/00001903-5/220153/1/1000008856600.pdf (accessed June 11, 2018).
Zararte LEM et al. 2018. Biodiversity loss along a gradient of deforestation in Amazonian agricultural landscapes. Conservation Biology **32**:1380–1391.

APPENDIX A

Supplementary Tables

Supplemental Table 1: Stable carbon isotope values (V-PDB) of tooth enamel for all taxa studied. Values of extinct taxa have not been adjusted to account for the Suess Effect (-1.5 ‰).

Specimen	Taxa	NALMA	Tooth	$\delta^{13}C$(‰)
UF424	*Protherohyus*	HMP	rm3	-6.2
UF429	*Protherohyus*	HMP	lm3	-11.3
UF430	*Protherohyus*	HMP	lm3	-5.8
UF431	*Protherohyus*	HMP	lm3	-6.7
UF103706	*Protherohyus*	HMP	rm3	-11.3
UF203140	*Protherohyus*	HMP	RM2	-12.1
UF203183	*Protherohyus*	HMP	rp4	-9.8
UF212394	*Protherohyus*	HMP	RM3	-9.4
UF16509	*Mylohyus*	BLC	m3/M3	-12.5
UF21957	*Mylohyus*	BLC	M3	-13.4
UF21958	*Mylohyus*	BLC	m3	-11.4
UF440	*Mylohyus*	HMP	LM3	-7.1
UF481	*Mylohyus*	HMP	lp4	-11.9
UF101982	*Mylohyus*	HMP	lm3	-11.2
UF203540	*Mylohyus*	HMP	LM3	-13.4
UF211795	*Mylohyus*	HMP	rm2	-14.3
UF211796	*Mylohyus*	HMP	rm2	-13.7
UF294749	*Mylohyus*	HMP	rp4	-12.3
UF63902	*Mylohyus*	IRV	RM3	-12.2[a]
UF63903	*Mylohyus*	IRV	lp4	-4.9[a]
UF67068	*Mylohyus*	IRV	RM3	-10.5[a]
UF67184	*Mylohyus*	IRV	RM3	-9.5[a]
UF81312	*Mylohyus*	IRV	P	-10.3[a]
UF84753	*Mylohyus*	IRV	RP3	-10.5[a]
UF84758	*Mylohyus*	IRV	RP4	-10.5[a]
UF87768	*Mylohyus*	IRV	lp3	-7.0[a]
UF87778	*Mylohyus*	IRV	rm3	-5.8[a]
UF209229	*Mylohyus*	IRV	lm1	-9.9[b]
UF3224	*Mylohyus*	RCH	lm3	-7.6[b]
UF3268	*Mylohyus*	RCH	lm3	-11.2[b]
UF3279	*Mylohyus*	RCH	LM3	-11.9[b]
UF8590	*Mylohyus*	RCH	M?	-10.8[c]

UF8593	*Mylohyus*	RCH	M?	-10.9[c]
UF10324	*Mylohyus*	RCH	LM3	-11.1[b]
UF12494	*Mylohyus*	RCH	R2	-9.1[b]
UF17699	*Mylohyus*	RCH	lm3	-9.6
UF24521	*Mylohyus*	RCH	m3	-8.4
UF148675	*Mylohyus*	RCH	M2/3	-10.0[c]
UF148677	*Mylohyus*	RCH	M2	-11.4[c]
UF207307	*Mylohyus*	RCH	NP	-9.8[d]
UF207308	*Mylohyus*	RCH	NP	-9.6[d]
UF207312	*Mylohyus*	RCH	NP	-11.3[d]
UF207313	*Mylohyus*	RCH	NP	-8.4[d]
UF207315	*Mylohyus*	RCH	NP	-10.8[d]
UF207318	*Mylohyus*	RCH	NP	-7.5[d]
UF207320	*Mylohyus*	RCH	NP	-9.0[d]
UF207321	*Mylohyus*	RCH	NP	-11.1[d]
UF207322	*Mylohyus*	RCH	NP	-10.0[d]
UF207327	*Mylohyus*	RCH	NP	-11.4[d]
UF207331	*Mylohyus*	RCH	NP	-12.1[d]
UF207332	*Mylohyus*	RCH	NP	-6.9[d]
UF207336	*Mylohyus*	RCH	NP	-8.0[d]
UF207339	*Mylohyus*	RCH	NP	-4.8[d]
UF207342	*Mylohyus*	RCH	NP	-10.7[d]
UF207344	*Mylohyus*	RCH	NP	-2.3[d]
UF207347	*Mylohyus*	RCH	NP	-7.6[d]
UF207350	*Mylohyus*	RCH	NP	-11.7[d]
UF18188	*Platygonus*	BLC	rm3	-11.5[a]
UF18203	*Platygonus*	BLC	rm3	-10.0[a]
UF45313	*Platygonus*	BLC	rm3	-10.4[a]
UF60027	*Platygonus*	BLC	rm3	-11.6[a]
UF60030	*Platygonus*	BLC	RM3	-13.1[a]
UF176742	*Platygonus*	BLC	LM1	-11.2[a]
UF227644	*Platygonus*	BLC	RM3	-10.9[a]
UF227645	*Platygonus*	BLC	RM3	-11.5[a]
UF12073	*Platygonus*	IRV	left M/m3	-12.6
UF12078	*Platygonus*	IRV	M?	-12.4[e]
UF12086	*Platygonus*	IRV	rm3	-10.5
UF12089	*Platygonus*	IRV	lm3	-10.3
UF12703	*Platygonus*	IRV	lm3	-12.6
UF62705	*Platygonus*	IRV	LM3	-7.9
UF62706	*Platygonus*	IRV	LM3	-9.1
UF63350	*Platygonus*	IRV	RM3	-7.8
UF63922	*Platygonus*	IRV	lm3	-8.0[f]

UF66669	*Platygonus*	IRV	rm3	-9.1
UF66670	*Platygonus*	IRV	rm3	-10.1
UF66686	*Platygonus*	IRV	lm3	-8.7
UF66689	*Platygonus*	IRV	lm3	-3.3
UF80117	*Platygonus*	IRV	lm3	-3.9[f]
UF81238	*Platygonus*	IRV	rm3	-7.4[f]
UF83122	*Platygonus*	IRV	rm3	-5.1[a]
UF83384	*Platygonus*	IRV	RM2	-6.5[a]
UF86760	*Platygonus*	IRV	frag	-12.7[g]
UF86948	*Platygonus*	IRV	LP4	-4.0[a]
UF87791	*Platygonus*	IRV	lm3	-7.7[a]
UF87830	*Platygonus*	IRV	lm3	-9.2[f]
UF87834	*Platygonus*	IRV	RM3	-6.6[f]
UF87850	*Platygonus*	IRV	rm3	-3.5[a]
UF211009	*Platygonus*	IRV	lm3	-7.8[b]
UF214391	*Platygonus*	IRV	lm3	-8.6
UF217659	*Platygonus*	IRV	rm3	-5.6
UF219564	*Platygonus*	IRV	rm3	-7.3
UF221021	*Platygonus*	IRV	RM3	-12.0
UF221282	*Platygonus*	IRV	RM3	-9.5
UF221528	*Platygonus*	IRV	RM3	-12.0
UF235900	*Platygonus*	IRV	lm3	-6.4
UFNC RSF-86	*Platygonus*	IRV	M?	-12.2[e]
UFNC RSF-87	*Platygonus*	IRV	M?	-11.3[e]
UF3098	*Platygonus*	RCH	M3	-11.5[e]
UF12497	*Platygonus*	RCH	rm2	-11.8
UF12498	*Platygonus*	RCH	M3	-12.4[e]
UF55264	*Platygonus*	RCH	m2	-10.8
UF126496	*Platygonus*	RCH	lm2	-13.7
UF126497	*Platygonus*	RCH	LM2	-10.9
UF126498	*Platygonus*	RCH	LM2	-12.6
UF126499	*Platygonus*	RCH	RM3	-13.9
UF131949	*Platygonus*	RCH	rm3	-9.6
UF131950	*Platygonus*	RCH	rm3	-10.7
UF207489	*Platygonus*	RCH	NP	-11.6[d]
UF207490	*Platygonus*	RCH	NP	-11.2[d]
UF212691	*Platygonus*	RCH	rm2	-13.5
UF212692	*Platygonus*	RCH	lm3	-7.9
UFNC (100)	*Platygonus*	RCH	lm3	-8.3[h]
UFNC RSF-40	*Platygonus*	RCH	P	-12.0[e]
UFNC RSF-41	*Platygonus*	RCH	P	-12.6[e]
WCSCRTP1	*Tayassu*	MOD	RM3	-15.0

WCSCRTP2	*Tayassu*	MOD	RM3	-13.4
WCSCRTP3	*Tayassu*	MOD	RM3	-13.9
WCSCRTP4	*Tayassu*	MOD	RM3	-14.5
WCSCRTP5	*Tayassu*	MOD	rm3	-15.5
WCSCRTP6	*Tayassu*	MOD	rm3	-14.2
WCSCRTP7	*Tayassu*	MOD	LM3	-12.7
WCSCRTP8	*Tayassu*	MOD	LM3	-14.3
WCSCRTP9A	*Tayassu*	MOD	rm2	-14.6
WCSCTP1	*Tayassu*	MOD	lm3	-14.7
WCSCTP10	*Tayassu*	MOD	rm3	-15.4
WCSCTP3	*Tayassu*	MOD	lm3	-13.9
WCSCTP4	*Tayassu*	MOD	rm3	-14.7
WCSCTP5	*Tayassu*	MOD	rm3	-14.2
WCSCTP9	*Tayassu*	MOD	RM3	-14.4
WCSF7TP14	*Tayassu*	MOD	lm3	-15.0
WCSF7TP35	*Tayassu*	MOD	RM3	-14.7
WCSF7TP36	*Tayassu*	MOD	rm3	-14.0
WCSF7TP37	*Tayassu*	MOD	rm3	-14.9
WCSF7TP4	*Tayassu*	MOD	lm3	-14.6
WCSF7TP51	*Tayassu*	MOD	rm3	-14.9
WCSF7TP52	*Tayassu*	MOD	rm3	-13.7
WCSF7TP54	*Tayassu*	MOD	lm3	-12.7
WCSF7TP57	*Tayassu*	MOD	rm3	-14.5
WCSF7TP62	*Tayassu*	MOD	lm3	-14.7
WCSUTP11	*Tayassu*	MOD	lm3	-15.1
WCSUTP12	*Tayassu*	MOD	lm3	-13.7
WCSUTP14	*Tayassu*	MOD	rm3	-15.0
WCSUTP15	*Tayassu*	MOD	RM3	-12.8
WCSUTP16	*Tayassu*	MOD	LM3	-13.5
WCSUTP18	*Tayassu*	MOD	rm3	-14.5
WCSUTP2	*Tayassu*	MOD	rm3	-14.3
WCSUTP6	*Tayassu*	MOD	rm3	-15.2
WCSUTP7	*Tayassu*	MOD	lm3	-15.1
WCSUTP8	*Tayassu*	MOD	lm3	-15.3

[a] DeSantis et al. (2009); [b]Yann and DeSantis (2014); [c]Koch et al. (1998); [d]D'Amo (2001); [e]Feranec and MacFadden (2000); [f]Feranec (2005); [g]Feranec and DeSantis (2014); [h]MacFadden and Cerling (1996); NP, not provided; NC = not catalogued; UF, University of Florida Museum of Natural History; WCS, Wildlife Conservation Society, Brazil and CENAP samples; HMP, Hemphillian; RCH, Rancholabrean; BLC, Blancan; IRV, Irvingtonian, MOD, Modern.

Supplemental Table 2: DMTA attribute values for all taxa studied.

Specimen	Taxon	NALMA	Tooth	*Asfc* median	*epLsar* median	*Tfv* median	$HAsfc_{3x3}$ median	$HAsfc_{9x9}$ median
UF408	*Protherohyus*	HMP	lm3	0.909	0.0048	11402	0.203	0.449
UF409	*Protherohyus*	HMP	lm3	0.451	0.0039	10858	0.203	0.449
UF424	*Protherohyus*	HMP	lm3	1.339	0.0024	9855	0.430	0.516
UF426	*Protherohyus*	HMP	lm3	4.811	0.0018	14330	0.379	0.741
UF428	*Protherohyus*	HMP	lm3	6.625	0.0022	13001	0.742	1.772
UF430	*Protherohyus*	HMP	lm3	2.257	0.0031	13678	1.104	1.929
UF431	*Protherohyus*	HMP	lm3	7.195	0.0006	12368	2.261	1.696
UF434	*Protherohyus*	HMP	RM3	1.361	0.0025	10499	0.528	1.272
UF435	*Protherohyus*	HMP	LM3	3.382	0.0022	12367	0.618	0.889
UF439	*Protherohyus*	HMP	RM2	3.369	0.0019	15517	1.189	1.581
UF455	*Protherohyus*	HMP	RM3	1.466	0.0043	11104	0.271	0.468
UF456	*Protherohyus*	HMP	RM3	13.792	0.0023	16313	0.691	1.021
UF458	*Protherohyus*	HMP	RM3	5.632	0.0023	11778	0.772	1.768
UF459	*Protherohyus*	HMP	LM3	2.369	0.0037	11934	0.386	0.747
UF460	*Protherohyus*	HMP	LM3	1.653	0.0026	8056	0.286	0.473
UF463	*Protherohyus*	HMP	LM2	3.405	0.0024	15136	0.561	0.902
UF464	*Protherohyus*	HMP	LM2	2.785	0.0026	10514	0.892	0.997
UF467	*Protherohyus*	HMP	LM1	4.686	0.0025	13406	0.573	0.770
UF203140	*Protherohyus*	HMP	RM2	0.751	0.0050	8488	0.490	0.719
UF203169	*Protherohyus*	HMP	M1	1.166	0.0018	14001	0.599	0.960
UF212392	*Protherohyus*	HMP	RM1	2.811	0.0017	14911	0.617	1.078
UF212419	*Protherohyus*	HMP	lm3	0.510	0.0010	0	0.304	0.406
UF16509	*Mylohyus*	BLC	m3/M3	10.509	0.0017	14855	0.638	0.902
UF21957	*Mylohyus*	BLC	M3	2.673	0.0010	13026	0.393	0.792
UF21958	*Mylohyus*	BLC	m3	11.734	0.0018	14922	0.649	0.942
UF60857	*Mylohyus*	BLC	lm1	4.132	0.0033	16447	0.422	0.800
UF97174	*Mylohyus*	BLC	rm3	10.454	0.0012	14537	0.402	0.722
UF412	*Mylohyus*	HMP	rm3	0.941	0.0017	11145	0.254	0.457
UF440	*Mylohyus*	HMP	LM3	3.261	0.0015	12587	0.430	0.749
UF12265	*Mylohyus*	HMP	LM3	2.190	0.0012	13491	0.160	0.296
UF26995	*Mylohyus*	HMP	LM1	1.775	0.0036	12557	0.642	2.126
UF101982	*Mylohyus*	HMP	lm3	2.673	0.0028	16781	0.414	0.835
UF203540	*Mylohyus*	HMP	LM3	2.900	0.0033	10891	0.756	1.359
UF211795	*Mylohyus*	HMP	lm1	7.087	0.0021	12982	1.424	2.263
UF211796	*Mylohyus*	HMP	rm2	3.535	0.0024	9421	0.329	0.777
UF14243	*Mylohyus*	IRV	M2	2.815	0.0016	16145	0.573	1.163
UF86301	*Mylohyus*	IRV	LM2	4.506	0.0022	15554	0.572	0.933
UF86691	*Mylohyus*	IRV	M2	4.063	0.0026	14057	0.586	1.283
UF214390	*Mylohyus*	IRV	LM3	12.827	0.0020	12422	0.639	0.815
UF2418	*Mylohyus*	RCH	lm1	4.927	0.0036	14429	0.439	0.673

UF2514	*Mylohyus*	RCH	lm1	8.001	0.0031	14289	0.229	0.657
UF3567	*Mylohyus*	RCH	RM1	2.004	0.0020	12339	0.987	1.340
UF4070	*Mylohyus*	RCH	lm3	10.026	0.0011	17121	0.501	0.745
UF4921	*Mylohyus*	RCH	rm3	9.223	0.0015	12055	0.268	0.730
UF10754	*Mylohyus*	RCH	ukn	5.585	0.0014	13928	0.485	0.970
UF12465	*Mylohyus*	RCH	lm3	6.098	0.0038	13157	0.479	0.925
UF12484	*Mylohyus*	RCH	rm1	24.085	0.0007	17918	0.352	0.777
UF13987	*Mylohyus*	RCH	molar	9.085	0.0035	12128	0.627	1.377
UF16513	*Mylohyus*	RCH	ukn	14.063	0.0007	13224	0.349	0.628
UF17699	*Mylohyus*	RCH	lm3	17.649	0.0020	15052	0.519	0.993
UF24521	*Mylohyus*	RCH	m3	7.645	0.0018	14622	0.777	1.605
UF309883	*Mylohyus*	RCH	LM2	1.934	0.0038	12230	0.242	0.397
UF12516AA	*Mylohyus*	RCH	molar	3.966	0.0013	13297	0.622	1.200
UF12516BB	*Mylohyus*	RCH	molar	0.933	0.0036	7699	0.240	0.404
UF15156	*Platygonus*	BLC	RM2	1.218	0.0036	9838	0.286	0.663
UF15158	*Platygonus*	BLC	lm2	5.883	0.0008	11217	1.168	3.293
UF18195	*Platygonus*	BLC	M2	10.322	0.0016	14054	1.725	2.591
UF45313	*Platygonus*	BLC	lm2	0.447	0.0046	11367	0.234	0.451
UF60028	*Platygonus*	BLC	lm3	2.163	0.0013	15669	0.445	0.913
UF176742	*Platygonus*	BLC	LM1	0.638	0.0067	5109	0.257	0.364
UF12073	*Platygonus*	IRV	rm2	8.177	0.0012	14630	0.548	0.983
UF12079	*Platygonus*	IRV	LM2	4.596	0.0054	13754	0.365	0.670
UF12086	*Platygonus*	IRV	rm3	22.774	0.0010	19873	0.423	1.018
UF12090	*Platygonus*	IRV	rm3	2.572	0.0016	13795	0.450	0.639
UF12094	*Platygonus*	IRV	m1	15.351	0.0029	11186	0.590	1.059
UF12703	*Platygonus*	IRV	lm3	3.493	0.0026	14296	0.349	0.883
UF62704	*Platygonus*	IRV	RM3	13.707	0.0022	15564	0.481	1.020
UF62708	*Platygonus*	IRV	LM3	2.155	0.0013	13306	0.325	0.470
UF63270	*Platygonus*	IRV	RM2	1.103	0.0041	9676	0.402	0.652
UF63337	*Platygonus*	IRV	RM2	2.144	0.0054	10539	0.398	0.738
UF63528	*Platygonus*	IRV	lm3	1.558	0.0010	11145	0.181	0.422
UF63907	*Platygonus*	IRV	lm3	1.878	0.0029	13202	0.557	1.098
UF63909	*Platygonus*	IRV	lm3	1.091	0.0037	10370	0.289	0.432
UF63924	*Platygonus*	IRV	LM3	3.527	0.0031	12550	0.948	1.222
UF63927	*Platygonus*	IRV	M2	2.232	0.0017	10814	0.487	0.855
UF65257	*Platygonus*	IRV	RM3	2.422	0.0019	12302	1.046	1.180
UF65258	*Platygonus*	IRV	RM3	1.623	0.0057	11112	0.253	0.511
UF65260	*Platygonus*	IRV	lm3	2.360	0.0039	9389	0.403	0.785
UF66651	*Platygonus*	IRV	rm3	3.738	0.0020	15604	0.388	1.007
UF66654	*Platygonus*	IRV	rm3	9.222	0.0017	15127	0.247	0.587
UF66656	*Platygonus*	IRV	rm2	0.578	0.0019	9395	0.216	0.415
UF66664	*Platygonus*	IRV	rm3	11.423	0.0014	17871	0.319	0.929
UF66665	*Platygonus*	IRV	rm2	15.931	0.0003	16503	0.351	0.764
UF66669	*Platygonus*	IRV	rm3	4.419	0.0033	12944	0.574	1.089
UF66676	*Platygonus*	IRV	rm3	9.547	0.0037	15123	0.848	1.645

UF66678	*Platygonus*	IRV	lm3	1.534	0.0047	11454	0.189	0.471
UF66683	*Platygonus*	IRV	lm3	14.894	0.0018	18076	0.509	0.936
UF66686	*Platygonus*	IRV	lm2	1.748	0.0031	14358	0.269	0.638
UF67177	*Platygonus*	IRV	lm3	4.568	0.0033	13900	0.324	0.656
UF67182	*Platygonus*	IRV	M2	1.672	0.0015	13818	0.257	0.466
UF67183	*Platygonus*	IRV	M3	3.341	0.0030	14596	1.129	1.597
UF80319	*Platygonus*	IRV	RM3	1.753	0.0055	12462	0.377	0.655
UF81556	*Platygonus*	IRV	m2	9.010	0.0016	18430	0.373	0.975
UF84402	*Platygonus*	IRV	lm3	2.134	0.0023	8533	0.510	0.956
UF86758	*Platygonus*	IRV	lm3	1.918	0.0013	11725	0.234	0.486
UF87819	*Platygonus*	IRV	lm3	2.178	0.0019	12748	0.399	0.702
UF87835	*Platygonus*	IRV	lm3	6.524	0.0018	15065	0.375	0.931
UF116009	*Platygonus*	IRV	LM3	10.259	0.0018	15419	0.358	0.726
UF211009	*Platygonus*	IRV	lm3	2.583	0.0035	14763	0.364	0.859
UF214391	*Platygonus*	IRV	lm3	1.121	0.0027	10133	0.611	0.985
UF217654	*Platygonus*	IRV	RM3	0.868	0.0033	4865	0.196	0.429
UF217659	*Platygonus*	IRV	m3/M3	2.780	0.0024	13261	0.631	1.680
UF219563	*Platygonus*	IRV	RM2	1.511	0.0026	4969	0.209	0.317
UF221016	*Platygonus*	IRV	lm3	0.838	0.0073	11650	0.237	0.427
UF221021	*Platygonus*	IRV	RM3	19.220	0.0018	14494	0.598	1.030
UF221173	*Platygonus*	IRV	LM2	4.018	0.0024	15103	0.197	0.399
UF221282	*Platygonus*	IRV	RM3	2.320	0.0020	11575	0.305	0.465
UF221528	*Platygonus*	IRV	RM3	4.362	0.0042	14161	0.380	0.892
UF221543	*Platygonus*	IRV	lm3	3.797	0.0024	14146	0.424	0.927
UF221767	*Platygonus*	IRV	lm3	2.406	0.0032	13428	0.697	1.071
UF235900	*Platygonus*	IRV	lm3	0.971	0.0031	11071	0.265	0.424
UF12078C	*Platygonus*	IRV	molar	14.979	0.0018	16107	0.586	0.728
UF12078D	*Platygonus*	IRV	molar	2.162	0.0040	16655	0.491	0.782
UFNC D	*Platygonus*	IRV	lm3	0.767	0.0046	2147	0.191	0.378
UF2924	*Platygonus*	RCH	molar	0.724	0.0041	5028	0.254	0.400
UF10130	*Platygonus*	RCH	M1	3.326	0.0019	11217	0.884	1.872
UF12497	*Platygonus*	RCH	rm2	4.545	0.0019	14464	0.491	0.764
UF12498	*Platygonus*	RCH	ukn	3.559	0.0072	10583	0.437	0.936
UF126495	*Platygonus*	RCH	lm1	2.389	0.0021	11744	0.396	1.027
UF126496	*Platygonus*	RCH	lm2	2.465	0.0042	13919	0.530	0.862
UF126498	*Platygonus*	RCH	LM2	4.325	0.0013	19021	0.356	0.844
UF126499	*Platygonus*	RCH	RM3	2.470	0.0028	9485	0.321	0.589
UF131950	*Platygonus*	RCH	rm3	20.200	0.0006	14582	0.316	0.516
UF131952	*Platygonus*	RCH	RM1	0.777	0.0051	7690	0.235	0.638
UF212691	*Platygonus*	RCH	rm2	5.696	0.0021	10491	0.233	0.462
UF212692	*Platygonus*	RCH	lm3	1.709	0.0052	13403	0.332	0.712
MZUSP107	*Tayassu*	MOD	rm2	1.739	0.0018	10983	0.513	0.628
MZUSP2998	*Tayassu*	MOD	rm2	2.887	0.0016	9081	0.226	0.373
MZUSP5437	*Tayassu*	MOD	rm2	3.326	0.0029	10971	0.436	0.642
MZUSP8087	*Tayassu*	MOD	rm2	11.011	0.0027	14229	0.661	0.976

MZUSP10346	*Tayassu*	MOD	rm1	2.813	0.0020	14169	0.622	0.744
MZUSP10350	*Tayassu*	MOD	lm1	2.896	0.0023	13866	0.352	0.718
MZUSP13489	*Tayassu*	MOD	rm2	14.679	0.0008	12961	0.519	0.935
MZUSP13491	*Tayassu*	MOD	rm2	2.613	0.0020	15281	0.533	1.442
MZUSP20015	*Tayassu*	MOD	lm2	2.080	0.0023	10769	0.124	0.254
MZUSP20017	*Tayassu*	MOD	RM1	1.958	0.0032	13250	0.882	1.312
MZUSP21607	*Tayassu*	MOD	rm2	6.340	0.0016	12567	0.423	0.935
MZUSP28146	*Tayassu*	MOD	rm1	1.681	0.0019	15781	0.170	0.411
MZUSP28547	*Tayassu*	MOD	rm2	16.800	0.0013	14806	0.754	1.504
MZUSP32288	*Tayassu*	MOD	rm1	2.344	0.0019	14280	0.214	0.483
WCSTPU10	*Tayassu*	MOD	rm1	4.234	0.0021	13373	0.518	0.930
WCSTPU11	*Tayassu*	MOD	rm3	2.252	0.0051	13144	0.176	0.327
WCSTPU12	*Tayassu*	MOD	rm3	2.066	0.0018	14390	0.662	0.881
WCSTPU13	*Tayassu*	MOD	rm3	2.876	0.0036	12090	0.266	0.575
WCSTPU14	*Tayassu*	MOD	rm3	5.954	0.0033	15083	0.216	0.500
WCSTPU17	*Tayassu*	MOD	RM3	11.463	0.0015	15964	0.820	1.419
WCSTPU2	*Tayassu*	MOD	rm3	5.653	0.0048	13252	0.558	1.049
WCSTPU3	*Tayassu*	MOD	rm3	1.831	0.0061	12219	0.287	0.534
WCSTPU7	*Tayassu*	MOD	rm3	3.577	0.0030	14724	0.333	0.585

Asfc, area-scale fractal complexity; *epLsar*, anisotropy; *Tfv*, textural fill volume; $HAsfc_{3x3}$, $HAsfc_{9x9}$, Heterogeneity of complexity in a 3 x 3 and 9 x 9 grid respectively; UF, University of Florida Natural History Museum; MZUSP, Museu de Zoologia da Universidade do São Paulo; WCS, Wildlife Conservation Society, Brazil and CENAP samples; HMP, Hemphillian; RCH, Rancholabrean; BLC, Blancan; IRV, Irvingtonian, MOD, Modern. R, upper right; r, lower right; L, upper left; l, lower left; m, molar; ukn, unknown tooth position.

Supplemental Table 3: Shapiro Wilk test for normality

Microwear Feature	p-value	Stable Carbon Isotopes	p-value
Asfc	**<0.0001**	*Mylohyus*	**0.035**
epLsar	**<0.0001**	*Platygonus*	**0.005**
Tfv	**<0.0001**	*Protherohyus*	0.198
$Hasfc_{3x3}$	**<0.0001**	*Tayassu*	**0.033**
$Hasfc_{9x9}$	**<0.0001**		

Asfc, area-scale fractal complexity; *epLsar*, anisotropy; *Tfv*, textural fill volume; $HAsfc_{3x3}$, $HAsfc_{9x9}$, Heterogeneity of complexity in a 3 x 3 and 9 x 9 grid respectively. Data with p-values less than 0.05 are considered non-normally distributed and indicated in bold font.

Supplemental Table 4: Statistical comparisons (P-values) for DMTA attributes between NALMAs for *Mylohyus*

		Rancholabrean	Irvingtonian	Blancan
Asfc	Irvingtonian	0.352		
	Blancan	0.355	0.273	
	Hemphillian	**0.007**	0.079	**0.013**
epLsar	Irvingtonian	0.476		
	Blancan	0.164	0.211	
	Hemphillian	0.398	0.448	0.139
Tfv	Irvingtonian	0.194		
	Blancan	0.093	0.384	
	Hemphillian	0.108	**0.047**	**0.016**
HAsfc3x3	Irvingtonian	0.085		
	Blancan	0.310	0.220	
	Hemphillian	0.416	0.134	0.388
HAsfc9x9	Irvingtonian	0.119		
	Blancan	0.495	0.158	
	Hemphillian	0.326	0.223	0.359

Asfc, area-scale fractal complexity; *epLsar*, anisotropy; *Tfv*, textural fill volume; $HAsfc_{3x3}$, $HAsfc_{9x9}$, Heterogeneity of complexity in a 3 x 3 and 9 x 9 grid respectively. P-values less than 0.05 are considered significant and noted here in bold.

Supplemental Table 5: Statistical comparisons (P-values) of DMTA attributes between NALMAs for *Platygonus*.

		Rancholabrean	Irvingtonian
Asfc	Irvingtonian	0.500	
	Blancan	0.170	0.133
epLsar	Irvingtonian	0.284	
	Blancan	0.331	0.466
Tfv	Irvingtonian	0.108	
	Blancan	0.453	0.146
$HAsfc_{3x3}$	Irvingtonian	0.320	
	Blancan	0.289	0.382
$HAsfc_{9x9}$	Irvingtonian	0.377	
	Blancan	0.348	0.413

Asfc, area-scale fractal complexity; *epLsar*, anisotropy; *Tfv*, textural fill volume; $HAsfc_{3x3}$, $HAsfc_{9x9}$, Heterogeneity of complexity in a 3 x 3 and 9 x 9 grid respectively

Supplemental Table 6: Pairwise comparison of DMTA attributes between *Mylohyus* and *Protherohyus* during the Hemphillian NALMA.

	Hemphillian
Asfc	0.765
epLsar	0.534
Tfv	0.801
$HAsfc_{3x3}$	0.558
$HAsfc_{9x9}$	0.833

Asfc, area-scale fractal complexity; *epLsar*, anisotropy; *Tfv*, textural fill volume; $HAsfc_{3x3}$, $HAsfc_{9x9}$, Heterogeneity of complexity in a 3 x 3 and 9 x 9 grid respectively

Supplemental Table 7: Statistical comparisons (P-values) of DMTA attributes between *Platygonus* and *Mylohyus* for each NALMA where the two genera co-occur.

	Irvingtonian	Blancan	Rancholabrean
Asfc	0.192	0.052	**0.025**
epLsar	0.434	0.537	0.152
Tfv	0.263	0.082	0.126
$HAsfc_{3x3}$	**0.028**	0.792	0.323
$HAsfc_{9x9}$	0.083	0.931	0.427

Asfc, area-scale fractal complexity; *epLsar*, anisotropy; *Tfv*, textural fill volume; $HAsfc_{3x3}$, $HAsfc_{9x9}$, Heterogeneity of complexity in a 3 x 3 and 9 x 9 grid respectively. P-values less than 0.05 are considered significant and noted here in bold.

Supplemental Table 8: Statistical comparisons (P-values) for stable carbon isotope analysis between NALMAs for *Mylohyus*.

	Rancholabrean	Irvingtonian	Blancan
Irvingtonian	0.282		
Blancan	**0.009**	**0.006**	
Hemphillian	**0.003**	**0.003**	0.331

P-values less than 0.05 are considered significant and noted here in bold.

Supplementary Table 8: Statistical comparisons (*P*-values) resulting from a Kruskal-Wallis test with a Dunn post hoc test for stable nitrogen isotope analyses among white-lipped peccary (*Tayassu pecari*) dietary resources from four Brazilian regions: Pantanal, Cerrado, semi-deciduous Atlantic Forest, and ombrophilous Atlantic Forest. *P*-values < 0.05 are considered significant and noted in bold. AF = Atlantic Forest.

Region Comparisons	$\chi 2$	Z	P	P (adjusted)
AF ombrophilous - AF semi-deciduous	15.200	-0.879	0.190	1
AF ombrophilous - Cerrado		-2.743	0.003	**0.018**
AF semi-deciduous - Cerrado		-2.204	0.014	0.083
AF ombrophilous - Pantanal		-3.034	0.001	**0.007**
AF semi-deciduous - Pantanal		-1.959	0.025	0.150
Cerrado - Pantanal		0.956	0.169	1

APPENDIX B

Overview, Design Concepts and Details

Model purpose

We developed a spatially-explicit, discrete agent-based model evaluating changes in large mammal habitat-use patterns as a function of habitat loss and fragmentation, here simplified to be percent of forest cover, the number of forested fragments, and the distance between forest fragments (a measure of connectivity). The purpose of the model is to determine how different fragmentation and loss scenarios result in differential use of the landscape by large mammals. This model was programmed in R version 3.3 and the version of the model used in this simulation can be found at https://github.com/jlbradha/IBM. To follow standard procedures with individual-based model description, we utilize the Overview, Design concepts, and Details method (Grimm et al. 2010).

Empirical peccary movement data

Model parameters that govern agent movement were derived from empirical movement data of white-lipped peccaries. Between 2013 and 2015, 12 white-lipped peccaries were captured and fitted with GPS collars in the southern Cerrado of central Brazil (Jorge et al. 2019). GPS locations were recorded every 3 to 6 hours through satellite transmission (Iridium). To quantify movement from GPS relocations, data were processed using adehabitatHR and adehabitatLS packages in R (Calenge 2006) to determine step length and relative turn angle (Bradham et al. unpublished). Step length is the straight-line distance between two GPS locations, while relative turn angle is the numerical change in angle between the continued trajectory direction from relocation one and the new trajectory direction from relocation two (Calenge 2006). Using Fitdistrplus package in R (Delignette-Muller and Dutang 2015) and associated AIC values, we established the empirical distributions that best fit the distribution of step lengths. The step lengths of all peccaries evaluated could be explained best by an exponential distribution. As the rate parameter of the associated exponential distribution varied per peccary, we took the median value for use in the model. Relative angles were also fitted to distributions using R and all peccary step angles could be explained through a circular uniform distribution.

Entities, state variables, and scales

The landscape of the model is divided into a grid of 167 x 167, 1-unit x 1-unit cells, with each cell representing 30 m x 30 m at our target field site. The state variable for each cell is the habitat type (i.e. forested or matrix) and number of times the cell has been visited by the agent. This model includes one type of agent, a single peccary herd, which moves across the landscape. State variables for the herd are their x and y coordinates. This model is spatially explicit and two-dimensional. Each time step represents a three-hour period in order to be consistent with the resolution from empirical movement data. The model run stops after the pre-specified amount of

time has passed (here 14600 steps or 5 years).

Process overview and scheduling

In each time step, the agent randomly chooses a step length and turn angle (90˚, 180 ˚, 270 ˚, 360˚) to map its next path. The model then checks to see if that path is within the boundary of the grid and whether the final coordinate of the move falls in a forested cell. If the final coordinate falls in a forest fragment but requires crossing the matrix, the peccary herd makes a stochastic decision whether to cross or to stay on the current cell. If the final coordinate falls on a forested cell but does not require crossing the matrix, the peccary herd always proceeds to that destination. The landscape state variable is updated after each peccary movement and each cell records the total number of visits from the peccary herd as it crosses from one location to another. Additional details from each of the actions executed here can be found in the Submodels section.

Design concepts

Basic principles – This model couples the fragmentation threshold hypothesis with empirical movement data to better understand the impact of fragmentation on animal habitat-use patterns. Parameters for animal movement and rules governing movement as utilized in this model can be found in Jorge et al. (2019).

Emergence – The spatial orientation and distribution of habitat-use intensity (measured in the model as visitation frequency) emerges as a function of the specified percent forest cover, the number of forest fragments on the landscape, and the distance between fragments.

Sensing – Agents can discern between a forested cell and a matrix cell. Agents preferentially stay in the forest and cross the matrix only under certain conditions (e.g. if the random step length and angle result in a distance below the maximum threshold for crossing and a stochastic process that prompts peccaries to cross the matrix).

Stochasticity – The configuration of the initial landscape and the decision whether or not to cross the matrix to arrive at another forested fragment are randomized.

Observation – For each fragmentation scenario and iteration, a csv file and an accompanying frequency histogram illustrate the distribution of visitation amount (i.e. visit count per cell). A csv file and an accompanying box plot show the percent of unvisited forested cells for each percent forest cover scenario. Finally, a csv file records the average distance between fragments and a scatterplot illustrates the number of unvisited forested cells as it relates to the distance between isolated forest fragments. In addition, the model generates a picture of the grid before a peccary herd has walked on it as well as the grid showing areas that are used more or less frequently after the peccary herd has walked over the landscape for the specified amount of time.

Initialization

The model is initialized by first creating a landscape, a grid with the specified dimensions where

all cells have the same state variable. Then, the model randomly selects a "seed" number between 1 and 4 depending on the fragmentation scenario. For one-fragment scenarios, the model randomly selects one cell on the landscape to be the seed cell. For two-fragment scenarios, the model randomly selects two cells on the landscape to be seed cells, and for three- and four-fragment scenarios, the model randomly selects three or four cells, respectively, as seed cells. Each seed cell converts their state variable to "forested". Then, seed cells convert the state variables of adjacent cells (up, down, left, or right – to the exclusion of diagonally connected cells) to 'forested' until the desired percent forest cover is reached for the entire landscape (i.e. the whole grid). Each forested seed cell and connected forested cells now form a forest fragment. Forest fragments are not uniform in size. Initialization continues by randomly placing one agent on a forested cell. From this location, the agent will choose a distance and an angle (90˚, 180 ˚, 270 ˚, 360˚) to inform movement to another cell location. The step length that the agent will take to move is chosen from an Exponential distribution with rate parameter of 6.67, while turn angles are chosen from a circular uniform distribution, in the form of four equally likely angles: 90˚, 180 ˚, 270 ˚, 360˚. The state variable for number of visits for each forested landscape cell is initially set to 0, while the state variable for matrix cells is permanently set to 'NA'.

Input

The model does not include any input of external data.

Submodels

Choose step length and turn angle – Since the turn angle was chosen from a circular uniform distribution, all directions on the grid are equally likely to be chosen. Thus, when choosing a turn angle, the agents randomly pick an integer between 1 and 4 where a value of "1" indicates movement to the left (270˚), '2' indicates movement up (360˚), '3' is to the right (90˚), and '4' is down (180˚). Step lengths were chosen from an exponential distribution with a parameter of 6.67 and multiplied by a specified maximum step distance and added to one to make the step-length scale comparable with the scale of the entire grid. After choosing the step length and the direction to travel in, the model locates the coordinates of the endpoint.

Check to see if the path is in bounds – To ensure that the agent remains on the map, the model checks to see whether the endpoint of the determined path lies within the grid boundaries. If the endpoint of the selected path is off the grid, the agent selects a new step length and turn angle. If the path is viable such that the endpoint lies on a forested cell and does not require crossing the matrix to arrive at that forested cell, the agent will proceed with the chosen movement trajectory.

Cross matrix or stay – If the endpoint of the determined path lies within an isolated forest fragment separated from the current forest fragment by matrix, the agent will decide whether or not to cross. If the distance to the endpoint requires crossing the matrix in which the matrix distance is greater than ¼ the pre-determined maximum step length, the agent will choose to stay. Otherwise, the agent will randomly choose to cross or stay with a probability of 0.5.

Update visit count to landscape – Each forested cell initially has a value of zero. As the agent moves across the forested landscape, the value of each cell increases according to the number of times the agent 'walks' across the cell. The frequency distribution of 'number of cell visits' is recorded in a data matrix for creating the frequency histogram and boxplot (see 'Observations').
Calculate distance between fragments – To calculate distance between two forested patches, the model draws an ellipse around each isolated forest fragment that includes 80% of the forested cells in that fragment using the dataEllipse function in the Car package (Fox and Weisburg, 2011). Once the ellipses are calculated, the model calculates the minimum distance between the ellipses. For one-fragment scenarios, there is no distance to be calculated. For two-fragment scenarios, a single distance between the two forested fragments is calculated. For scenarios involving three or more forest fragments, the distances between all fragments are calculated and the average of the n –1 shortest distance is recorded, where n is the number of forest fragments. In each simulation, this distance is used to calculate the scatterplot (see Observations) that relates distance between forest fragments to the number of forested cells where the visitation count is zero, as this provides an estimation of the maximum distance between fragments where white-lipped peccary movement is not impeded by the matrix.